博士論文

Characterization of human monoclonal antibodies against influenza A virus and its application to antibody therapy

（A 型インフルエンザウイルスに対するヒトモノクローナル抗体の性状解析と抗体治療への応用）

Atsuhiro Yasuhara

安原　敦洋

CONTENTS

CHAPTER III

Antigenic drift originating from changes to the lateral surface of the neuraminidase head of influenza A virus

PREFACE

Influenza virus is an RNA virus that circulates among humans, causing acute respiratory infections. It is estimated that three to five million people are infected with influenza virus every year, causing a serious health burden and economic impact due to reduced productivity (1). The young and the elderly are particularly susceptible to severe disease (2). Therefore, influenza virus poses a constant and serious public health threat.

Influenza viruses belong to the *Orthomyxoviridae* family and can be classified into four distinct types: influenza A, influenza B, influenza C, and influenza D (3, 4). Although influenza A, B, and C viruses commonly circulate and cause disease in humans, only influenza A virus has caused serious disease outbreaks; in fact, influenza A virus has caused some of the most serious infectious outbreaks in history (5). Influenza A viruses are further classified into subtypes based on the antigenic properties of their two viral surface glycoproteins, hemagglutinin (HA) and neuraminidase (NA); to date 18 HA (H1–H18) and 10 NA (N1–N10) antigenic subtypes been identified (6, 7). The current subtypes of influenza A viruses found in people are H1N1 and H3N2 viruses.

To counter the threat of influenza virus, antiviral therapy is one of the main protective strategies. In particular, NA inhibitors are currently used to treat influenza virus infection (8). NA is a tetrameric transmembrane protein with enzymatic activity that cleaves the interaction between viruses and the host cell surface, allowing release of progeny viruses (9, 10). NA inhibitors bind to the active site on NA molecules and inhibit virus release (8). These inhibitors have been employed successfully

for more than a decade. However, almost all H1N1 viruses isolated between 2007 and 2009 acquired resistance to oseltamivir, which is the most commonly used NA inhibitor (11, 12). Although the current dominant strains are susceptible to NA inhibitors, the emergence of resistant viruses is always a concern. Therefore, several therapies that target highly conserved features of influenza virus, such as antibodies to the HA conserved region, are being developed (13, 14).

The virus surface protein HA consists of a globular head and a stem region, and mediates binding of the virus to host cells via interactions between its receptor binding site (RBS) and the terminal sialic acids on host cell glycans (15, 16). During the past several years, antibodies targeting conserved epitopes in the head or stem region of HA have been isolated (14, 17-20). Given their potential, some of these antibodies are being evaluated in clinical trials (21-23). Antibodies targeting the functionally conserved residues within the RBS of the HA head possess high protective efficacy by directly blocking sialic acid receptor binding; such antibodies would be expected to be powerful anti-influenza agents. However, it is not clear how readily mutant viruses can escape from anti-RBS antibodies or whether such mutants are biologically fit to compete with wild-type viruses.

Another powerful tool to control influenza virus infection is vaccination, which can induce protective antibody responses (24, 25). However, influenza viruses can evade virus-specific host immunity through antigenic drift. Since influenza virus genomes do not have RNA proofreading enzymes, point mutations accumulate in the antigenic site through successive rounds of replication (26). Therefore, influenza vaccines must be reformulated frequently to antigenically match circulating

strains (14). For the development of a long-term effective vaccine, it is important to know the exact antigenicity of the circulating strains and predict their future antigenic drift. However, the antigenicity of NA is not as well understood as that of HA. And, although some studies have shown the importance of anti-NA antibodies for protection, the current vaccine does not efficiently elicit antibodies against NA (27-31).

In this study, I aimed to improve protection strategies through isolation and characterization of human monoclonal antibodies induced by vaccination or infection. In chapter I, I predicted potential antigenic variants that may emerge in nature by use of in vitro selection using human monoclonal antibodies. In chapter II, I isolated and characterized human neutralizing monoclonal antibodies that recognize the RBS of HA and investigated the ease with which resistant variants emerged. Finally, in chapter III, I evaluated the antigenic properties of NA by characterizing human monoclonal antibodies that recognize the lateral surface of the NA head.

CHAPTER I

Diversity of antigenic mutants of influenza A(H1N1)pdm09 virus escaped from human monoclonal antibodies

Abstract

Since the 2017 Southern Hemisphere influenza season, the A(H1N1)pdm09-like virus recommended for use in the vaccine was changed because human, but not ferret, sera distinguish A(H1N1)pdm09 viruses isolated after 2013 from the previously circulating strains. An amino acid substitution, lysine to glutamine, at position 166 (H3 numbering) in the major antigenic site of HA was reported to be responsible for the antigenic drift. Here, I obtained two anti-A(H1N1)pdm09 HA monoclonal antibodies that failed to neutralize viruses isolated after 2013 from a vaccinated volunteer. Escape mutations were identified at position 129, 165, or 166 in the major antigenic site of HA. Competitive growth of the escape mutant viruses with the wild-type virus revealed that some escape mutants possessing an amino acid substitution other than K166Q showed superior growth to that of the wild-type virus. These results suggest that in addition to the K166Q mutation that occurred in epidemic strains, other HA mutations can confer resistance to antibodies that recognize the K166 area, leading to emergence of epidemic strains with such mutations.

Introduction

The first influenza pandemic of the 21st century began in 2009 with the emergence of the A(H1N1)pdm09 virus, which replaced the previous seasonal H1N1 (sH1N1) virus (32, 33). Surveillance of circulating A(H1N1)pdm09 viruses has revealed some genetic variations in the viral surface glycoproteins, hemagglutinin (HA) and neuraminidase (NA) (34, 35). However, until recently, the antigenicity of the circulating A(H1N1)pdm09 viruses was similar to the vaccine strain (A/California/7/2009) in assays with panels of antiserum obtained from infected ferrets (34). Therefore, the World Health Organization (WHO) recommended using A/California/7/2009-like virus as a vaccine seed virus until the 2016–2017 Northern hemisphere influenza season (34). However, human sera distinguished the antigenicity of recent A(H1N1)pdm09 viruses from that of the A/California/7/2009-like vaccine virus, whereas ferret antisera failed to detect this antigenic difference (36, 37). Accordingly, since the 2017 Southern Hemisphere influenza season, the WHO has recommended A/Michigan/45/2015-like virus be used as the vaccine seed virus (36, 37).

The HA protein is the major influenza viral antigen and the primary target of neutralizing antibodies (38). A(H1N1)pdm09-HA has five major antigenic sites, which were identified by studies using A/Puerto Rico/8/34 (H1N1) (39-42). Two immunodominant sites (Sa and Sb) are located proximal to the receptor-binding pocket and elicit high potency neutralizing antibodies (39, 41). The Ca sites (Ca1 and Ca2) are at the subunit interface, and the Cb site is close to the stalk region of HA (39, 41). A(H1N1)pdm09 viruses isolated after the 2012–2013 influenza season, which are classified

into the genetic group 6B, possess a lysine-to-glutamine substitution at position 166 (K166Q, H3 numbering) within the Sa antigenic site (43). This mutation affects the antigenicity of recent A(H1N1)pdm09 viruses (44). In the 2016–2017 influenza season, A(H1N1)pdm09 viruses classified into genetic group 6B.1 circulated among humans (36). The 6B.1 viruses obtained a serine-to-asparagine substitution at position 165 (S165N) in the Sa antigenic site that resulted in the generation of an N-glycosylation site (35, 45).

Previous reports have described several human monoclonal antibodies that recognize an epitope around position 166 of A(H1N1)pdm09-HA and neutralize A(H1N1)pdm09 and sH1N1 viruses. However, these antibodies failed to neutralize A(H1N1)pdm09 viruses isolated after the 2012–2013 season, which possessed the K166Q mutation, or sH1N1 viruses isolated between 1986 and 2008, which had a potential glycosylation site (129-NHT-131) masking the epitope around position 166 (46-48). Middle-aged adults (i.e., born between 1965 and 1979) were reported to have a high antibody titer against the epitope around position 166 of the HA of A(H1N1)pdm09 viruses that were circulating before 2012, since they had been exposed to sH1N1 viruses that were circulating before 1985 and whose HA lacked the 129-NHT-131 glycosylation site. These middle-aged adults suffered from A(H1N)pdm09 virus infection with substantial morbidity and mortality during the 2013–2014 influenza season because of low neutralization antibody titers against the viruses possessing the K166Q substitution (43). These reports demonstrate that the epitope around position 166 plays a role in the antigenic drift recently detected in assays with human, but not ferret, sera. Another group

confirmed this phenomenon by using a panel of human monoclonal antibodies from a middle-aged adult (48). In vitro selection of escape mutants from these monoclonal antibodies revealed that a mutation at position 166 of HA was responsible for the resistance to neutralization, suggesting that the antigenic drift was caused by the selective pressure of the human antibodies recognizing the epitope around position 166 (48).

Here, I established two human anti-A(H1N1)pdm09 HA monoclonal antibodies that recognized the epitope around position 166. I then attempted to obtain escape mutants possessing an amino acid substitution other than at position 166 and compared their growth ability with that of the wild-type virus.

Results

Establishment of human monoclonal antibodies recognizing A(H1N1)pdm09-HA. PBMCs separated from a human volunteer vaccinated with the 2014-2015 seasonal influenza vaccine were fused with fusion partner SPYMEG cells to generate hybridomas that expressed a human antibody (17). After screening by ELISA using recombinant H1-HA, hybridomas positive for anti-HA antibody production were biologically cloned. As a result of screening with 444 hybridoma clones, I obtained two monoclonal antibodies (mAbs), 1429B72/2-7 and 1429C45/1-5, which recognized A(H1N1)pdm09-HA but not H3, H5, H7, or type B-HAs. Nucleotide sequence analysis of the variable regions of each antibody (Table 1) revealed that the two monoclonal antibodies used the same VH and VL genes, suggesting that these two antibodies could be derived from the same B cell ancestor. The VH regions of 1429B72/2-7 and 1429C45/1-5 had 94.9% and 95.6% identities, respectively, compared with the germline sequence, IGHV3-7*01 (Fig. 1). Similar homologies were also observed for other genes (D, JH, VL, and JL). These results indicate that 1429B72/2-7 accumulated somatic mutations compared with 1429C45/1-5.

Table 1. Genetic features of human mAbs that recognize A(H1N1)pdm09-HA

mAb	Heavy chain		Light chain	
	VH[a]	CDR3[b]	VL[c]	CDR3
1429B72/2-7	IGHV3-7*01	ARAGSYGDYVPYYNWFDS	IGKV3-15*01	QQYNNWPPWT
1429C45/1-5	IGHV3-7*01	ARAGSYGDYRPLYNWFDS	IGKV3-15*01	QQYNNWPPWT

[a] Variable genes for the heavy chain

[b] Complementarity determining region 3

[c] Variable genes for the light chain.

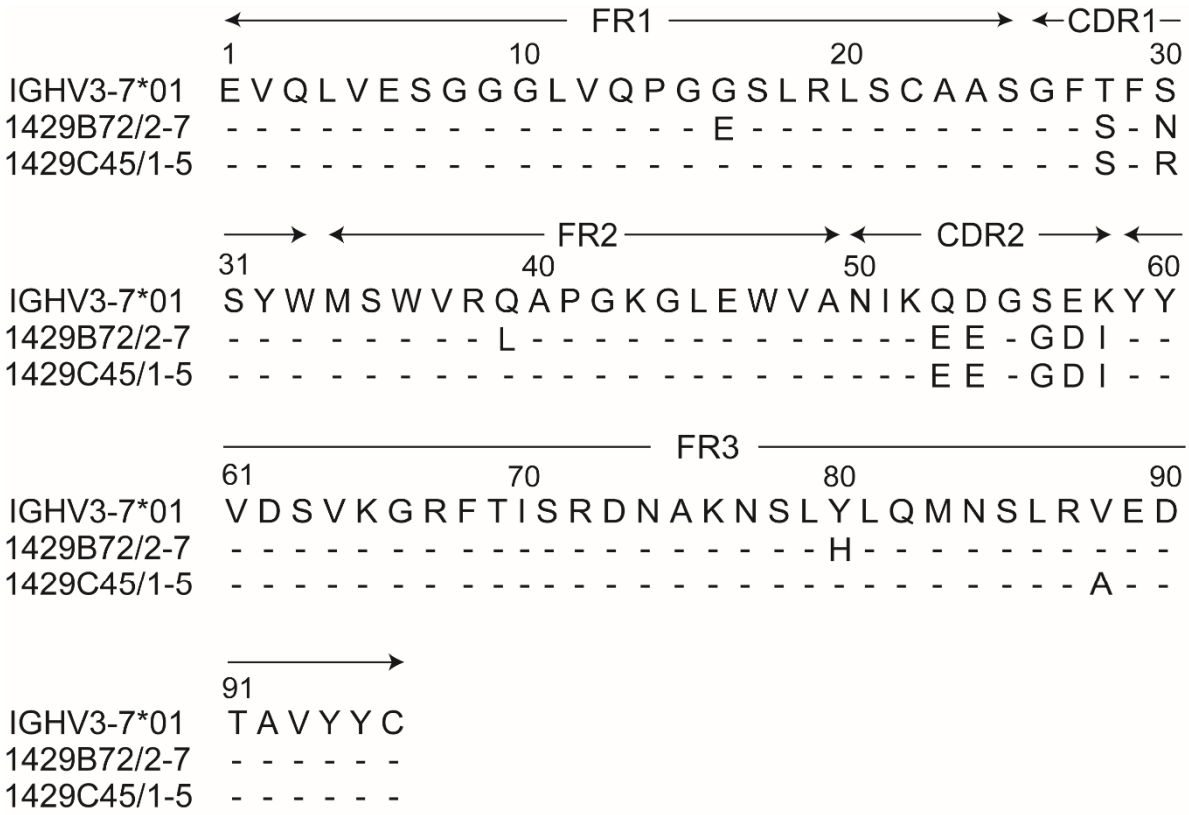

Figure 1. Sequence alignment of the variable regions of the heavy chains. The VH regions of 1429B72/2-7 and 1429C45/1-5 were compared with the germline sequence, IGHV3-7*01. Dashes indicate identities with respect to the germline sequence. The amino acid numbering corresponds to the Kabat numbering scheme.

Human mAbs fail to recognize A(H1N1)pdm09 viruses isolated after the 2013–2014 season. To characterize the two mAbs I obtained, I performed a microneutralization assay against A(H1N1)pdm09 viruses isolated in different influenza seasons. 1429B72/2-7 and 1429C45/1-5 neutralized A(H1N1)pdm09 viruses isolated between the 2009 and 2013 seasons with 50% inhibitory concentration (IC_{50}) values of 0.08–0.12 and 0.24–0.39 μg/ml, respectively (Table 2). However, these mAbs failed to neutralize A(H1N1)pdm09 viruses isolated after the 2013–2014 season even at the highest concentration (50 μg/ml) tested. CR9114, which recognizes the HA stalk (49), inhibited replication of all A(H1N1)pdm09 viruses tested, yielding an IC_{50} value of 0.92–9.92 μg/ml under the same experimental conditions. These results indicate that a key amino acid in the epitope recognized by the two mAbs changed after the 2013–2014 season. To identify this key amino acid substitution, I compared the amino acid sequences of A(H1N1)pdm09 HA obtained from the Global Initiative on Sharing All Influenza Data (GISAID). As previously reported (34, 36), this analysis revealed that A(H1N1)pdm09 viruses acquired the K166Q mutation in the major antigenic site Sa after 2013 (Table 3 and Fig. 2). The correlation between the loss of neutralization activity of the two mAbs and the acquisition of the K166Q mutation suggested that these mAbs may recognize an epitope that includes position 166.

In previous reports (46-48), some mAbs recognizing the epitope around position 166 of A(H1N1)pdm09 HA failed to neutralize sH1N1 viruses isolated between 1986 and 2008, because these viruses acquired an N-linked glycosylation at position 129, which likely covers the epitope that

includes position 166. To investigate whether 1429B72/2-7 and 1429C45/1-5 have identical neutralization properties to previously reported 166-specific mAbs (46, 47), I tested the neutralization activities of our mAbs in a microneutralization assay using four sH1N1 viruses isolated in 1979, 1980, 1988, and 1992. As expected, our two monoclonal antibodies efficiently neutralized the sH1N1 viruses isolated in 1979 and 1980 but failed to neutralize the sH1N1 viruses isolated in 1988 and 1992, which contained the additional glycosylation site created by the K129N substitution, which shielded the epitope around position 166 (Table 4). CR9114 inhibited the replication of all of the sH1N1 viruses tested at an IC_{50} value of 12.50–17.68 μg/ml. These results indicate that our two mAbs recognized the epitope in a manner similar to that of previously reported mAbs (46-48).

Table 2. Neutralization activity of mAbs against A(H1N1)pdm09 viruses

mAb	IC_{50} value (μg/ml) against A(H1N1)pdm09 virus isolated in						
	2009[a]	2010–2011[b] (Clade 5[h])	2011–2012[c] (Clade 7)	2012–2013[d] (Clade 6C)	2013–2014[e] (Clade 6B)	2014–2015[f] (Clade 6B)	2015–2016[g] (Clade 6B.1)
1429B72/2-7	0.10	0.08	0.12	0.10	>50	>50	>50
1429C45/1-5	0.39	0.25	0.31	0.39	>50	>50	>50
CR9114	6.25	3.94	3.94	9.92	0.92	1.24	1.24

[a] A/California/04/2009, [b] A/Hiroshima/66/2011, [c] A/Osaka/83/2011, [d] A/Osaka/33/2013, [e] A/Osaka/6/2014, [f] A/Yokohama/50/2015 and [g] A/Yokohama/94/2015 were used in this experiment.

[h] Phylogenetic clades are listed for each isolate.

Table 3. Sequence variation of H1N1pdm09 HA at position 166.

Amino acid position[a]	Residue	Percentage of isolates possessing the indicated residue isolated in							
		2009–2010[b, d]	2010–2011[e]	2011–2012[f]	2012–2013[g]	2013–2014[h]	2014–2015[i]	2015–2016[j]	2016–2017[c, k]
166	K	99.1	96.4	97.7	72.4	4.6	0.5	0.3	0.5
	Q	0	0.1	0.4	7.7	93.8	98.2	98.9	99.1
	Others	0.9	3.5	1.9	19.9	1.6	1.3	0.8	0.4

[a] H3 numbering.

[b] Northern Hemisphere influenza season (from October to May).

[c] The sequences were obtained from October, 2016 to January, 2017.

[d] 3616, [e] 1022, [f] 468, [g] 1057, [h] 1632, [i] 1139, [j] 5838, and [k] 424 HA amino acid sequences were used.

Table 4. Neutralization titers of mAbs against sH1N1 viruses

mAb	IC_{50} value (μg/ml) against sH1N1virus isolated in			
	1979[a]	1980[b]	1988[c]	1992[d]
1429B72/2-7	0.28	0.28	>50	>50
1429C45/1-5	0.25	0.14	>50	>50
CR9114	17.68	12.50	15.75	12.50

[a] A/Kumamoto/37/79, [b] A/Kamata/8/80, [c] A/Tokyo/913/88, and [d] A/Minato/131/92 were used in this experiment.

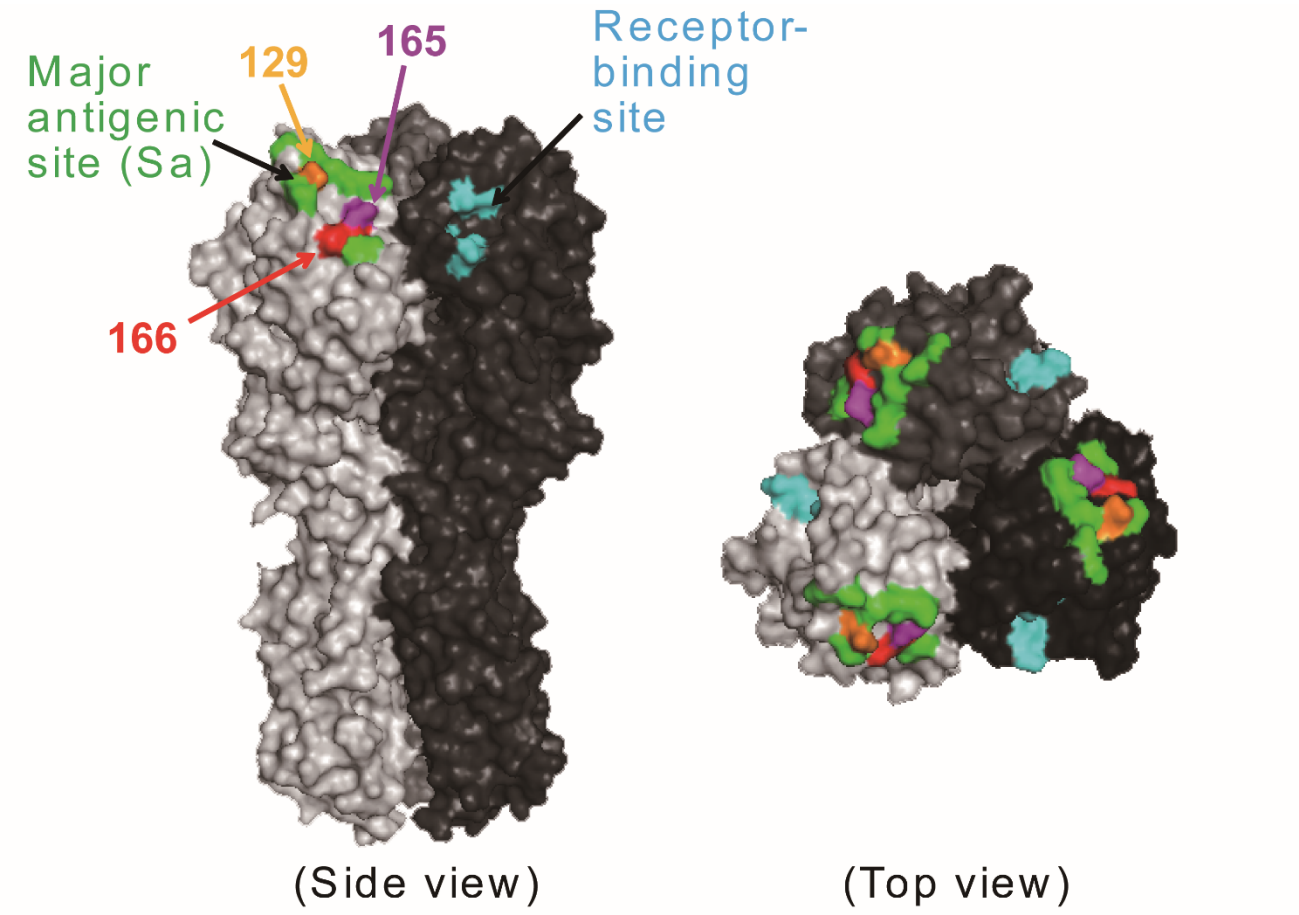

Figure 2. Positions 129, 165, and 166 on the HA molecule. Each HA monomer is indicated in white, gray, and black. Cyan indicates the residues involved in receptor binding; green indicates the Sa antigenic site. Amino acids at positions 129 (orange), 165 (magenta), and 166 (red) are shown on the HA of A/California/04/2009.

Escape mutants from 1429B72/2-7 and 1429C45/1-5. Recent A(H1N1)pdm09 viruses possessing the K166Q mutation do not react with antibodies that recognize the epitope that includes position 166 (36, 43, 48). In addition, an in vitro-selected mutant possessing K166E did not react with such antibodies (48). To examine whether antigenic variants possessing mutations at positions other than 166 would be selected by antibodies recognizing the epitope that includes position 166, I attempted to select escape mutant viruses in triplicate by passaging CA04 virus with various concentrations of 1429B72/2-7 or 1429C45/1-5. After 3–15 passages, I identified escape mutants for each mAb. These mutants possessed the N129D, S165C, S165N, K166E, or K166N mutation in their HA (Table 5). All of these mutations are located in the major antigenic site Sa (Fig. 2). No amino acid mutations were identified in the NA proteins. The results of selecting escape mutants indicate that an amino acid substitution at position 129 or 165, in addition to 166, conferred resistance to A(H1N1)pdm09 virus against human antibodies that recognized the epitope around position 166.

Table 5. Amino acid substitutions in the HA of escape mutants.

mAb	Amino acid substitution in the HA of the escape mutant		
	Clone 1[a]	Clone 2	Clone 3
1429B72/2-7	K166E[b]	S165C	N129D
1429C45/1-5	N129D	S165N	K166N

[a] Clones 1–3 were independently obtained.

[b] H3 numbering.

Growth kinetics of the escape mutant viruses in cultured cells. To examine the fitness of the viruses possessing mutations that allowed them to escape from 1429B72/2-7 and 1429C45/1-5, I compared the growth kinetics of the escape mutant viruses in cultured cells with those of the wild-type virus. I infected A549 cells with the wild-type CA04 virus or a mutant virus possessing an escape mutation (i.e., HA-N129D, -S165C, -S165N, -K166E or -K166N) or the naturally occurring HA-K166Q substitution at a multiplicity of infection (MOI) of 0.0001. Virus titers at 12, 24, 48, and 72 hours post-infection (hpi) were determined by use of plaque assays with MDCK cells (Fig. 3). The virus with the N129D or K166E mutation replicated to higher titers than the wild-type virus ($P < 0.01$). The K166Q or K166N mutant viruses replicated to slightly higher titers compared with the wild-type virus. The S165C mutant virus replicated as efficiently as the wild-type virus, whereas the S165N mutant virus showed slightly lower titers at 12, 24, and 72 hpi. These results demonstrate that the fitness of some of the antigenic variant viruses in these human cells was increased by the escape mutation.

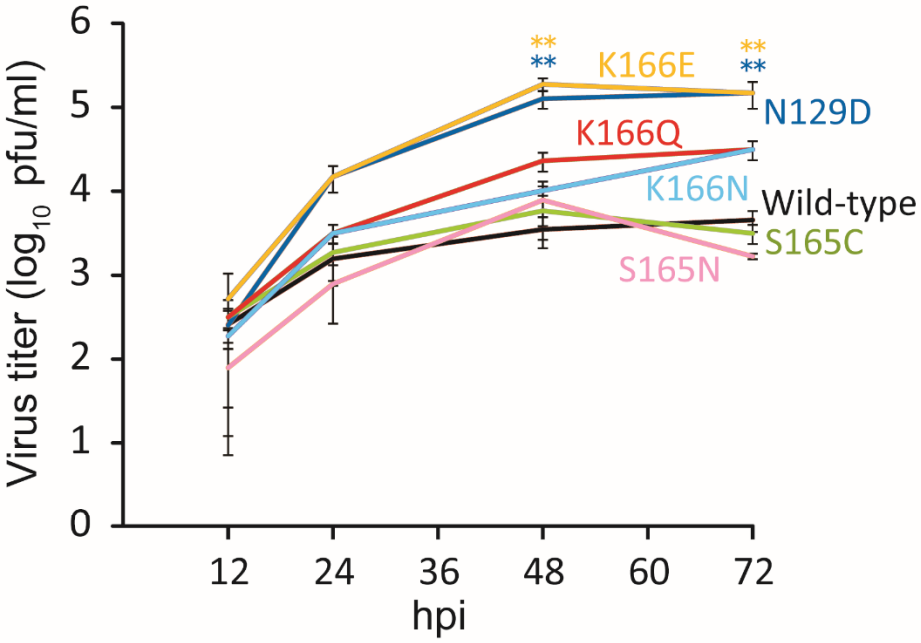

Figure 3. Replication kinetics of the wild-type virus and escape mutants. The growth kinetics of the wild-type CA04 virus and the indicated mutant viruses in A549 cells were compared. Cell culture supernatants of A549 cells infected at an MOI of 0.0001 were collected at 12, 24, 48, and 72 hpi. Virus titers are presented as the mean ± SD (n=3). **P < 0.01 (two-way ANOVA followed by Dunnett' s tests).

Competitive growth of the escape mutant viruses with wild-type virus. To further examine the fitness of the escape mutant viruses, I performed a competitive replication assay against the wild-type virus (Fig. 4). Briefly, I co-infected A549 cells with a 1:1 ratio of the wild-type CA04 virus and a mutant virus each possessing an escape mutation or the naturally occurring HA-K166Q. The populations of wild-type and mutant viruses were then measured by using a droplet digital PCR (ddPCR) system at 12, 24, 48, and 72 hpi. I found that the population of mutant viruses with HA-N129D or -K166E became dominant at 72 hpi (~75%), whereas the mutant viruses with HA-S165C or -S165N was detected at relatively low levels (~30%) at 72 hpi. The proportion of mutant viruses with HA-K166N or -K166Q remained at the same level as that of the wild-type virus at even 72 hpi. These results show that some escape mutant viruses are as competitive as the naturally occurring HA-K166Q mutant with the wild-type virus. Next, I performed the competitive replication assay using the HA-N129D or -K166E virus and the currently circulating HA-K166Q mutant virus (Fig. 5). Again, I co-infected A549 cells with a 1:1 ratio of the K166Q mutant virus and the N129D or K166E virus, and determined the populations of each mutant virus by using a ddPCR system at 12, 24, 48, and 72 hpi. I found that the relative proportion of mutant viruses with N129D or K166E became dominant over the K166Q mutant virus (70%–84%), suggesting that the N129D or K166E mutant virus has the potential to overcome the currently circulating viruses as well as the pre-2013 isolates. Therefore, it remains unclear why the virus with HA-K166Q, rather than HA-N129D, -S165C, -S165N, -K166E, or -K166N

became dominant in nature. Nevertheless, our results suggest that the escape mutants identified here had the potential to be dominant strains in the world.

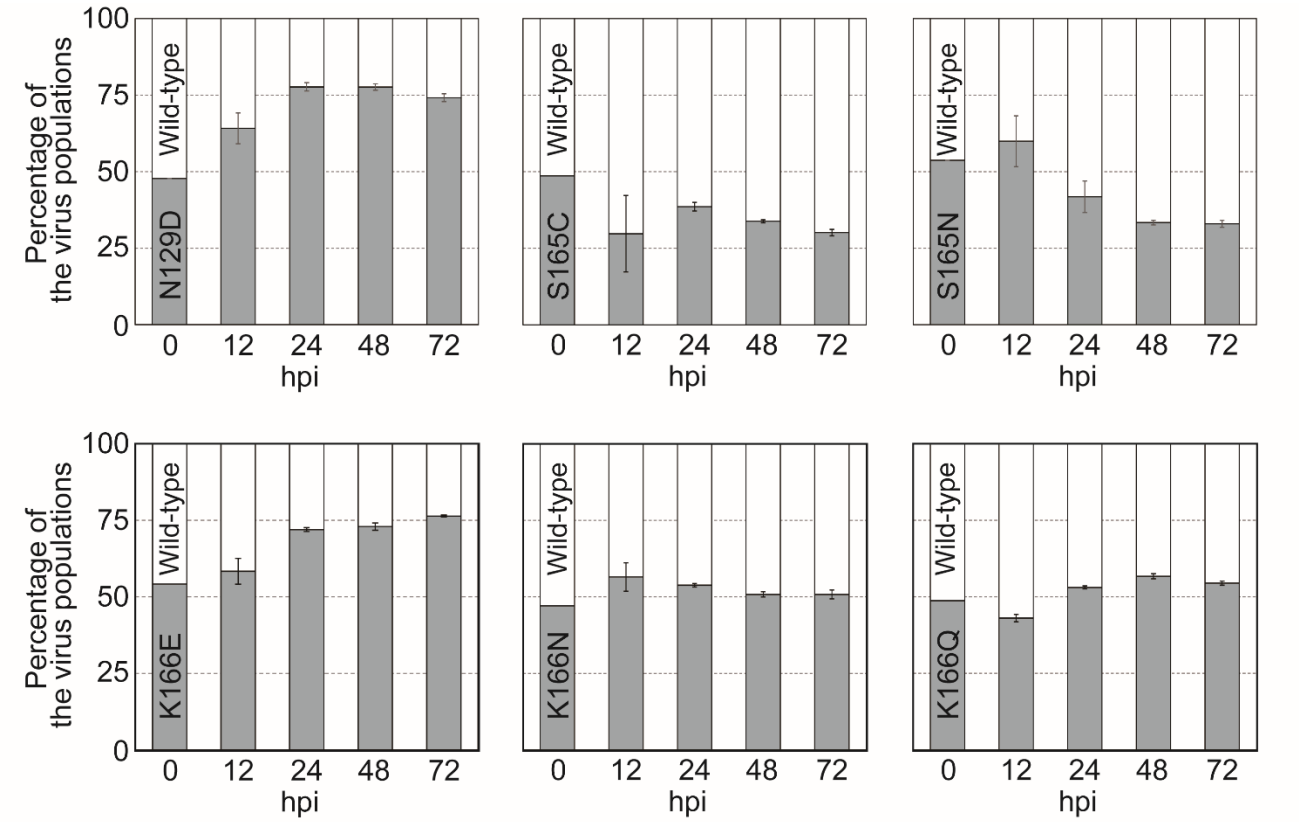

Figure 4. Competitive growth of escape mutant viruses with wild-type virus in cultured cells. The relative proportions of the indicated escape mutant virus and the wild-type virus are showed in the panels (grey bars show the percentage of mutant virus; white bars show the proportion of wild-type virus). The wild-type virus and the mutant viruses possessing each escape mutation were premixed at a 1:1 ratio based on their PFU titers. A549 cells were infected with the mixed viruses at an MOI of 0.0001, and supernatants were harvested at 12, 24, 48, and 72 hpi. The relative proportions of wild-type and mutant viruses were determined by using a QX200 droplet digital PCR system. The average values were measured in three technically independent experiments, and the SDs are shown as error bars.

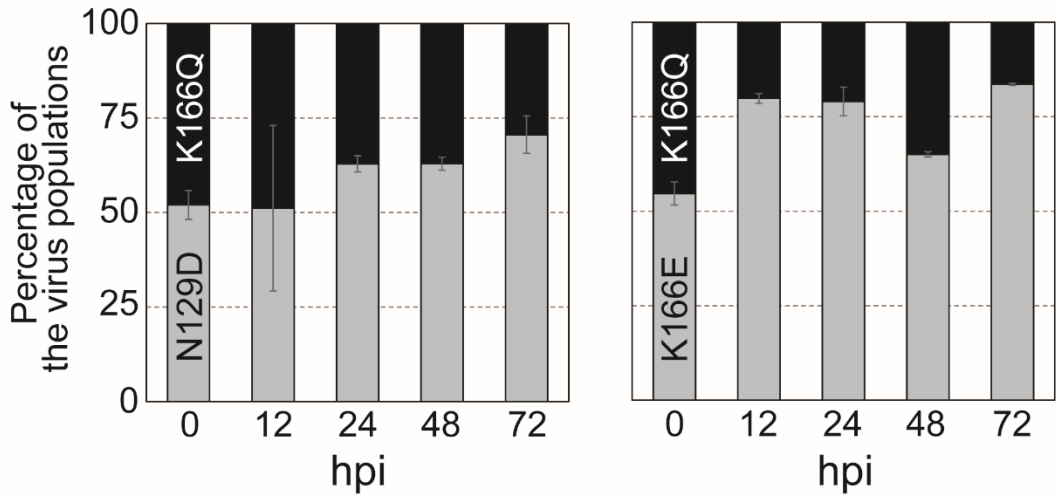

Figure 5. Competitive growth of escape variants with the naturally occurring K166Q mutant. The relative populations of the mutant viruses possessing HA-N129D or -K166E and the K166Q mutant virus were examined by using the competitive replication assay in A549 cells (MOI = 0.0001). The grey bars show the percentage of the mutant viruses with N129D or K166E and the black bars show the proportion of the K166Q mutant virus. The relative proportions of the indicated viruses at 12, 24, 48, and 72 hpi were determined by using ddPCR systems. The average values were measured in three technically independent experiments, and the SDs are shown as error bars.

Discussion

Here, I established two human anti-A(H1N1)pdm09 HA monoclonal antibodies, 1429B72/2-7 and 1429C45/1-5, which failed to neutralize A(H1N1)pdm09 viruses isolated after 2013. By passaging the CA04 virus in the presence of these monoclonal antibodies, I obtained escape mutant viruses that possessed an amino acid substitution at position 129, 165, or 166. Some escape mutants showed better growth kinetics and became the dominant population in the competitive replication assay. These findings indicate that antigenic variant viruses with a mutation at position 129 or 165 could be selected by the immunological pressure of human antibodies that recognize the epitope around position 166 that are abundant in some individuals (43, 48), leading to the emergence of epidemic strains with such mutations.

Although an antigenic variant with the HA-K166Q mutation was selected in nature and became an epidemic strain in the 2012–2013 season, A(H1N1)pdm09 viruses possessing the N129D or S165N mutation temporarily appeared in the 2010–2011 season (50, 51). The S165N substitution did not affect the antigenicity of A(H1N1)pdm09 viruses in assays with ferret anti-serum (52, 53) but no information is available in this regard with human serum. The N129D substitution led to a significant reduction in the hemagglutination inhibition (HI) titer with human sera obtained from infected or vaccinated subjects (54). Although viruses with the N129D or S165N mutation were obtained in vitro and those with N129D showed high replicative ability in the competitive replication assay, the viruses with N129D did not spread in human populations. These findings suggest that the

emergence of antigenic drift strains is a stochastic event in which an epidemic strain emerges randomly from viruses with similar epidemic potential, or that factors other than HA antigenicity and replicative ability in vitro (e.g., transmissibility) play roles in determining which antigenic variants become epidemic strains. Nonetheless, the selection of antigenic variants in vitro provides useful information for identifying future epidemic strains. Further studies are needed to understand exactly what determines which antigenic mutants became dominant in the field.

1429B72/2-7 and 1429C45/1-5 did not neutralize A(H1N1)pdm09 isolates from after 2013 or sH1N1 isolates from after 1985 even at the highest concentration (50 μg/ml) tested. The neutralization properties of these two mAbs were similar to those of K166-specific antibodies that were reported previously (46-48). In these previous studies, the K166-specific antibodies were found in individuals who were born before 1979, so they had been exposed to sH1N1 viruses that circulated prior to 1985 and lacked the glycosylation site at position 129 (43). 1429B72/2-7 and 1429C45/1-5 were obtained from a volunteer who was born in 1976, which is consistent with this pattern. The age in humans at which antigenic drift mutants are selected in nature is not known. However, our studies, together with those of others, suggest that at least the K166Q mutants may have been selected in individuals who had been exposed to sH1N1 that circulated prior to 1985, which lacked a glycosylation site near the 166 epitope (43, 55); namely, individuals who are over 30 years old.

Sequence analysis of variable heavy and light chain genes revealed that 1429B72/2-7 and 1429C45/1-5 share the VH3-7*01 gene, and somatic mutations are accumulated in 1429B72/2-7

compared with 1429C45/1-5. Together with the IC_{50} values against A(H1N1)pdm09 viruses, these data suggest that 1429B72/2-7 may have acquired its higher neutralizing activity via these accumulated somatic mutations. Nine human monoclonal antibodies, clones 4A10, 2O10, 4K8, 6D9, 2K11, SFV009-3F05, T2-9A, T2-6A, and T2-7D, which were reported to recognize the epitope around HA-166K of A(H1N1)pdm09 and to neutralize sH1N1 viruses isolated between 1986 and 2008, utilize the VH3-7*01 gene in combination with various DH, JH, VL, and JL genes (46-48). Although the Sa antigenic site could be recognized by human antibodies harboring various kinds of VH genes (56, 57), the VH3-7*01 gene might play an important role in developing an antibody specific for the epitope that includes position 166 of both sH1N1-HA that circulated between 1986 and 2008 and H1N1pdm09-HAs that circulated before 2013.

In conclusion, amino acid substitutions other than at position 166 in major antigenic site Sa can be selected by the immunological pressure of antibodies, such as 1429B72/2-7 and 1429C45/1-5, that recognize an epitope including position 166. In combination with computational analyses and other methods (58), in vitro selection of potential antigenic drift mutants may improve the selection of vaccine seed viruses.

CHAPTER II

Isolation and characterization of human monoclonal antibodies that recognize the influenza A(H1N1)pdm09 virus hemagglutinin receptor-binding site and rarely yield escape mutant viruses.

Abstract

The influenza A virus rapidly mutates to escape from antibodies. Here, I isolated and characterized three human monoclonal antibodies (mAbs) that neutralize A(H1N1)pdm09 viruses. Generation of escape mutant viruses suggested that these antibodies recognized conserved residues of the receptor-binding site (RBS) of hemagglutinin (HA) and that mutant viruses that escaped from these mAbs rarely appeared. Moreover, the escape mutant viruses grew significantly slower than wild-type virus, indicating their reduced fitness. These results indicate that these three human mAbs against the RBS of HA have the potential to be anti-influenza agents with a low propensity for the development of resistant viruses.

Introduction

The surface glycoprotein hemagglutinin (HA) of influenza virus mediates attachment to host cells via binding to its receptor, sialyloligosaccharides (60, 61). Antibodies against the immunodominant globular head of HA are generated after infection or vaccination (62). Previously, a panel of murine monoclonal antibodies was used to identify five antigenic sites (Sa, Sb, Ca1, Ca2, and Cb) on the H1-HA head domain (39, 41, 63).

Recently, structural analysis of monoclonal antibodies (mAbs) bound to HAs showed that the CDRH3 loop of the antibodies was inserted into the receptor-binding site (RBS), making a direct interaction with the conserved amino acid residues in the RBS (18, 64-71). Among these anti-RBS mAbs, C05, F045-092, and 2G1 interact with heterosubtypic HA (65, 72, 73). C05, which neutralizes pre2009H1, H2, H3, and H9 viruses in vitro, extends its CDRH3 loop to the RBS, resulting in direct inhibition of receptor binding (65). The CDRH3 of F045-092 mimics sialic acid to fit in the RBS of pre2009H1-, H2-, H3-, and H5-HA (73). 2G1 inhibits the hemagglutination activity of H2- and H3-HA by binding to the RBS (72). In addition, subtype-specific anti-RBS mAbs have also been reported (18-20, 69, 70, 72, 74-77). CH65, 1F1, and H2526 neutralize pre2009H1 virus (18, 19, 69), whereas 5J8, CH67, and 641 I-9 neutralize both pre2009H1 and H1pdm09 viruses (19, 20, 69). 8F8 and 8M2, H5.3, FLA5, FLD21, AVFluIgG03, and AVFluIgG01, or HNIgGA6 and HNIgGB5 specifically recognize the RBS of H3-HA (72), H5-HA (70, 74-76), or H7-HA (77), respectively. Among these RBS-binding antibodies, the frequency with generation of escape mutants (after five passages) has

been reported only for HNIgGA6 and HNIgGB5 (77).

Antiviral therapy can reduce the burden of seasonal influenza and provides the first line of defense against pandemic influenza before vaccines are available. Because the emergence of NA inhibitor-resistant viruses is always a concern, novel classes of anti-influenza agents are needed. Antibodies that bind to the functionally conserved residues within the RBS could fulfill the need for an anti-influenza agent with a low propensity for the development of resistant viruses. However, it is not clear how readily mutant viruses can escape from anti-RBS mAbs or whether such mutants are biologically fit to compete with wild-type viruses.

Here, I obtained three human mAbs that recognize the RBS of H1pdm09-HA and characterized their protective potential in vitro and in vivo. I also evaluated the ease with which escape mutant viruses emerged and their growth capability in vitro.

Results

Three human monoclonal antibodies recognizing H1pdm09-HA. PBMCs were obtained from human volunteers who were vaccinated with the 2014–2015 seasonal influenza vaccine (78) or with the influenza H5N1 pre-pandemic vaccine (79). These cells were then fused with fusion partner SPYMEG cells to generate hybridomas that expressed a human antibody. After screening by ELISA using recombinant H1pdm09-HA, positive hybridomas were biologically cloned. Eventually, I obtained three monoclonal antibodies: 1428A33/1 and 1428B5/1from volunteers that received the seasonal vaccine and F3A19 from a volunteer who received the H5N1 vaccine. The nucleotide sequences of the VH and VL regions of all three human mAbs were obtained, and the CDR3 sequences were analyzed to determine the closest germline gene by using the IgBlast software in the NCBI database (Table 6); 1428A33/1 used the IGHV2-70*01 germline gene and the IGLV3-9*01 germline gene, whereas 1428B5/1 and F3A19 used the IGHV4-39*01 and IGLV3-21*01 germline genes. The VH region of 1428A33/1 differed from the IGHV2-70*01 germline sequence by 2.4% (Table 6 and Fig. 6), whereas those of 1428B5/1 and F3A19 differed by 7.7% and 12.3% from the IGHV4-39*01 germline sequence, respectively.

Table 6. Genetic features of human mAbs that recognize A(H1N1)pdm09-HA.

mAb	Heavy chain			Light chain		
	VH [a]	Mismatches [b] (mutation rate, %)	CDR3 [c]	VL [d]	Mismatches (mutation rate, %)	CDR3
1428A33/1	IGHV2-70*01	7/297 (2.4)	ARYMYGDHVHYFDY	IGLV3-9*01	7/283 (2.5)	QVWDSNTEVV
1428B5/1	IGHV4-39*01	23/299 (7.7)	ARHLRGDTVGGVIDY	IGLV3-21*01	17/288 (5.9)	QVWDSGSDHVI
F3A19	IGHV4-39*01	34/300 (12.3)	ARVNRGWLPDKADWFDT	IGLV3-21*01	24/288 (8.3)	QVWDLSSDHVV

[a] Variable genes for the heavy chain.

[b] The sequences of the VH or VL regions of each mAb were compared with their germline sequence.

[c] Complementarity determining region 3.

[d] Variable genes for the light chain.

Figure 6. Sequence of the heavy chain variable regions. The VH regions of 1428A33/1 (A), 1428B5/1, and F3A19 (B) were compared with the indicated germline sequence. Dashes indicate no changes for the residue.

Binding and neutralization capability of the three mAbs. To determine the specificity of the binding activity of the three mAbs, I performed an ELISA using recombinant H1-, H3-, H5-, and H7-HA proteins. I found that 1428A33/1 and 1428B5/1 showed specific binding to H1pdm09-HA (OD_{405} values = 1.52 and 1.49, respectively), whereas F3A19 bound to pre2009H1-HA derived from a 2007 isolate, H5-HA, and H1pdm09-HA (OD_{405} values = 1.21–1.32, Table 7). CR9114, which recognizes the HA stem (49), bound to all HA proteins tested under the same experimental conditions (OD_{405} values = 1.03–1.32). Furthermore, I determined the binding kinetics of 1428A33/1, 1428B5/1, and F3A19 with H1pdm09-HA by using BLI and an Octet Red 96 instrument. 1428A33/1, 1428B5/1, F3A19, and CR9114 showed rapid binding to H1pdm09-HA with k_{on} values of 8.1×10^5, 7.9×10^5, 4.7×10^5, and 1.0×10^6 (1/Ms), respectively (Table 8). None of these mAbs detached from HA, resulting in k_{off} values of $< 1.0 \times 10^{-7}$ (1/s) (Table 8). Therefore, the K_D values of these four mAbs to H1pdm09-HA was less than 1.0×10^{-12} M, indicating that our mAbs exhibited high binding affinities, comparable to that of CR9114.

Next, I investigated whether these mAbs had in vitro neutralizing potency by using a microneutralization assay that included five H1N1pre2009 viruses, two A(H1N1)pdm09 viruses, and one H3N2 virus. Both 1428A33/1 and 1428B5/1 neutralized the two A(H1N1)pdm09 viruses, which were isolated in 2009 and 2015, respectively, with 50% inhibitory concentration (IC_{50}) values of 0.06–0.46 μg/ml (Table 9). Both mAbs failed to neutralize the H1N1pre2009 or H3N2 viruses even at the highest concentration (50 μg/ml) tested. F3A19 neutralized both the A(H1N1)pdm09 viruses and

H1N1pre2009 viruses isolated after 1988, with IC_{50} values of 0.14–0.62 μg/ml. CR9114 inhibited the replication of all viruses tested, yielding an IC_{50} value of 1.24–17.68 μg/ml under the same experimental conditions. These results indicate that F3A19 shows broader neutralization activity than 1428A33/1 and 1428B5/1, which possess similar neutralization capability.

Table 7. Reactivity of mAbs with different subtypes of HA.

mAb	OD_{405} values at 1 μg/ml of mAb					
	H1pre2009		H1pdm09[c]	H3 [d]	H5 [e]	H7 [f]
	1918 [a]	2007 [b]				
1428A33/1	0.03 [g]	0.02	1.52	0.04	0.02	0.01
1428B5/1	0.03	0.02	1.49	0.01	0.03	0.05
F3A19	0.02	1.23	1.21	0.05	1.32	0.02
CR9114	1.23	1.25	1.05	1.32	1.15	1.03

HA proteins were derived from [a]A/Brevig Mission/1/18, [b]A/Brisbane/59/2007, [c]A/California/07/2009, [d]A/Perth/16/2009, [e]A/Egypt/N05056/2009, and [f]A/Netherland/219/2003.

Table 8. Binding kinetics of mAbs with recombinant H1pdm09-HA.

mAb	k_{on} (1/Ms)	k_{off} (1/s)	K_D (M)
1428A33/1	8.1E + 5	<1.0E - 7	<1.0E - 12
1428B5/1	7.9E + 5	<1.0E - 7	<1.0E - 12
F3A19	4.7E +5	<1.0E - 7	<1.0E - 12
CR9114	1.0E + 6	<1.0E - 7	<1.0E - 12

Table 9. Neutralization activity of mAbs against influenza A viruses.

mAb	IC_{50} value (μg/ml) against							
	H1N1pre2009					A(H1N1)pdm09		H3N2
	1979 [a]	1980 [b]	1988 [c]	1992 [d]	2007 [e]	2009 [f]	2015 [g]	2009 [h]
1428A33/1	>50	>50	>50	>50	>50	0.06	0.46	>50
1428B5/1	>50	>50	>50	>50	>50	0.08	0.10	>50
F3A19	>50	>50	0.39	0.62	0.46	0.16	0.14	>50
CR9114	17.68	12.50	15.75	12.50	11.81	6.25	1.24	6.25

[a]A/Kumamoto/37/79, [b]A/Kamata/8/80, [c]A/Tokyo/913/88, [d]A/Minato/131/92, [e]A/Brisbane/59/2007, [f]A/California/04/2009, [g]A/Yokohama/94/2015, and [h]A/Perth/16/2009 were used in this experiment.

In vivo protection of mice by the three mAbs against lethal challenge. To evaluate the dose-dependent protective efficacy of 1428A33/1, 1428B5/1, and F3A19, I examined whether these three mAbs protected mice from lethal challenge with the A(H1N1)pdm09 virus. Each of our mAbs, CR9114, or anti-influenza B virus HA mAb 1430E3/9 at 15, 3, 0.6, or 0.12 mg/kg, or PBS was intraperitoneally administrated to four mice per group 24 h before challenge with the mouse-adapted A/California/04/2009 strain. 1428A33/1, 1428B5/1, and F3A19 protected all of the mice from death when dosed at 0.6 mg/kg or greater (Fig. 7A). At 0.12 mg/kg, 1428A33/1 partially protected mice, 1428B5/1 completely protected mice, and F3A19 failed to protect the mice. Most mice that received the 0.6 mg/kg or greater dose of CR9114 survived the 14-day observation period. All mice that received PBS or 1430E3/9 died within 10 days of the challenge. Furthermore, I assessed virus titers at 3 and 6 days post-infection in the nasal turbinates and lungs of infected mice that received each mAb at 3 mg/kg. On day 3 post-infection, virus titers in the lungs of infected mice that received 1428B5/1 or F3A19 were significantly lower than those in the lungs of mice that received the negative control 1430E3/9 (Fig. 7B). On day 6 post-infection, mice that received 1428A33/1, 1428B5/1, or F3A19 had significantly lower virus titers in the lungs than mice that received 1430E3/9 (Fig. 7B). In the nasal turbinates, virus titers were not affected by administration of any mAb. These results demonstrate that 1428A33/1, 1428B5/1, and F3A19 directly suppress virus propagation following lethal infection with A(H1N1)pdm09 virus.

Next, I examined the protective efficacy of F3A19 against H5N1 and H1N1pre2009 viruses,

since F3A19 recognized H1pre2009-HA and H5-HA in our ELISA. F3A19, CR9114, or 1430E3/9 at 3 mg/kg was intraperitoneally administered to mice. One day later, the mice were intranasally infected with 10 MLD_{50} of the H5N1 virus or 10^6 PFU of the H1N1pre2009 virus. Body weights of four mice per group were monitored daily for 14 days, and three mice per group were euthanized on days 3 and 6 post-infection for virus titrations of the nasal turbinates and lungs. F3A19 partially protected mice from lethal infection with H5N1 virus, whereas all mice that received 1430E3/9 died within 10 days of the challenge infection (Fig. 8A). F3A19 reduced virus titers of H5N1 virus in nasal turbinates on day 6 post-infection (Fig. 8B). In addition, F3A19 significantly suppressed the body weight loss of mice infected with H1N1pre2009 virus (Fig. 8A), and suppressed H1N1pre2009 virus propagation in the lungs of mice on day 6 (Fig. 8C). Taken together, these results suggest that F3A19 broadly protects mice from infection with group 1 viruses (e.g., A(H1N1)pdm09, H5N1, and H1N1pre2009 viruses) albeit with less efficacy against H5N1 virus than the other viruses.

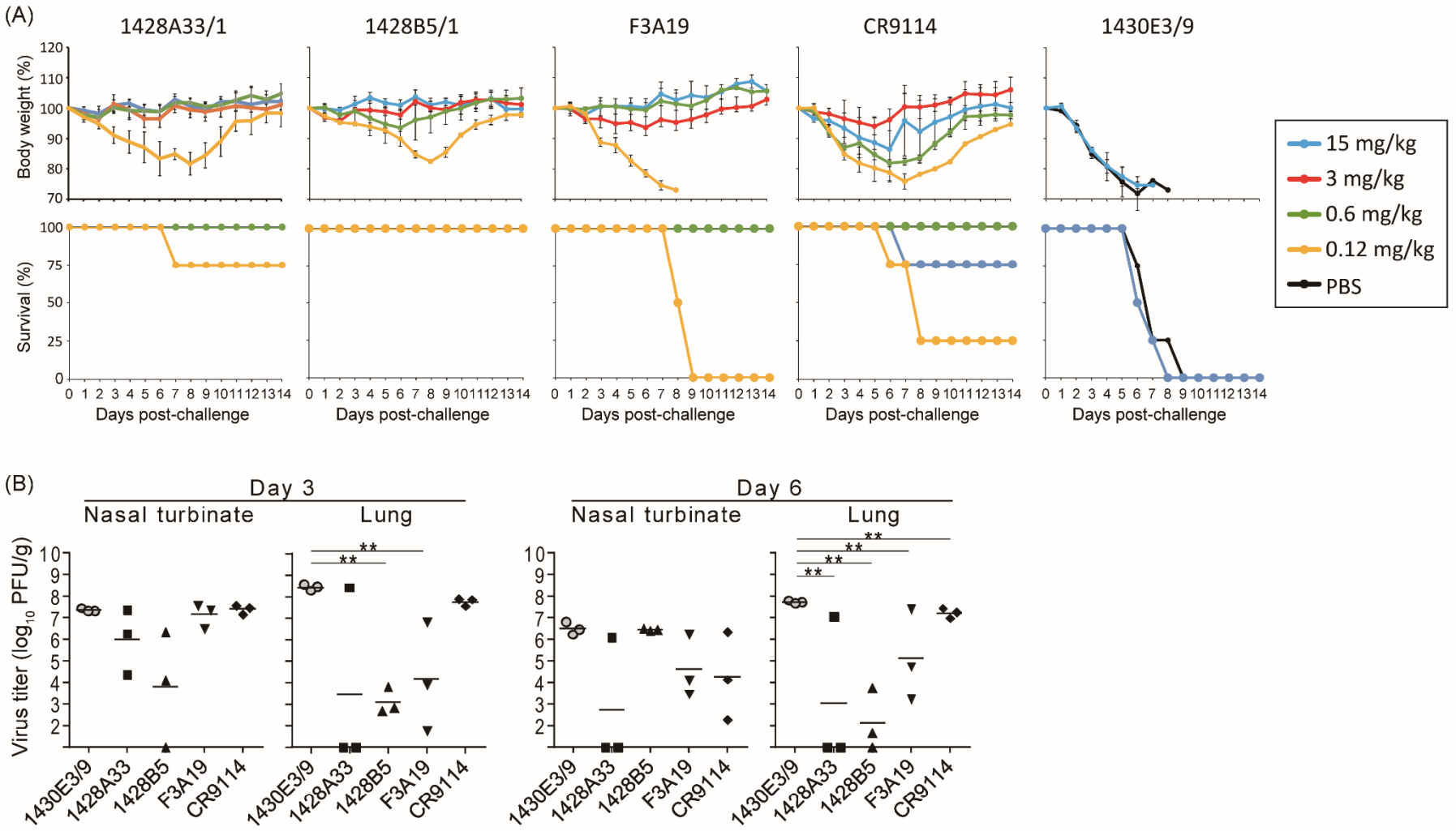

Figure 7. In vivo protective activity of mAbs. (A) Four mice per group were intraperitoneally injected with PBS or the indicated antibodies at 15, 3, 0.6, or 0.12 mg/kg. One day later, the mice were challenged with 10 MLD50 of MA-CA04 virus. Body weight and survival were monitored daily for 14 days. CR9114 and 1430E3/9 were used as a positive control and a negative control antibody, respectively. Mouse body weights are expressed as mean ± SD. (B) Three mice per group were intraperitoneally injected with the indicated antibodies at 3 mg/kg. One day later, the mice were challenged with 10 MLD50 of MA-CA04 virus. On days 3 and 6 post-infection, virus titers in the nasal turbinates and lungs were examined. **P < 0.01 (one-way ANOVA followed by Dunnett' s tests)

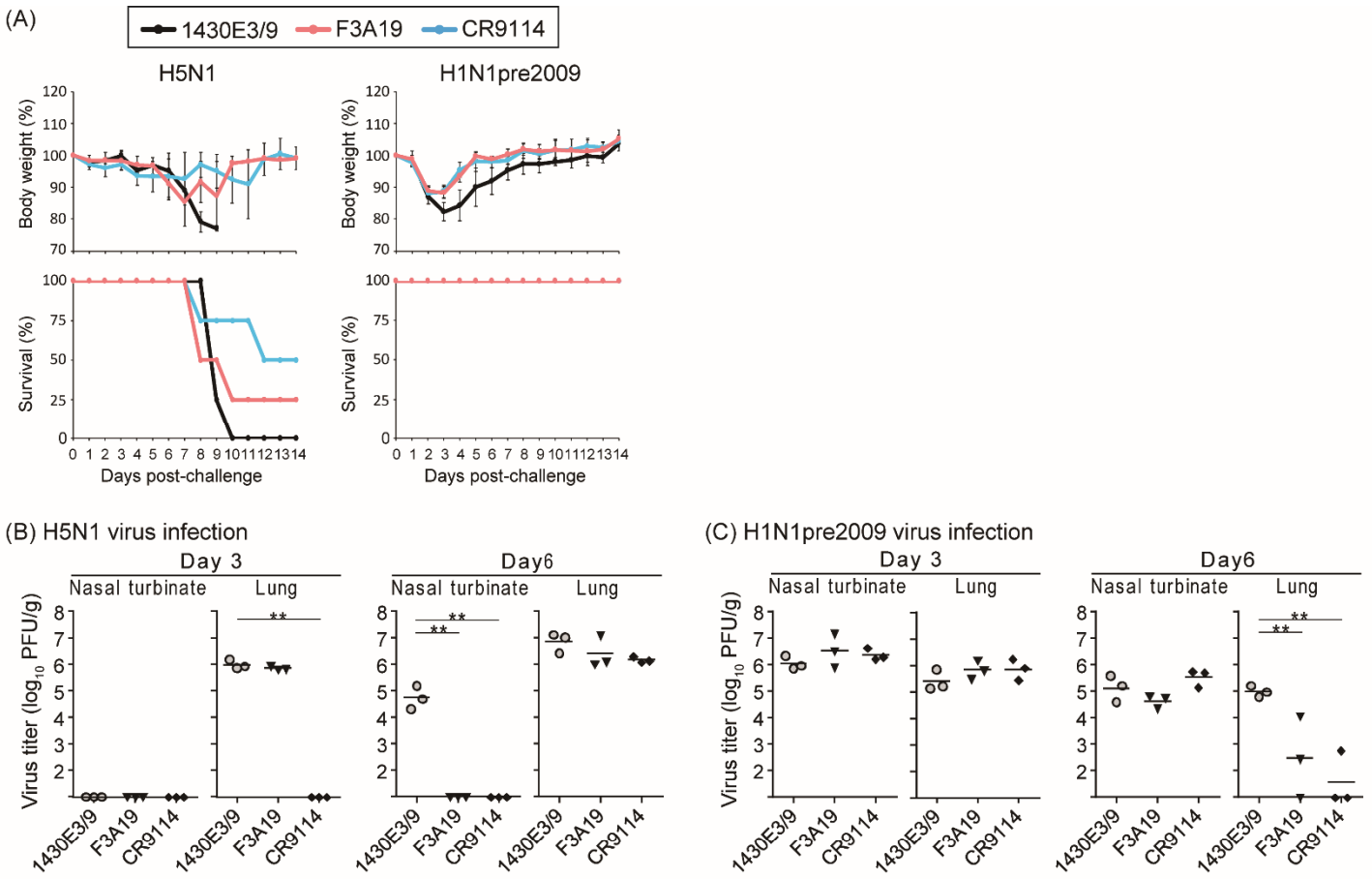

Figure 8. In vivo protective efficacy of F3A19 against H5N1 and H1N1pre2009 viruses. (A) Four mice per group were intraperitoneally injected with F3A19, 1430E3/9, or CR9114 at 3 mg/kg. One day later, the mice were intranasally challenged with 10 MLD50 of the H5N1 virus (A/Vietnam/1203/2004) or 106 PFU of the H1N1pre2009 virus (A/Brisbane/59/2007). Body weight was monitored daily for 14 days. CR9114 and 1430E3/9 were used as a positive control and a negative control, respectively. Mouse body weights are expressed as means ± SD. ** indicates $P < 0.01$ (two-way ANOVA followed by Dunnett' s tests). (B and C) Three mice per group were intraperitoneally injected with the indicated antibodies at 3 mg/kg. One day later, the mice were challenged with 10 MLD50 of the H5N1 virus (B) or 106 PFU of the H1N1pre2009 virus (C). On days 3 and 6 post-infection, virus titers in the nasal turbinates and lungs were determined. **$P < 0.01$ (one-way ANOVA followed by Dunnett' s tests)

Mutations that permit escape from 1428A33/1, 1428B5/1, and F3A19. I attempted to select escape mutant viruses in triplicate (I called them lines 1, 2 and 3) by passaging CA04 virus in the presence of various mAb concentrations to identify the epitopes of 1428A33/1, 1428B5/1, and F3A19. Although mutant viruses that escaped from human mAbs against the Sa antigenic site were obtained previously by 3–15 passages, as described elsewhere (78), at least one out of the three lines did not escape from 1428A33/1, 1428B5/1, or F3A19 even after 30 passages in the presence of each mAb (Table 10). When escape mutants were obtained, 9–25 passages were required. Given that escape mutants were obtained from the anti-RBS mAbs HNIgGA6 and HNIgGB5 after five passages (77), I conclude that it is relatively challenging for viruses to escape from our three mAbs.

To identify mutations that occurred during passages, I analyzed the nucleotide sequences of the HA, NA, PB2, PB1, and PA proteins by direct sequencing (Table 10). I found that escape mutant 1428A33/1 line 1 possessed the K125E, D190V, and D348Y mutations in its HA and that 1428B5/1 line 3 possessed the G143E and K145E mutations in its HA (Table 10). F3A19 line 1 or line 2 possessed the A137T, K145E, and D190V mutations, or the K125N, A137T, S165N, A189T, D190N, and S193N mutations, respectively. In addition, 1428A33/1 lines 1 and 2 had the K125N mutation, and the A189D and E501K mutations in the HA, respectively. 1428B5/1 line 2 possessed the K125N and D366E mutations, whereas F3A19 line 3 possessed the K125N and S193R mutations. 1428B5/1 line 1 had no mutations in its HA even after 30 passages. In other segments, amino acid mutations were found in the PB2, PB1, or PA proteins of seven virus lines and mutations in the NA protein were detected in five

lines (Table 10).

To confirm that the passaged viruses indeed escaped from the mAbs, I generated mutant CA04 viruses possessing substitutions in HA that were found in each passaged virus and the seven remaining wild-type segments by use of reverse genetics and performed the neutralization assay. Mutant viruses possessing the substitutions K125E+D190V+D348Y (found in 1428A33/1 line 1), G143E+K145E (1428B5/1 line 3), A137T+K145E+D190V (F3A19 line 1), or K125N+A137T+S165N+A189T+D190N+S193N (F3A19 line 2) in their HA grew well even in the presence of the highest concentrations of mAbs (Table 11), indicating that these mutations were important for escape from the mAbs. Of note, the mutant virus with the G143E+K145E substitutions (1428B5/1 line 3) in HA escaped from 1428A33/1 and the mutant virus with the A137T+K145E+D190V substitutions (F3A19 line 1) in HA was resistant to both 1428A33/1 and 1428B5/1. Other passaged viruses showed similar IC_{50} values against the homologous mAbs to that of the wild-type virus. These results suggest that some of the mutations found in the escape mutants may be responsible for their resistance to the mAbs.

To determine which amino acid substitutions contributed to escape from each mAb, I prepared mutant CA04 viruses possessing single amino acid substitutions and investigated their sensitivity to each mAb. 1428A33/1 failed to neutralize mutant virus possessing the D190V or K145E substitution, and 1428B5/1 failed to neutralize virus possessing the K145E substitution (Table 12). Although the IC_{50} values of F3A19 against the mutant viruses possessing A137T, D190V, or D190N were higher

than against wild-type virus, these single amino acid substitution mutant viruses were neutralized by the mAbs with IC50 values of less than 19.8 μg/ml. Therefore, I generated mutant viruses possessing the double mutations of A137T and D190V or D190N and then tested the neutralization capability of F3A19 against these double mutant viruses. F3A19 failed to neutralize the double mutant viruses even at the highest concentration tested (Table 12). Similarly, the double mutant viruses were not neutralized by either 1428A33/1 or 1428B5/1. These results demonstrate that amino acid mutations at positions 137, 145, and 190 play an important role in escape from 1428A33/1, 1428B5/1, and F3A19. To visualize these positions, I mapped these residues on the HA molecule (Fig. 9). The amino acids at positions 137 and 190 are located in the 130-loop and the 190-helix of the RBS (80, 81), respectively. The amino acid at position 137 is also found near the RBS, suggesting that 1428A33/1, 1428B5/1, and F3A19 target the RBS of HA.

Table 10. Amino acid substitutions in HA, NA, PB2, PB1, and PA of viruses passaged in the presence of mAbs.

Escaped from	Virus line [a]	Passage number	Amino acid substitution(s) in				
			HA [b]	NA [c]	PB2	PB1	PA
1428A33/1	1	10 [d]	K125E+D190V+D348Y	-	-	-	T32N
	2	30 [e]	K125N	-	D680N+D740N	-	-
	3	30	A189D+E501K	G27E	-	-	-
1428B5/1	1	30	- [f]	K111N	T751N	-	-
	2	30	K125N+D366E	-	-	N533S+V640I	T162S+I483L+I592V
	3	15	G143E+K145E	E119K	-	-	-
F3A19	1	9	A137T+K145E+D190V	S153I	-	-	N222S
	2	25	K125N+A137T+S165N +A189T+D190N+S193N	-	-	R220K	I554M
	3	30	K125N+S193R	S341F	-	I164V+M339I	-

[a] Lines 1–3 were independently obtained.

[b] H3 numbering.

[c] N2 numbering.

[d] The passage number at which escape mutants were obtained.

[e] The passage was aborted when escape mutants did not emerge by 30 passages.

[f] '-' indicates that no mutation occurred.

Table 11. Neutralization activity against mutant viruses possessing amino acid substitutions in HA.

mAb	**IC_{50} value (μg/ml) against mutant viruses possessing amino acid substitutions found after passaging viruses in the presence of**								
	1428A33/1			1428B5/1		F3A19			Wild-type CA04 [a]
	K125E+D190V +D348Y	K125N	A189D +E501K	K125N +D366E	G143E +K145E	A137T+K145E +D190V	K125N+A137T+S165N+ A189T+D190N+S193N	K125N +S193R	
1428A33/1	>50	0.10	0.14	0.10	>50	>50	14.7	0.28	0.06
1428B5/1	0.39	0.11	0.55	0.14	>50	>50	0.55	0.06	0.08
F3A19	19.3	0.14	0.11	0.62	25	>50	>50	0.16	0.16
CR9114	4.96	9.92	7.87	4.96	1.83	1.56	6.25	1.83	6.25

[a] IC_{50} values against the parental virus are from Table 9.

Table 12. Neutralization activity of mAbs against variant viruses with each escape mutation.

mAb	**IC_{50} value (μg/ml) against variant viruses each possessing amino acid substitutions of escape mutants obtained from:**												
	1428A33/1			1428B5/1		F3A19							
	K125E	D190V[a]	D348Y	G143E	K145E[a]	A137T	K125N	S165N	A189T	D190N	S193N	A137T+ D190V	A137T+ D190N
1428A33/1	0.11	>50	0.12	0.16	>50	0.14	0.28	0.14	0.16	17.7	0.28	>50	>50
1428B5/1	0.25	0.39	0.14	0.11	>50	0.28	0.11	0.10	0.14	0.49	0.10	>50	>50
F3A19	0.29	10.6	0.14	0.06	0.14	1.39	0.49	0.16	0.14	19.8	0.11	>50	>50
CR9114	7.87	9.92	2.48	2.48	3.94	3.94	1.24	1.24	1.97	2.48	6.25	0.98	4.42

[a] Escape mutants obtained from F3A19 also possessed the indicated mutation.

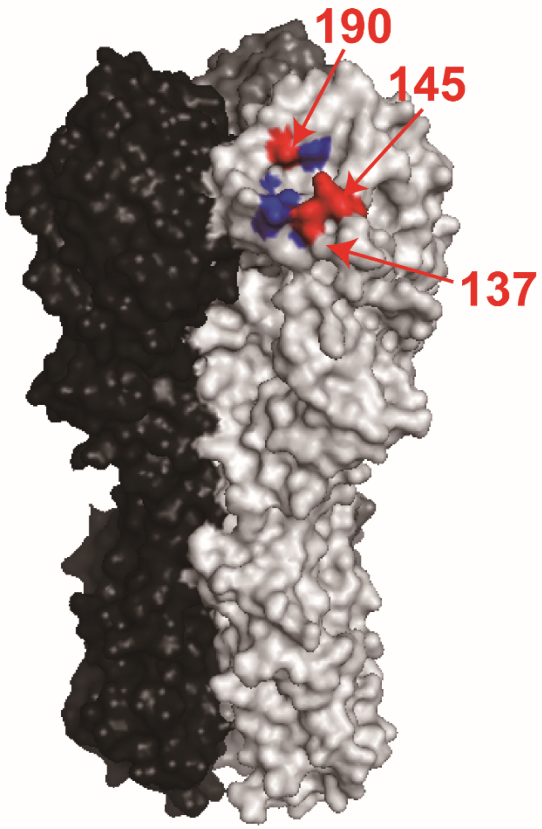

Figure 9. Positions of escape mutations on the HA molecule. Blue indicates the residues involved in receptor binding. Red indicates the amino acid positions involved in escape from 1428A33/1, 1428B5/1, and F3A19. These amino acids are shown on the HA of A/California/04/2009. Each HA monomer is indicated in white, gray, and black.

Growth kinetics of the escape mutant viruses in vitro. To examine the fitness of the viruses possessing mutations that allowed them to escape from 1428A33/1, 1428B5/1, and F3A19, I compared the growth kinetics of mutant viruses possessing the escape mutations (i.e., HA-D190V, -K145E, -A137T+D190V, or -A137T+D190N) in A549 and MDCK cells with those of the wild-type virus. All mutant viruses tested replicated to significantly lower titers than the wild-type virus at 24–72 hpi (Fig. 10). These results demonstrate that the fitness of the escape mutants was decreased.

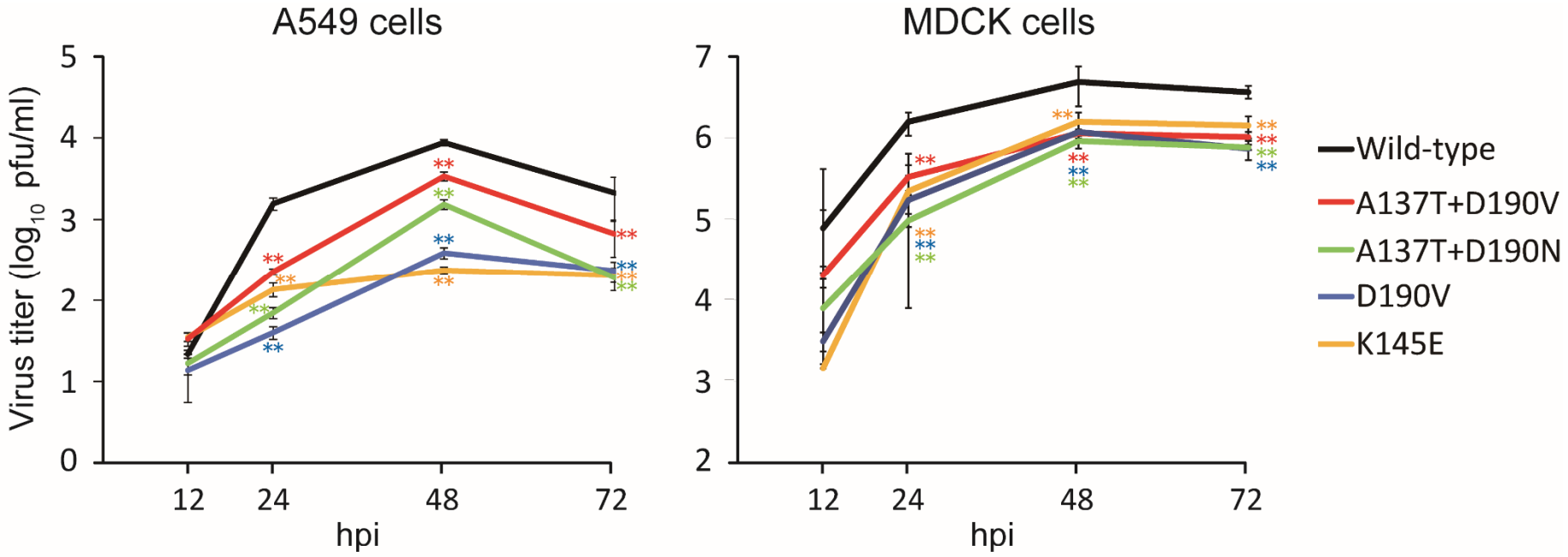

Figure 10. Growth kinetics of wild-type and escape mutant viruses. The growth kinetics of the wild-type CA04 virus and the indicated mutant viruses in A549 cells and MDCK cells were compared. Cell culture supernatants of A549 and MDCK cells infected at an MOI of 0.0001 were collected at 12, 24, 48, and 72 hpi. Virus titers are presented as the mean ± SD (n=3). **P < 0.01 (two-way ANOVA followed by Dunnett' s tests).

Serum neutralization titers of vaccinated individuals against escape mutant viruses. To examine the proportion of antibodies that recognize epitopes similar to those recognized by the mAbs characterized in this study (i.e., 1428A33/1, 1428B5/1, and F3A19) in the individuals from whom I generated the mAbs (SeaV-28 and H5V-3, Table 13), I examined the neutralization titers against escape mutant viruses of sera from the two individuals. The virus neutralization assay revealed that the neutralizing activity of these sera against escape mutant viruses was similar to that against the wild-type virus (Table 13). These results suggest that antibodies that target epitopes similar to those recognized by mAbs 1428A33/1, 1428B5/1, and F3A19 are not predominant in these individuals.

Table 13. Virus neutralization titers of sera from the two individuals from whom mAbs were isolated.

Volunteer ID[a]	Neutralization titer against the CA04 virus possessing HA of				
	Wild-type	D190V	K145E	A137T+D190V	A137T+D190N
SeaV-28	1024	512	512	1024	512
H5V-3	256	128	128	128	128

[a] Serum samples were taken 30 day after vaccination.

Discussion

Here, I obtained three human mAbs that recognize the RBS of HA: 1428A33/1 and 1428B5/1 were specific to H1pdm09-HA, whereas F3A19 recognized both H1pdm09- and H5-HA. I passaged viruses 9–25 times to obtain escape mutants and in some instances failed to obtain such mutants even after 30 passages. Although information about the frequency with which mutant viruses escape from anti-RBS mAbs is limited, one report indicated that such viruses escaped from HNIgGA6 and HNIgGB5 after only five passages (77). Therefore, compared with HNIgGA6 and HNIgGB5, our results suggest that it is more difficult for viruses resistant to our three mAbs to emerge. Furthermore, the escape mutant viruses showed significantly less efficient replication in vitro, indicating that mutant viruses that are able to escape from these three anti-RBS mAbs would be unlikely to dominate the parental viruses. Given that the potential emergence of escape mutant viruses is one of the main disadvantages of mAbs as antiviral treatments, mAbs such as ours that rarely produce escape mutant viruses should be useful as protective antibodies.

The human mAb 5J8, which recognizes the RBS of H1pdm09-HA, shares the epitope at positions 137, 145, and 190 with our anti-RBS mAbs (20, 70). Since 5J8 neutralizes a broad array of H1N1 viruses isolated between 1918 and 2009, the exact binding mode of our mAbs should be compared to that of 5J8 by co-crystal structure analysis. Such an analysis may reveal structural reasons why the breadth of reactivity of these mAbs differs.

The amino acids at positions 145 and 190 are located in the Ca and Sb antigenic sites,

respectively (39-42), which are the major targets of neutralizing antibodies, suggesting that these amino acids are exposed to the selective pressure of human neutralizing antibodies. Nevertheless, lysine at position 145 (99.5%) and aspartic acid at position 190 (99.7%) are highly conserved among the 18,308 A(H1N1)pdm09 viruses whose HA sequences are available in the GISAID database, suggesting functional and/or structural restrictions at positions 145 and 190. Among field isolates, viruses possessing mutations at position 145 or 190 have occasionally been reported but such viruses have not spread extensively most likely due to reduced fitness in humans. These data further support the usefulness of our three mAbs as protective antibodies.

F3A19 was isolated from a healthy donor who received the pre-pandemic H5N1 vaccine. In a previous study that analyzed antibodies obtained from individuals vaccinated with the H5 vaccine, human mAbs that were specific to H5 had fewer mutations (an average of 12.3 amino acid substitutions in the heavy variable domain) than mAbs recognizing heterosubtypic HA (an average of 21.6 amino acid substitutions in the heavy variable domain) (71). Other studies have shown that broadly reactive mAbs likely arise through stimulation of memory B cells since these mAbs possess significantly more mutations (82, 83). In the heavy variable region of F3A19, which recognized both H1- and H5-HA, 20 amino acid changes from the germline sequence were observed, suggesting that this mAb was stimulated by memory B cells and not newly induced by H5 vaccination.

The epitopes of anti-RBS human mAbs have been studied by using various methods. The epitopes of 13 anti-RBS mAbs (C05, F045-092, 2G1, CH65, 1F1, H2526, 5J8, CH67, 641 I-9, 8F8,

8M2, H5.3, and HNIgGA6) were identified by structural analysis (18, 64-71), and those of other mAbs (FLA5, FLD21, AVFluIgG03, AVFluIgG01, and HNIgGB5) were investigated by using whole-genome–fragment phage display libraries or evaluating reactivity to mutated HA proteins (74, 76, 77). Among them, mutant viruses that escaped from six anti-RBS mAbs (5J8, 8F8, 8M2, 2G1, HNIgGA6, and HNIgGB5) were isolated and characterized previously (20, 72, 77). The escape mutants selected from these mAbs possessed one or two substitutions in their HA, whereas escape mutants selected from our mAbs possessed two to six substitutions in HA. Among the mutations found in the passaged viruses, only one or two mutations were responsible for escape from our mAbs. Since the mutant viruses possessing escape mutations replicated to significantly lower titers than the wild-type virus, additional mutations in HA might contribute to emergence of mutant virus escaped from our mAbs.

The replication of escape mutant viruses in MDCK cells was similar, whereas that in A549 cells differed (Fig. 10). An escape mutation at position 137, 145, or 190 of HA affects the binding properties of the H1N1 virus to the cellular receptor (84, 85). Therefore, the growth of escape mutant viruses might be affected by the amount and balance of α2,3-linked and α2,6-linked sialic acids on the cells; the expression of α2,3-linked and α2,6-linked sialic acids on MDCK cells differs from that on A549 cells (86, 87).

Co-crystal structure analysis revealed that some mAbs that recognize the RBS utilize an aspartic acid residue of HCDR3 to insert a carboxylate in the RBS that would be occupied by the carboxylate of the sialic acid of the alpha-2,6 sialoglycan receptor (66, 70, 71, 88, 89). Clone 5J8

inserts a proline of HCDR3 into a universally conserved hydrophobic pocket in the RBS. 1428A33/1, 1428B5/1, and F3A19 possess aspartic acid in each HCDR3, and F3A19 possesses proline in HCDR3, suggesting that the mAbs in our study may bind to the RBS by the mode of receptor mimicry that has been observed with previously reported anti-RBS mAbs (18, 66, 70, 90).

In conclusion, mutant viruses that could escape from 1428A33/1, 1428B5/1, or F3A19 were difficult to obtain in vitro. Moreover, the escape mutants that did emerge showed significantly less efficient replication than their wild-type counterparts. These findings show the potential of the three mAbs obtained in this study as antiviral agents and provided information for the design of a universal vaccine.

CHAPTER III

Antigenic drift originating from changes to the lateral surface of the neuraminidase head of influenza A virus.

Abstract

Influenza viruses possess two surface glycoproteins, hemagglutinin (HA) and neuraminidase (NA). Although HA plays a major role as a protective antigen, immunity to NA also contributes to protection. The NA protein consists of a stalk and a head portion, the latter of which possesses enzymatic NA (or sialidase) activity. Like HA, NA is under immune pressure, which leads to amino acid alterations and antigenic drift. The amino acid changes accumulate around the enzymatic active site, which is located at the top of the NA head. However, amino acid alterations also accumulate at the lateral surface of the NA head. The reason for this accumulation remains unknown. Here, I isolated seven anti-NA monoclonal antibodies (mAbs) from individuals infected with A(H1N1)pdm09 virus. I found that amino acid mutations on the lateral surface of the NA head abolished the binding of all of these mAbs. All seven mAbs activated Fcγ receptor (FcγR)-mediated signaling pathways in effector cells, and five of the mAbs possessed neuraminidase inhibition (NI) activity, but the other two did not; yet all seven protected mice from lethal challenge infection via their NI activity or FcγR-mediated antiviral activity or both. Serological analysis of individuals who were infected with A(H1N1)pdm09 virus revealed that some possessed or acquired the anti-NA lateral surface antibodies upon infection. I also found antigenic drift on the lateral surface of the NA head between 2009 isolates and 2015 isolates. Our results demonstrate that anti-lateral surface mAbs without NI activity can provide protection by activating FcγR-mediated antiviral activity and can drive antigenic drift at the lateral surface of the NA head. These findings have implications for NA antigenic characterization in that they demonstrate that

traditional neuraminidase inhibition assays are inadequate to fully characterize NA antigenicity.

Introduction

Influenza A virus harbors two major glycoproteins on its envelope: hemagglutinin (HA) and neuraminidase (NA). HA and NA play pivotal roles in both the early and late stages of the virus replication cycle. HA binds to cellular receptors (sialic acid) on the cell surface to initiate entry (60, 61), while the enzymatic activity of NA cleaves off the sialic acid, allowing release of progeny viruses from the cell surface (9, 10). The enzymatic activity of NA also contributes to virus entry by removing receptor decoys that present in the airways (92).

Antibodies against HA and NA are elicited upon influenza virus infection in infected individuals (31, 93-95). Antibodies against the head region of HA inhibit virus attachment to the receptor primarily by preventing receptor binding (62) and those against the stem region of HA inhibit viral fusion or egress (79, 80, 96). Although antibodies to HA are typically considered the mediators of protection from influenza virus infection, some studies have indicated the importance of anti-NA antibodies for protection (27-31). Among the NA-specific monoclonal antibodies (mAbs), some restrict virus spread by interfering with virus NA activity, resulting in aggregation of progeny virions on the cell surface. Such neuraminidase-inhibiting (NI) antibodies are known to reduce viral load and symptoms in infected mice, ferrets, and humans (27, 28, 97-100). Although the major antiviral ability of anti-NA antibodies seems to be its NI activity, one study reported that, for in vivo protection, a broadly reactive NI mAb required Fc-FcγR interactions (between an Fc region of IgG and Fcγ receptors (FcγRs)) to activate effector cells such as natural killer (NK) cells, macrophages, and neutrophils (101).

NK cells express FcγRIIIa (102) and macrophages and neutrophils expressed FcγRIIa (103, 104). The activated NK cells, macrophages, and neutrophils suppress virus propagation via antibody-dependent cellular cytotoxicity (ADCC), antibody-dependent cellular phagocytosis (ADCP), and antibody-dependent neutrophil-mediated phagocytosis (ADNP), respectively (105, 106). This study suggested the possibility that anti-NA mAbs could trigger FcγRs-mediated effecter cell activation to promote in vivo protection. These functions have been studied by analyzing anti-NA mAbs that possess NI activity and recognize epitopes around the enzymatic center of the NA head. However, the contribution of anti-NA antibodies that recognize regions other than those near the enzymatic center remains unknown.

To evade neutralizing antibodies, influenza viruses with amino acid changes in the epitopes of the major surface proteins (HA and NA) emerge (antigenic drift) (107-109). Similar to the antigenic drift of HA, the antigenicity of NA changes as a result of amino acid mutations in the NA head that allow escape from anti-NA antibodies (110, 111). Several amino acid changes that allow viruses to escape from NI antibodies have been mapped around the enzymatic center of the NA head (112). However, amino acid substitutions also accumulate at the lateral surface of the NA head, which is far from the enzymatic center, (112); the reason why mutations accumulate in this region remains unknown.

Here, I obtained seven mAbs that recognize the lateral surface of the NA head from two individuals naturally infected with A(H1N1)pdm09 virus during the 2015–2016 influenza season, and characterized these mAbs to understand their properties, particularly their roles in in vivo protection

and antigenic drift.

Results

Isolation of human monoclonal antibodies that recognize A(H1N1)pdm09 virus. Peripheral blood mononuclear cells (PBMCs) were obtained from two human volunteers who were infected with A(H1N1)pdm09 virus during the 2015–2016 influenza season. The PBMCs were fused with SPYMEG cells to generate hybridomas that express a human antibody. After several rounds of screening by ELISA using purified A/California/04/2009 (CA/04/09) virus and A/Yokohama/94/2015 (YO/94/15) virus, which were isolated during the first wave of the 2009 pandemic and in the 2015–2016 season, respectively, and classified into the genetic clades 1 and 6B.1 based on their respective HA sequences, hybridomas expressing antibodies bound to YO/94/15 virus but not to CA/04/09 virus were biologically cloned. Of 701 hybridomas screened, I obtained seven clones (DA05C23, HP02C70, DA05B02, HP02B69, HP02E74, HP02E63, and HP02B24) that expressed a monoclonal antibody (mAb) specific to YO/94/15 virus. Nucleotide sequence analysis of their variable regions revealed that all seven mAbs used the same VH gene (IGHV3-15*01), although the CDR3 sequence of each heavy chain varied (Table 14). Five mAbs used IGLV3-1*01, whereas HP02B24 and HP02E63 used IGLV3-21*01 and IGLV6-57*01, respectively.

Table 14. Genetic features of human mAbs that recognize A(H1N1)pdm09-NA

mAb	Heavy chain		Light chain	
	VH[a]	CDR3[b]	VL[c]	CDR3
DA05C23	IGHV3-15*01	TTDSYDLLTGFHRPGLFAS	IGLV3-1*01	QAWDSSTVV
HP02C70	IGHV3-15*01	TNDDFNWKYGVAY	IGLV3-1*01	QAWDTSTGV
DA05B02	IGHV3-15*01	TTDSFNWNYGMDV	IGLV3-1*01	QAWDTNIVV
HP02B69	IGHV3-15*01	TTAGQWLYYDHMDV	IGLV3-1*01	QAWDSSTVV
HP02E74	IGHV3-15*01	TTGPYWTHNDY	IGLV3-1*01	QAWDSSIVV
HP02E63	IGHV3-15*01	TTDPPPYCGHDCYSSY	IGLV6-57*01	QSYDTSNHLI
HP02B24	IGHV3-15*01	TTEILRGVNDAFNM	IGLV3-21*01	QVWDSITDHYV

[a] Variable genes for the heavy chain

[b] Complementarity determining region 3

[c] Variable genes for the light chain.

The seven human mAbs mainly recognize the NA of A(H1N1)pdm09 virus isolated in the 2015–16 influenza season. To determine the breadth of recognition of the seven mAbs I obtained, I performed an ELISA using A(H1N1)pre2009, A(H3N2), and YO/94/15 viruses. None of the mAbs recognized A(H1N1)pre2009 or A(H3N2) virus (Fig. 11A). A broadly reactive human anti-N1-NA mAb clone 1000-3C05 (95, 101) bound to A(H1N1)pre2009 and YO/94/15 viruses, whereas the broadly reactive human anti-HA stem mAb clone CR9114 (49) recognized all three viruses tested (Fig. 11A). A negative control, anti-B HA 1430E3/9, did not bind to any of these viruses. These results indicate that the seven mAbs isolated here are specific to A(H1N1)pdm09 virus. Next, I performed an ELISA using A(H1N1)pdm09 viruses isolated during different influenza seasons. HP02C70, DA05B02, HP02E74, HP02E63, and HP02B24 showed specific binding to YO/94/15 virus, whereas HP02B69 and DA05C23 bound preferentially to YO/94/15 virus and weakly to A/Osaka/6/2014 virus (Fig. 11B). EM-3C02, which was reported to be a strain-specific human anti-N1-NA mAb (95, 101), bound to CA/04/09 and A/Hiroshima/66/2011 viruses, whereas the broadly reactive mAb 1000-3C05 recognized all viruses tested. The anti-influenza B HA mAb clone 1430E3/9 failed to recognize any of the viruses tested. These results indicate that the seven mAbs obtained are not broadly reactive but mainly recognize YO/94/15 virus.

To determine which viral protein was recognized by these mAbs, I performed an ELISA using purified reassortant viruses possessing HA and NA derived from YO/94/15 or CA/04/09 virus. All seven mAbs bound to viruses possessing NA derived from YO/94/15 virus, whereas EM-3C02

recognized a virus possessing NA derived from CA/04/09, but not YO/94/15, virus (Fig. 11C). 1000-3C05 detected all of the viruses tested. These results demonstrate that these seven human mAbs are against the NA of A(H1N1)pdm09 virus.

I next determined the binding affinity of the seven mAbs to NA derived from YO/94/15 virus by use of a Scatchard analysis (Fig. 12). DA05C23 and HP02C70 possessed high binding affinities (K_D = 0.86 and 0.73 nM, respectively), which were comparable to that of 1000-3C05 (K_D = 0.82 nM). However, DA05B02, HP02B69, HP02E74, HP02E63, and HP02B24 showed relatively lower binding affinities than that of 1000-3C05 (K_D = 2.57, 3.24, 4.18, 3.22, and 3.62 nM, respectively).

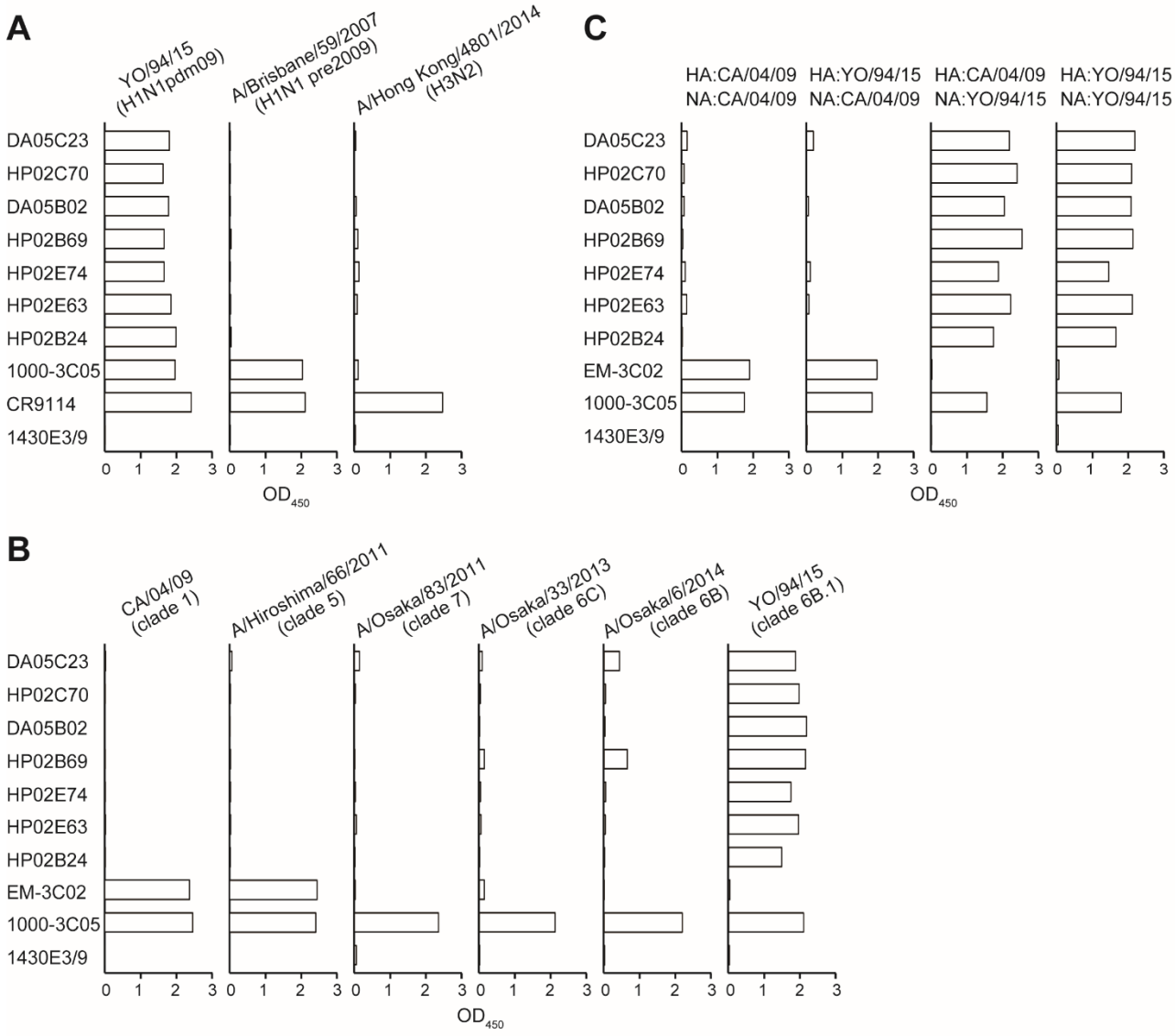

Figure 11. Breadth of reactivity of seven isolated mAbs. (A) The breadth of mAb recognition was examined in an ELISA using purified YO/94/15, A(H1N1)pre2009, and A(H3N2) viruses. Binding is shown as the OD450 value. 1000-3C05 broadly binds to N1-NA. CR9114, which targets the HA stem, and 1430E3/9, which recognizes the HA of influenza B virus, were used as positive and negative controls, respectively. (B) The reactivity of mAbs against six A(H1N1)pdm09 viruses [CA/04/09 (clade 1), A/Hiroshima/66/2011 (clade 5), A/Osaka/83/2011 (clade 7), A/Osaka/33/2013 (clade 6C), A/Osaka/6/2014 (clade 6B), and YO/94/15 (clade 6B.1) viruses] isolated in different influenza seasons was evaluated by ELISA. Binding is shown as the OD450 value. EM-3C02 specifically binds to the NA of A(H1N1)pdm09 virus. (C) The viral protein targeted by the isolated mAbs was determined by use of an ELISA using purified reassortant viruses, harboring HA and NA segments derived from YO/94/15 or CA/04/09 virus. Binding is shown as the OD450 value. All ELISAs were performed twice independently and yielded similar results.

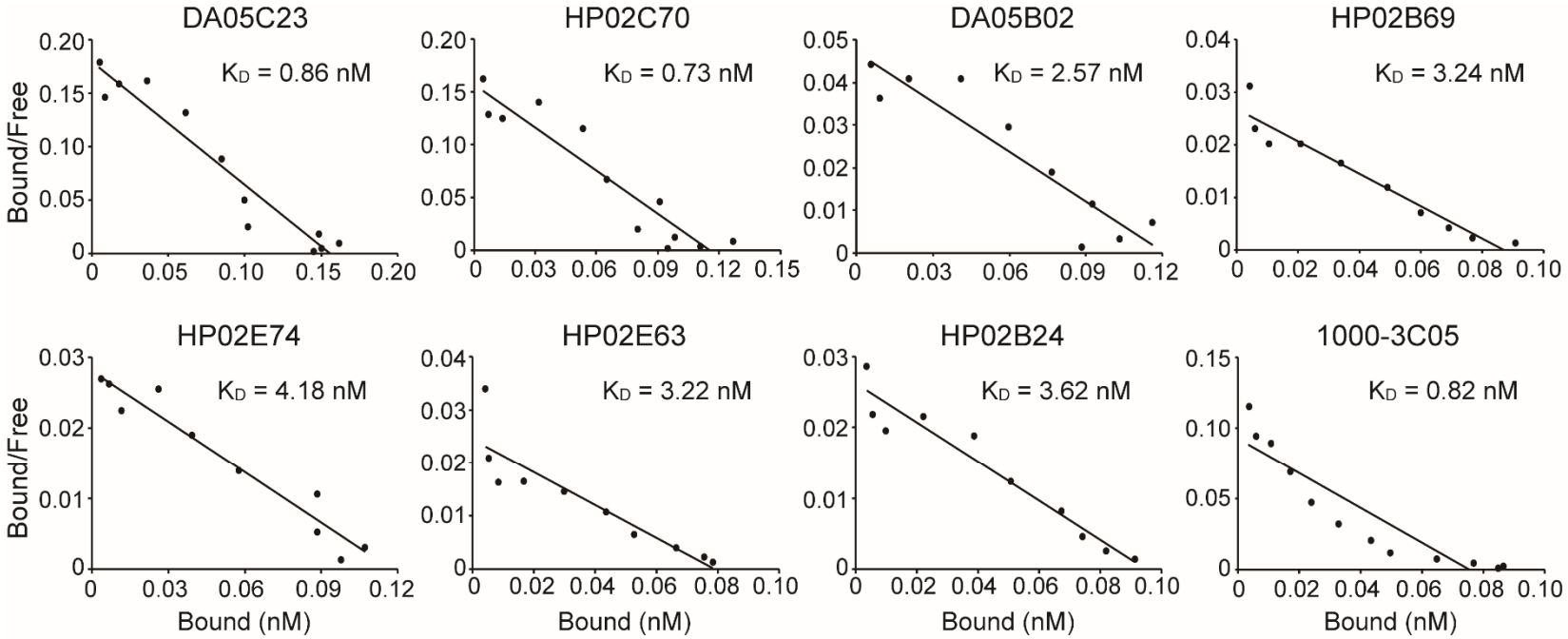

Figure 12. Binding affinity of anti-NA mAbs. K_D values were determined from Scatchard plots of ELISA data. VP40-induced VLPs presenting YO/94/15-NA were used as the antigen. Based on the average OD450 values in three technically independent experiments, the concentrations of antibody bound to antigen and of free antibody were calculated. When the ratio of bound to free antibody concentration was plotted against the bound antibody concentration, the negative inverse of the resulting slope was determined as the K_D.

The seven mAbs recognize the lateral surface of the NA head. To determine the amino acids that are important for the binding of the seven anti-NA mAbs, I compared the amino acid sequences of the NA protein from the six viruses used in Fig. 11B and identified six unique amino acids in the NA of YO/94/15 virus (Fig. 13A, 13I, 44I, 263I, 268K, 314M, and 390K; N2 numbering). I then generated mutant YO/94/15 viruses possessing single amino acid substitutions (I13V, I44L, I263V, K268N, M314I, or K390N) in their NA and examined the binding of the seven mAbs in an ELISA. HP02C70, DA05B02, HP02E74, HP02E63, and HP02B24 did not bind to virus possessing the K390N substitution in its NA but did bind to viruses possessing the I13V, I44L, I263V, K268N, or M314I substitution (Fig. 13B). DA05C23 and HP02B69 recognized all of the NA mutant viruses that possessed single amino acid substitutions, but showed decreased reactivity against the K390N mutant virus. Since these two clones weakly bound to A/Osaka/6/2014 virus (see Fig. 11B), I selected three amino acids shared only by the A/Osaka/6/2014 and YO/94/15 viruses (i.e., 38V, 321V, and 432E) for additional mutant generation. I generated mutant viruses possessing two substitutions (V38I and K390N, V321I and K390N, or E432K and K390N) in their NA and tested mAb binding. DA05C23 and HP02B69 did not bind to the virus possessing the K390N and E432K mutations in NA but still bound to the viruses possessing V38I and K390N or V321I and K390N (Fig. 13B). These results suggest that the amino acid at position 390 and the amino acids at positions 390 and 432 are important for the recognition of five and two of the monoclonal antibodies, respectively. Therefore, I mapped positions 390 (orange) and 432 (blue) together with the neuraminidase catalytic residues (cyan) on the

NA head molecule (Fig. 13C). Position 390 is located at the lateral face of the NA head, whereas position 432 is located at the edge of the enzymatic center on the upper surface of NA (Fig. 13C). The distance between positions 390 and 432 based on the crystal structure of the NA head molecule is approximately 3 nm. Since an antibody footprint is typically 4–10 nm^2 (38, 113), both amino acids are likely to be covered by one mAb. Therefore, I suggest that the five anti-NA mAbs that recognize an epitope around position 390, mainly recognize the lateral surface of NA and that the other two anti-NA mAbs, which lose binding to NA with mutations at positions 390 and 432, recognize an epitope that spans the upper and lateral surfaces.

A

Strain name	Amino acid (N2 numbering) at position																					
	13	38	44	48	106	155	199	240	247	263	268	274	283	298	314	321	372	390	398	401	415	432
A/California/04/2009	V	I	L	N	V	Y	N	V	N	V	N	H	D	S	I	I	N	N	V	N	L	K
A/Hiroshima/66/2011	·	·	·	·	I	·	·	·	D	·	·	Y	·	A	·	·	·	·	·	·	·	·
A/Osaka/83/2011	·	·	·	S	I	H	·	I	D	·	·	Y	·	·	·	·	K	·	·	·	M	·
A/Osaka/33/2013	·	·	·	S	·	·	S	I	D	·	·	·	G	·	·	·	K	·	·	·	·	·
A/Osaka/6/2014	·	V	·	S	·	·	S	I	D	·	·	·	·	·	·	V	K	·	I	K	·	E
A/Yokohama/94/2015	I	V	I	S	·	·	S	I	D	I	K	·	·	·	M	V	K	K	·	·	·	E

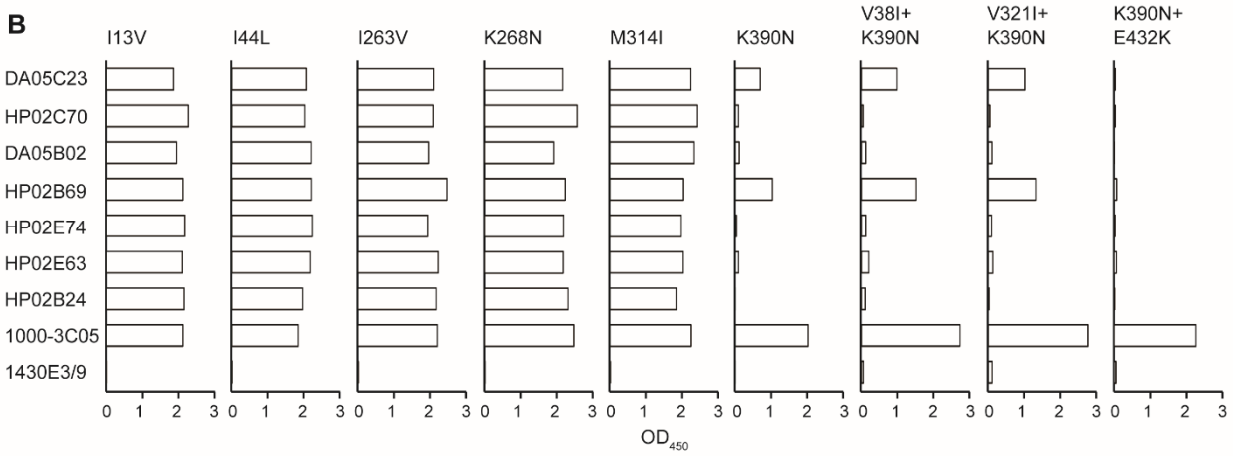

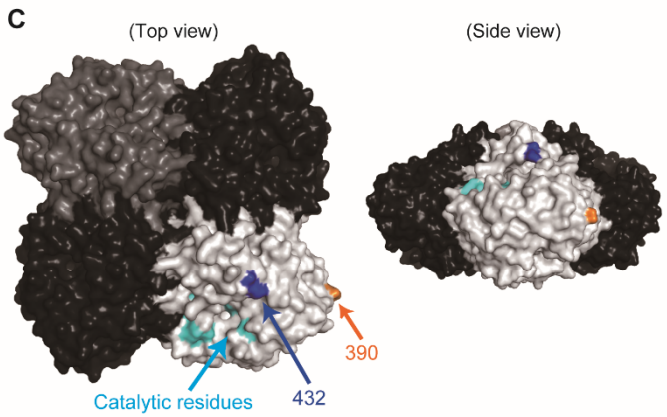

Figure 13. Epitope analysis of isolated anti-NA mAbs. (A) The NA amino acid sequences of A/Hiroshima/66/2011, A/Osaka/83/2011, A/Osaka/33/2013, A/Osaka/6/2014, and YO/94/15 viruses were compared with that of CA/04/09 virus. Bullets indicate an identical residue to the CA/04/09 sequence. (B) Binding of mAbs to mutant viruses possessing the indicated mutations in YO/94/15-NA was examined by means of an ELISA. Binding is shown as the OD450 value. These experiments were performed twice independently and yielded similar results. (C) Positions of amino acids that are important for mAbs binding are shown on the NA structure of CA/04/09 virus. Each NA monomer is indicated in white, grey, or black. Cyan indicates the catalytic residues; orange and blue indicate the amino acids that are important for mAb binding.

The seven anti-NA mAbs differ in their NI activity. To further characterize the seven anti-NA mAbs, I assessed their ability to inhibit viral sialidase activity in an enzyme-linked lectin assay (ELLA). DA05C23, HP02C70, and DA05B02 strongly inhibited NA activity with 50% inhibition concentration (IC_{50}) values of 0.38, 0.60, and 0.73 nM, respectively (Fig. 14A). HP02B69 weakly inhibited NA activity with an IC_{50} value of 7.52 nM, which was similar to that of 1000-3C05 (IC_{50} = 12.05 nM). HP02E74 slightly inhibited NA activity at high concentrations (IC_{50} = >26.67 nM), whereas HP02B24 and HP02E63 possessed no NI activity at all. To further confirm the NI activity in vitro, I performed a plaque size reduction assay. In this assay, DA05C23, HP02C70, and DA05B02 decreased viral plaque size by 50% or more at the highest concentration (Fig. 14B). The plaques that formed in the presence of HP02B69 and HP02E74 were about 30% smaller than those that formed in the absence of a mAb. In contrast, the plaque size reduction induced by HP02B24, HP02E63, and 1000-3C05 was approximately 10% at any concentration tested. Taken together, these results indicate that DA05C23, HP02C70, and DA05B02 possess relatively high NI activity, HP02B69 and HP02E74 possess relatively low NI activity, and HP02B24 and HP02E63 fail to inhibit NA activity.

The seven anti-NA mAbs activate the FcγR-mediated signaling pathway in effector cells. I next asked whether these anti-NA mAbs elicit antibody-dependent cellular cytotoxicity (ADCC) or antibody dependent cellular phagocytosis (ADCP) by using ADCC and ADCP reporter bioassays. By using these reporter bioassays, I found that the three mAbs that possess high NI activity, HP02C70,

DA05C23, and DA05B02, efficiently activated the ADCC and ADCP signaling pathways in effector cells co-cultured with both virus-infected and NA-expressing cells, except for the ADCC reporter assay with DA05C23 and NA-expressing cells, which was moderately activated (Fig. 14C). HP02B69 and HP02E74, which possessed low NI activity, moderately activated the ADCC signaling pathway and efficiently activated the ADCP signaling pathway in the effector cells co-cultured with infected and NA-expressing cells. HP02B24 and HP02E63, which had no NI activity, induced low or similar ADCC and ADCP signaling activation to that induced by the other five mAbs. 1000-3C05, which protected mice from lethal infection by activating FcγR-mediated effector cells (101), triggered ADCC and ADCP signal activation via both virus-infected and NA-expressing cells. All of the mAbs that possessed the N297Q mutation, which abolishes the interaction with FcγRs, and 1430E3/9 caused little-to-no activation in both reporter assays. These results indicate that our seven anti-NA mAbs have the potential to activate ADCC and ADCP.

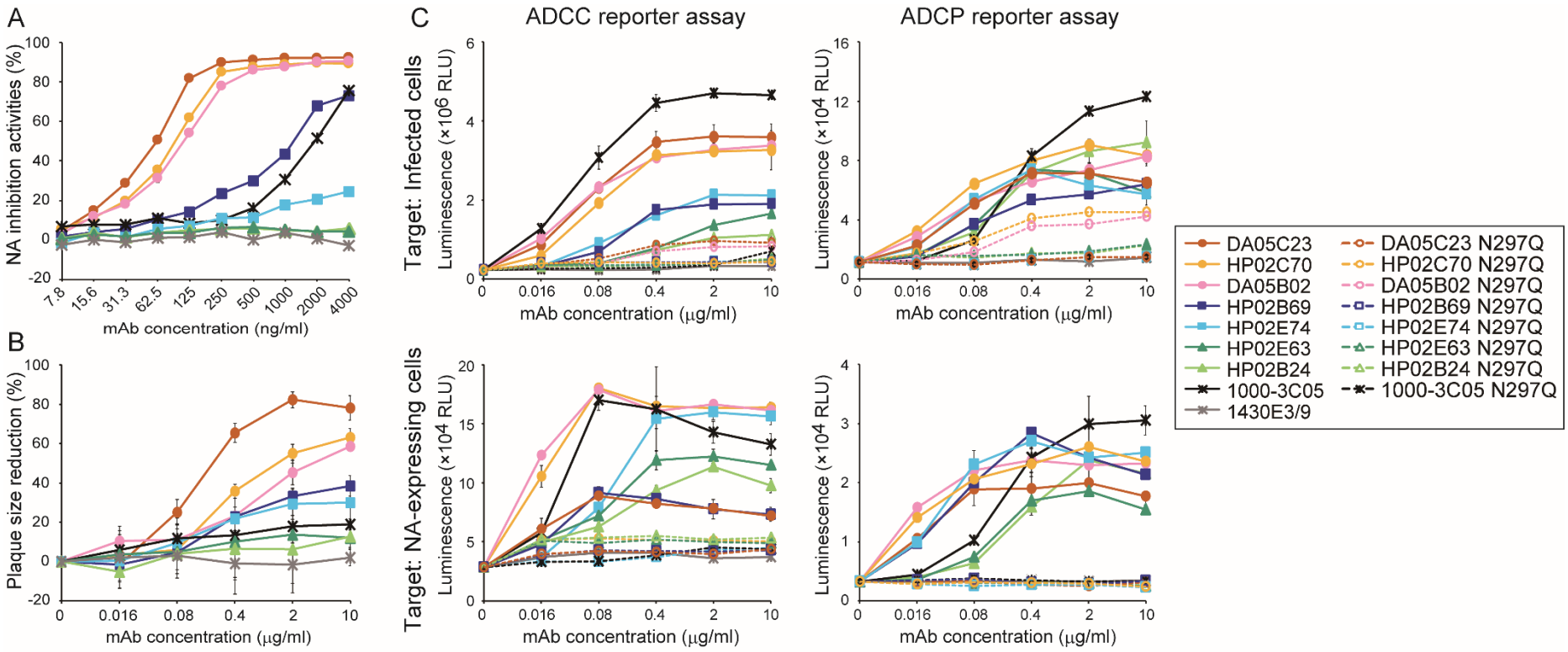

Figure 14. In vitro characterization of the isolated anti-NA mAbs. (A) mAb inhibition of NA activity was examined in an ELLA. This assay uses fetuin as a substrate and the purified YO/94/15 virus as the antigen/enzyme. NA cleaves terminal sialic acids from fetuin and the exposed galactose is detected by horseradish peroxidase-conjugated peanut agglutinin (PNA). NA activities in the presence of each mAbs were normalized to those in the absence of antibodies, and are expressed as relative NA inhibition activities. Data are shown as the mean ± standard deviations (SDs) of three technically independent experiments. (B) The inhibition of plaque formation was calculated by comparing the average plaque size in the presence of each mAb with that in the absence of mAb. Average plaque size was measured in three technically independent experiments, and SDs are shown as error bars. (C) Activation of the ADCC and ADCP signaling pathways. FcγR-mediated signaling activation in effector cells expressing human FcγRIIIa (ADCC) or FcγRIIa (ADCP) was induced by co-culture with A549 cells that were infected with YO/94/15 virus, or 293T cells transfected with an NA-expressing plasmid. Signaling activation was measured in three technically independent experiments and error bars reflect SDs. The N297Q mutant mAbs did not interact with FcγRs. 1430E3/9, which is an anti-influenza B HA mAb, was used as a negative control.

The anti-NA mAbs protect mice from lethal infection via their NI and FcγR-mediated antiviral activities. Since our mAbs possessed various levels of NI activity and activated FcγRIIIa- and FcγRIIa-mediated signaling pathways to various extents, I examined their in vivo protective efficacy against lethal influenza virus infection. For these in vivo tests, I monitored the body weight loss and survival of mice infected with 10 MLD_{50} (50% mouse lethal dose) of a challenge virus after administration of the wild-type or mutant N297Q mAb at 30 mg/kg (results of administration at 5 or 1 mg/kg are shown in Fig. 15). 1000-3C05, which requires FcγR-mediated effector cell activation to provide in vivo protection (101), or 1430E3/9, which is an anti-influenza B HA antibody, served as positive and negative controls, respectively. All of the wild-type anti-NA mAbs, except for DA05B02, protected all of the mice from lethal challenge infection, with the mice experiencing transient weight loss (Fig. 16). Of the mutant N297Q mAb-administrated groups, 75% of the mice that received HP02C70 or DA05B02, which possessed high NI activity, survived (Fig. 16). In particular, the N297Q mutant mAb DA05B02 showed similar in vivo protective potency to that of its wild-type counterpart. The N297Q mutants of DA05C23, HP02B69, and HP02E74, which possessed NI activity, protected 25% of the mice that experienced severe weight loss. The N297Q mutants of HP02E63 and HP02B24, which showed no NI activity, failed to protect any mice. Wild-type 1000-3C05 showed protection with transient weight loss, whereas no mice that received the N297Q mutant of 1000-3C05 survived. Mice that received 1430E3/9 experienced similar weight loss to that experienced by mice that received PBS. These results suggest that both the NI activity and FcγR-mediated antiviral activity of the anti-NA

mAbs contribute to protection against influenza virus infection. Moreover, FcγR-mediated antiviral activity played central roles in the in vivo protection provided by the anti-NA mAbs that lacked NI activity.

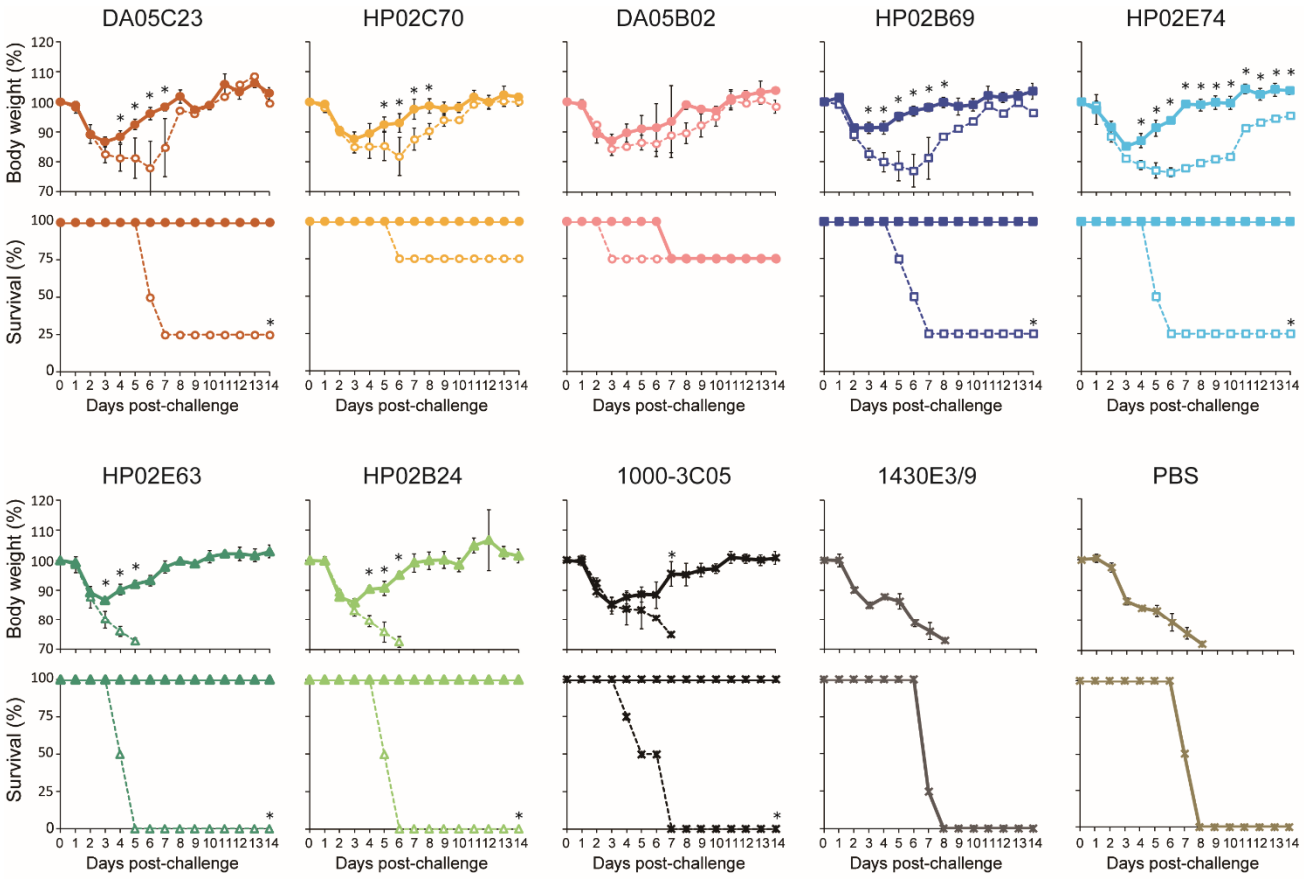

Figure 15. In vivo protective efficacy of anti-NA mAbs. Four mice per group were intraperitoneally injected with PBS or the indicated mAbs at 30 mg/kg. One day later, the mice were challenged with 10 MLD50 of the challenge virus. Body weight changes and survival were monitored daily for 14 days. Solid lines or dashed lines indicate the group that was exposed to the wild-type mAb or the N297Q mutant mAb, respectively. 1430E3/9 and PBS were used as negative controls. Body weight changes are shown as the mean ± SDs. * indicates $P < 0.01$. A two-way ANOVA followed by Dunnett' s tests and the two-sided log-rank test were used to obtain the body weight curves and the Kaplan-Meier survival curves, respectively.

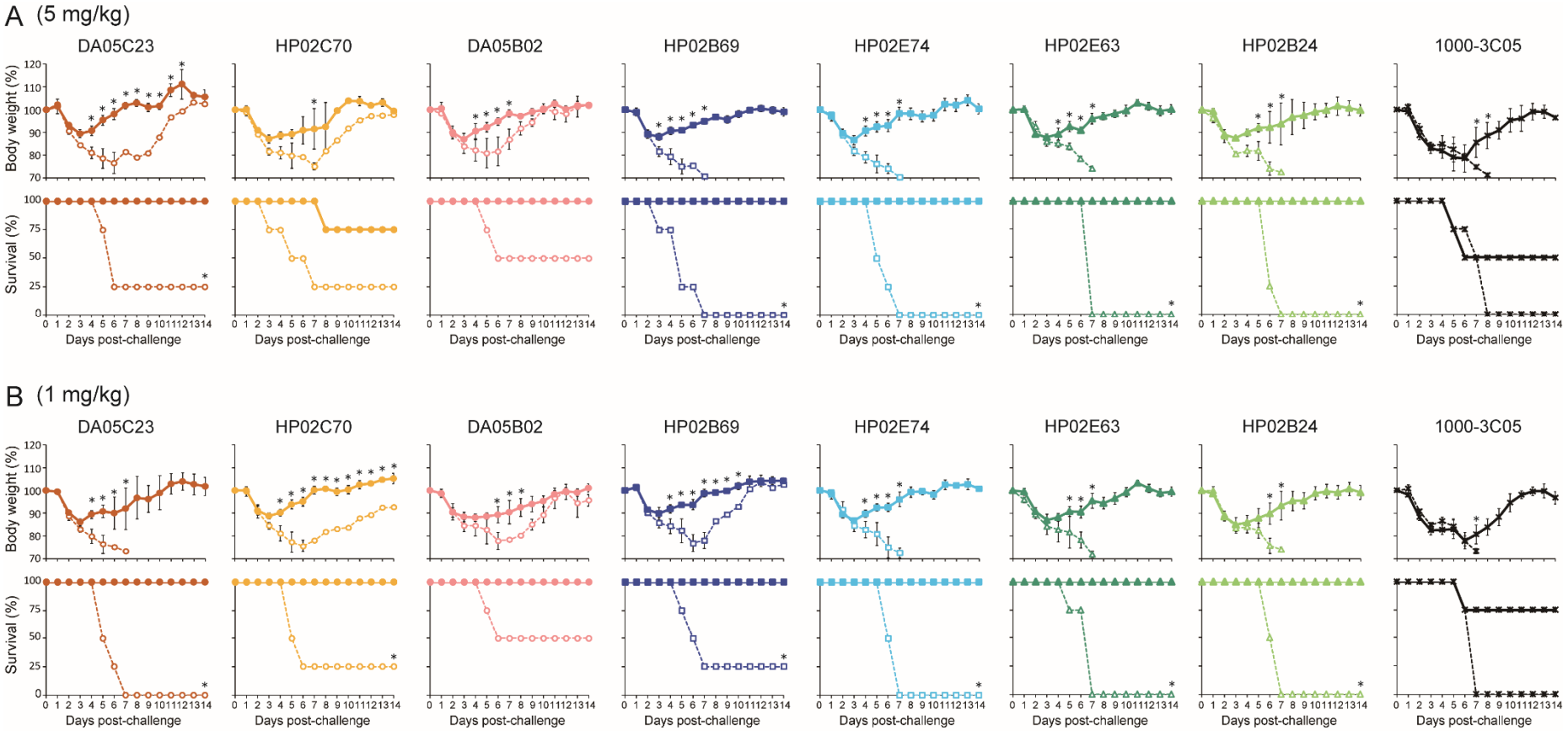

Figure 16. In vivo protective efficacy of low-dose mAbs. Four mice per group were intraperitoneally injected with PBS or the indicated mAbs at 5 mg/kg (A) or 1 mg/kg (B). One day later, the mice were challenged with 10 MLD50 of the challenge virus. Body weight changes and survival were monitored daily for 14 days. Solid lines or dashed lines indicate the group exposed to the wild-type mAb or the N297Q mutant mAb, respectively. Body weight changes are shown as the mean ± SDs. * indicates $P < 0.01$. A two-way ANOVA followed by Dunnett' s tests and the two-sided log-rank test were used to obtain the body weight curves and the Kaplan-Meier survival curves, respectively.

Antibodies recognizing the lateral surface of the NA head of A(H1N1)pdm09 virus in patient sera.

To evaluate whether individuals who were infected with the A(H1N1)pdm09 virus possessed antibodies targeting the lateral surface of the NA head on the day they visited the hospital or 1 month after infection, I performed a competitive binding ELISA using a protective mAb without NI activity, HP02E63 or HP02B24, or a cocktail of our seven anti-NA mAbs (Fig. 17A). The Fc region of these mAbs was replaced with that of mouse IgG2a so as not to be recognized by the HRP-conjugated antibody. In the presence of the mAb cocktail or each mAb, I assessed antibody binding in the serum samples of patients infected with A(H1N1)pdm09 virus during the 2015–2016 influenza season to VLPs displaying YO/94/15-NA; the NA-displaying VLPs were produced by expressing Ebola virus VP40 and NA since humans do not have antibodies to VP40. All of the patients were found to possess antibodies that competed with the anti-NA mAb cocktail 30 days after infection (Fig. 17B). Serum samples from patients HP001, HP002, HP014, and HP021 or from HP002 and HP021 collected 30 days after infection contained significant amounts of antibodies that competed with antibodies HP02E63 or HP02B24, respectively (Fig. 17C and 17D). On the day that each patient visited the hospital, HP001 and HP021 had antibodies that competed with the anti-NA mAbs cocktail, HP02E63, and/or HP02B24 (Fig. 17). These results demonstrate that substantial amounts of antibodies targeting epitopes on the lateral surface of the NA head were induced upon virus infection.

A Schematic diagram of the competitive binding assay

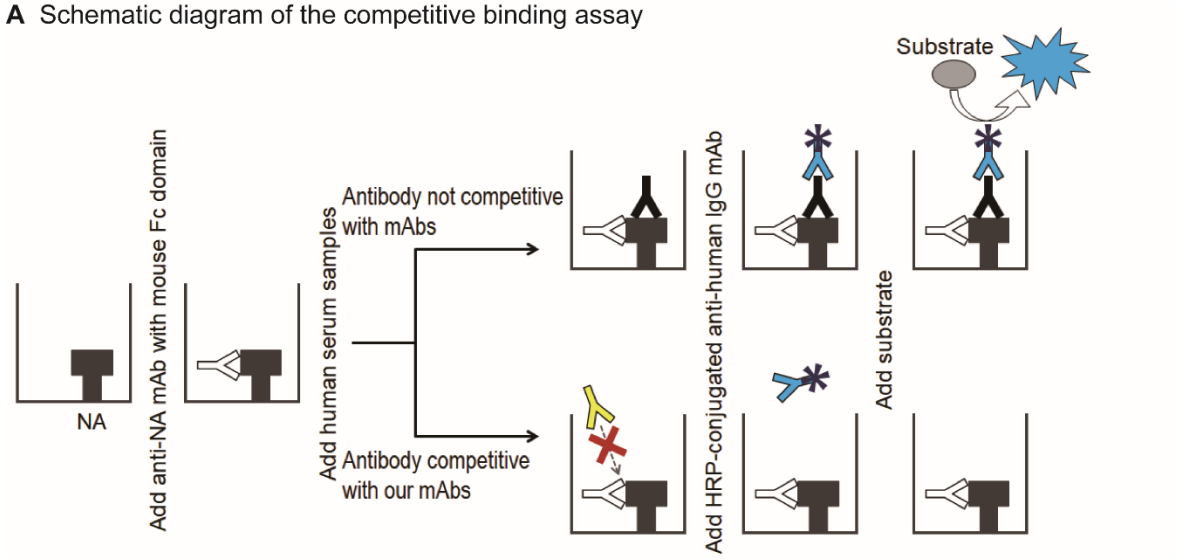

B The cocktail of seven anti-NA mAbs

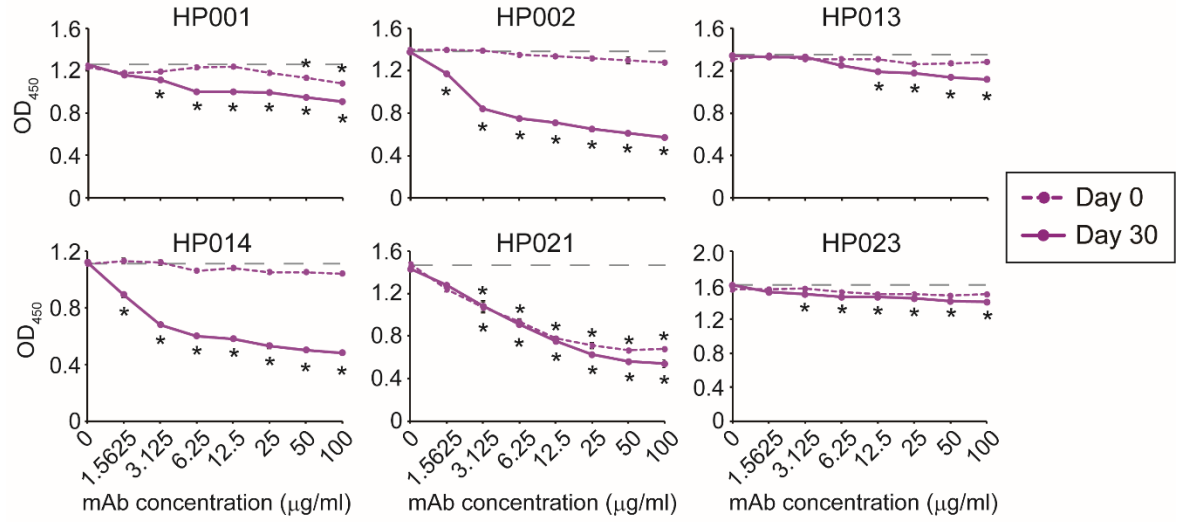

C HP02E63

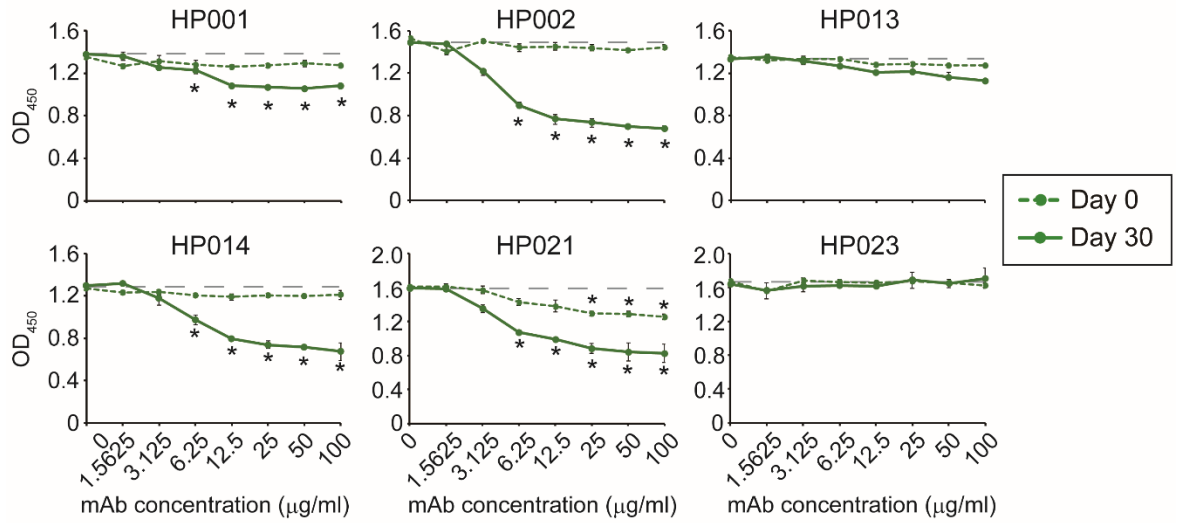

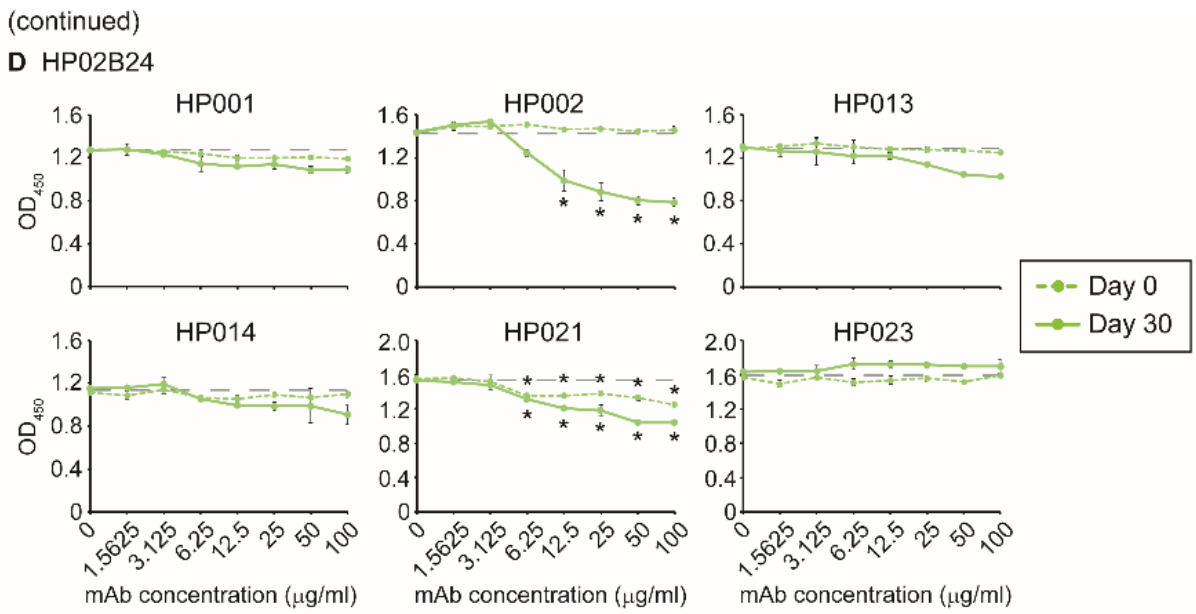

Figure 17. Competitive binding between antibodies in the sera of infected individuals and mAbs targeting the lateral surface of the NA head. (A) Schematic diagram of the competitive binding assay. For the competitive ELISA assay, ELISA plates were coated with VP40-induced VLPs presenting YO/94/15-NA. The antigen-coated plates were then incubated with the anti-NA mAbs of interest that possessed the mouse Fc region (shown as a white antibody). The plates were then washed and six serum samples were added. Antibodies in the serum that did not compete with our mAbs (shown as a black antibody) bound to the antigen, whereas antibodies that did compete with our mAbs (shown as a yellow antibody) failed to bind to the antigen. The bound antibodies were detected by using the HRP-conjugated anti-human Fc antibody and then visualized by using the substrate TMB. (B-D) VP40-induced VLPs presenting YO/94/15-NA were used as the antigen. A cocktail of seven anti-NA mAbs (B) or mAb HP02E63 (C) or HP02B24 (D), whose Fc region was exchanged with the Fc region of mouse IgG2a, was incubated with antigen-coated plates to block their epitope before incubation with the serum. Serum samples used here were collected from patients who were infected with A(H1N1)pdm09 virus in the 2015–2016 influenza season. Dashed lines or solid lines indicate sera collected on day 0 or 30 post-infection, respectively. Wells treated with PBS instead of monoclonal antibody were used as control wells; the grey dashed line indicates the OD450 values of the control wells for the Day 0 serum samples. The average OD450 values were measured in three technically independent experiments, and the SDs are shown as error bars. * indicates $P < 0.01$ (one-way ANOVA followed by Dunnett' s test).

NA antigenicity differs between 2009 and 2015 isolates of A(H1N1)pdm09 virus. Influenza viruses constantly evade suppressive antibodies by acquiring mutations in the epitopes of not only HA, but also NA. Therefore, I investigated the antigenicity of CA/04/09-NA and YO/94/15-NA in an ELISA using 22 serum samples that were collected during the 2009–2010 influenza season from volunteers who had neutralization antibodies against A(H1N1)pdm09 virus (114). I found that end-point titers to YO/94/15-NA were significantly lower than those to CA/04/09-NA (Fig. 18A). These results indicate that YO/94/15-NA differed antigenically from CA/04/09-NA.

To determine which amino acid mutations are responsible for the antigenic change in NA, I compared the amino acid sequences of CA/04/09-NA and YO/94/15-NA and found 6, 4, and 3 amino acid differences around the enzymatic center of the NA head (blue; positions 199, 240, 247, 321, 372, and 432), on the lateral surface of the NA head (orange; positions 263, 268, 314, and 390), and in the stalk region (not shown in the structure; position 38, 44, and 48), respectively (Figs. 13A and 18B). Then, I performed a cell-based ELISA by using the 22 A(H1N1)pdm2009-positive sera and cells transiently expressing wild-type CA/04/09-NA or its mutants that possessed amino acid changes found in YO/94/15-NA. If the end-point titer of each serum against the mutant NA was at least 4 times lower than that against wild-type NA, I concluded that that mutation affected the antigenicity of NA. Half of the sera (11/22, blue dots) showed reduced reactivity to NA possessing mutations around the enzymatic center (Fig. 18C, left). Two of these sera (2/11) also showed decreased binding to the stalk region mutant (Fig. 18C, right). Two serum samples (2/22) mainly targeted the lateral surface of the NA head

(red or orange dot in Fig. 18C, middle) and reacted with the NA mutants of the enzymatic center and stalk region with similar titers. These results indicate that the antigenic drift of NA involves mutations on the lateral surface of the NA head and that the antibodies of some individuals mainly recognize the lateral surface of the NA head.

Furthermore, I investigated whether a single mutation at position 390, which is the key residue for the binding of our mAbs, contributes to the antigenic drift on the lateral surface of the NA head by using a cell-based ELISA. Cells transiently expressing CA/04/09-NA with the N390K mutation as the antigen were incubated with the 22 A(H1N1)pdm2009-positive human sera used in Fig. 18C. I found that one sample (red dot) also showed decreased binding to the N390K mutant (Fig. 18D). These results suggest that the single N390K mutation is partially involved in the NA antigenic drift.

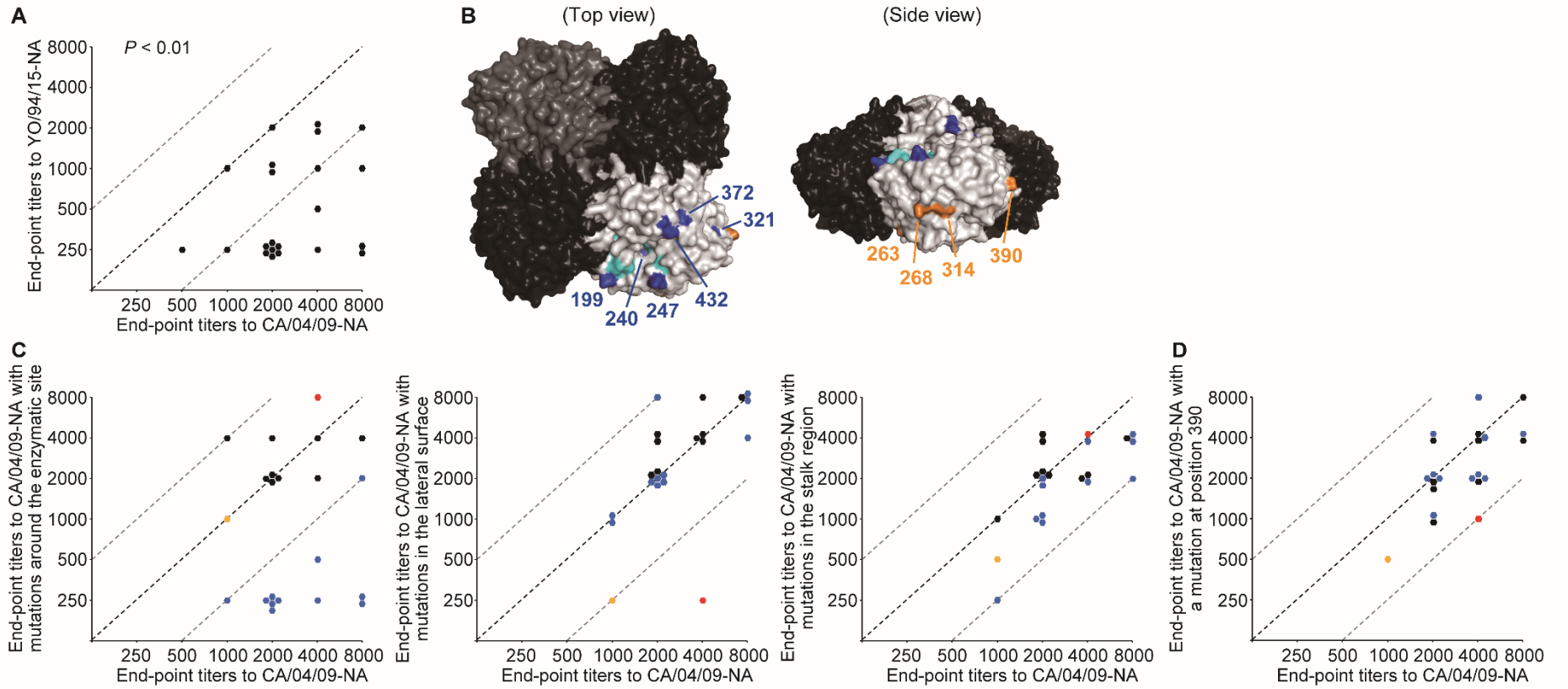

Figure 18. Antigenic differences between CA/04/09 and YO/94/15-NA. (A) The antibody titers of sera collected from volunteers in the 2009–2010 influenza season against the NA of CA/04/09 or YO/94/15 virus were determined by using an ELISA. 293T cells transiently expressing CA/04/09-NA or YO/94/15-NA were used as the antigen. The reciprocal of the highest dilution providing an OD450 value of greater than 0.1 was expressed as the end-point titer. End-point titers to YO/94/15-NA were plotted against those to CA/04/09-NA. The black dashed line indicates a 1:1 ratio of YO/94/15-NA end-point titers to CA/04/09-NA end-point titers and the grey dashed lines indicate the 1:4 or 4:1 ratios. The P value was calculated by using the two-sided Wilcoxon signed rank test. (B) Amino acid substitutions in YO/94/15-NA are shown on the NA structure. Cyan indicates the catalytic residues; blue or orange indicate the amino acids located around the enzymatic center or on the lateral surface of the NA head, respectively. The stalk region of NA is not included in this structure. (C-D) We determined end-point titers of sera, collected during the 2009–2010 influenza season, against CA/04/09-NA with (C) mutations around the enzymatic center (left), on the lateral surface (middle), or in the stalk region (right), or (D) the N390K single mutation. End-point titers to each CA/04/09-NA mutant were plotted against those to the wild-type CA/04/09-NA. The black dashed line indicates the 1:1 ratio and the grey dashed lines indicate the 1:4 or 4:1 ratios of the y-axis end-point titers to the x-axis titers. The blue dots indicate individuals whose sera showed weak binding to CA/04/09-NA with mutations around the enzymatic center, and the red and orange dots indicate individuals whose sera showed weak binding to CA/04/09-NA with mutations on the lateral surface.

Discussion

Antibodies that inhibit virus sialidase activity are produced in infected individuals and are important for protection against seasonal influenza virus infection (99, 100, 115). To evade such NI antibodies, amino acid mutations are accumulated around the enzymatic center of NA (112, 116). Although many amino acid changes accumulate on the lateral surface of the NA head over time, which is far away from the enzymatic center, the role of these mutations remained unknown (112). Here, I isolated human mAbs that recognize the lateral surface of the NA head of A(H1N1)pdm09 virus isolated during the 2015–2016 influenza season. These anti-NA lateral surface mAbs protected mice from lethal virus infection via their NI activity and/or FcγR-mediated antiviral activity. I also found that some individuals acquire anti-NA lateral surface antibodies after infection and that the antigenicity of the lateral surface of the NA head has changed during A(H1N1)pdm09 virus replication in humans since 2009. Taken together, the findings of this study suggest that anti-NA antibodies similar to our anti-NA antibodies are likely to be involved in the antigenic drift on the lateral surface of the NA head. To reveal whether amino acids are changed frequently at the lateral surface of the NA head, I compared the NA sequences derived from A(H1N1)pdm2009, A(H1N1)pre2009, and A(H3N2) viruses, which were obtained from the Global Initiative on Sharing All Influenza Data (GISAID) database, and then calculated the Shannon entropy to determine the sequence variability. The calculated Shannon entropy was then mapped onto the NA structure (Fig. 19). This analysis revealed that amino acid mutations at the lateral surface of the NA head occur in all subtypes of human virus NA at a frequency equal to or

higher than that around the enzymatic center. Although further epitope analysis is required to fully understand this phenomenon, the selective pressure of anti-NA lateral surface mAbs due to FcγR-mediated antiviral activity as well as NI activity likely contribute to the antigenic drift at the lateral surface.

Recent studies report that, in vaccinated humans, the levels of anti-NA antibodies correlate with a reduced disease severity score, decreased symptoms, and even a reduction in the duration of virus shedding (99, 117), indicating that anti-NA antibodies are an important mediators of protection against influenza virus infection. Therefore, attention has been paid to the importance of NA in influenza vaccines (29-31). In this context, antigenic characterization of NA is essential to select appropriate vaccine strains, as has been done with HA. Traditionally, the antigenic properties of NA are evaluated by using the NI assay, which detect mainly antigenic changes caused by amino acid changes around the enzymatic active center and may not detect some changes in the lateral surface of NA. Our results demonstrate that anti-lateral surface mAbs without NI activity are potentially involved in the antigenic drift of NA, suggesting that the traditional NI assays are not sufficient to fully characterize NA antigenicity. To this end, it is vital that I develop a new assay to properly characterize NA antigenicity.

Studying human anti-NA antibodies, DiLillo *et al.* (101) reported that the broadly reactive mAb clone 1000-3C05, which possesses low NI activity, requires FcγR-mediated effector cell activation to provide in vivo protection, whereas the strain-specific mAb EM-3C02, which possesses

high NI activity, does not. Taken together with our results, these findings suggest that human anti-NA antibodies suppress virus pathogenicity by at least two distinct mechanisms: NI activity and FcγR-mediated effector cell activation. An anti-NA mAb with high NI activity could reduce virus spread in vivo mainly via its NI activity, whereas an anti-NA mAb without NI activity could suppress virus replication mainly through FcγR-mediated effector cell activation (e.g., ADCC, ADCP, and/or ADNP). For anti-NA mAbs with low NI activity, both NI activity and FcγR-mediated effector cell activation are required to reduce virus growth in vivo. Thus, the sum of the NI activity and the FcγR-mediated effector cell activation determines the potency of an anti-NA antibody in vivo.

Of the seven anti-NA mAbs isolated, binding to the NA protein of five clones (HP02C70, DA05B02, HP02E74, HP02E63, and HP02B24) was abolished by an amino acid substitution at position 390, located on the lateral surface, and that of two clones (DA05C23 and HP02B69) was eliminated by two amino acid mutations at positions 390 and 432, located on the upper and lateral surfaces. The amino acid at position 390 was essential for recognition. Of the former five mAbs, three (HP02C70, DA05B02, and HP02E74) showed NI activity, whereas the other two (HP02E63 and HP02B24) did not. The mouse mAb clone CD6, which recognizes an epitope located on the lateral surface of NA, possesses potent NI activity (118, 119). Co-crystallization revealed that CD6 could hinder NA activity by either preventing sialic acid substrates from accessing the enzymatic center (due to its size) or by cross-linking adjacent NA tetramers (118). I hypothesize that our anti-NA mAbs (HP02C70, DA05B02, and HP02E74) may inhibit NA activity through a similar mechanism. However,

I cannot explain why HP02E63 and HP02B24 do not possess NI activity even though they share the key amino acid for binding. Co-crystallization of NA with these mAbs would help us to understand the lack of NI activity of such mAbs that recognize an epitope on the lateral surface of NA.

In summary, I found that anti-NA mAbs with low or no NI activity can contribute to protection from influenza virus infection. Furthermore, these mAbs are potentially involved in the antigenic drift of NA via FcγR-mediated antiviral activity. These findings suggest that the assessment of antigenic drift by using the NI assay alone is insufficient and that methods that allow us to consider antigenic changes that cannot be detected using NI assays need to be developed for better selection of vaccine candidate strains.

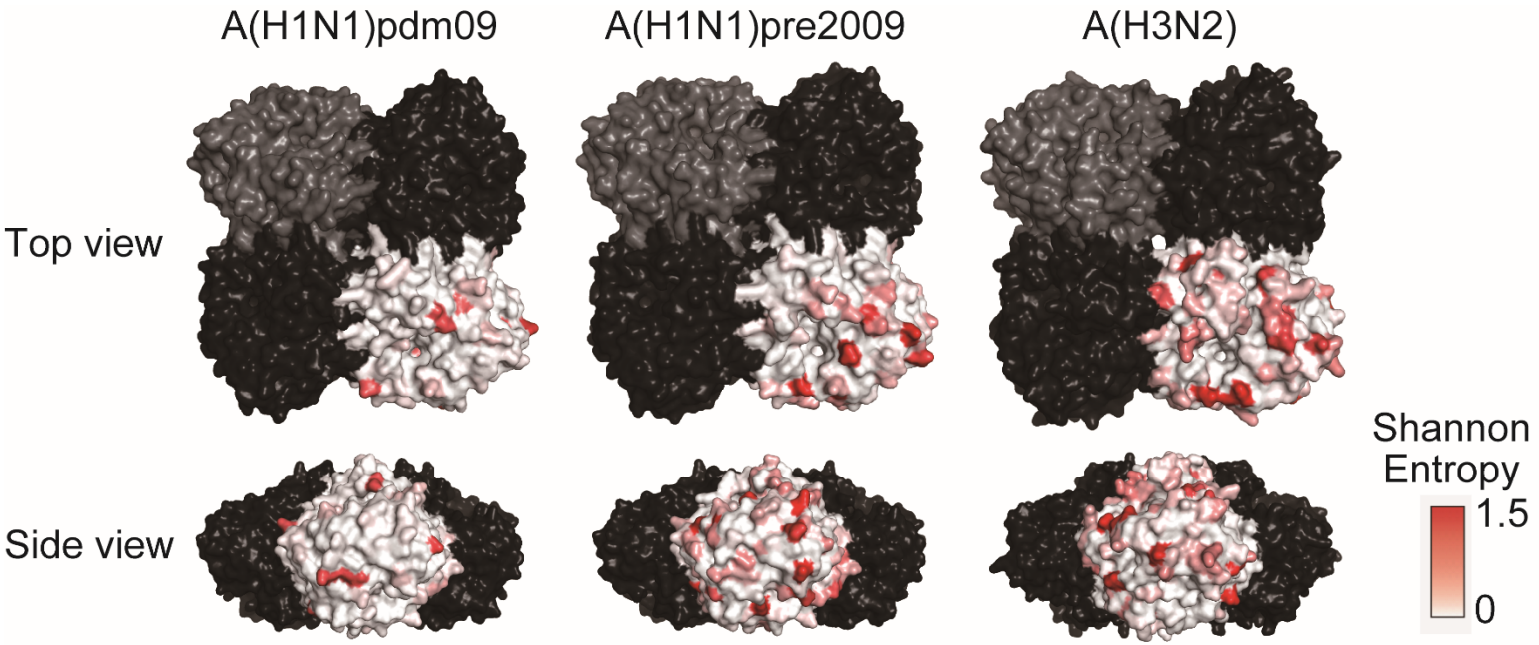

Figure 19. Mapping of amino acid variability onto the NA structure. The variability of the NA sequence was computed as the Shannon entropy for each position, based on the NA sequences of 19,034 A (H1N1)pdm09, 4,626 A(H1N1)pre2009, and 40,516 A(H3N2) isolates. Residues are colored based on the computed entropy values, on a scale of white (complete conservation; 0) to red (variable; 1.5).

MATERIAL AND METHODS

Ethics. Human blood was collected from two volunteers by following a protocol approved by the Research Ethics Review Committee of the Institute of Medical Science, the University of Tokyo. Written informed consent was obtained from each participant. All experiments with mice were performed in accordance with the University of Tokyo's Regulations for Animal Care and Use and were approved by the Animal Experiment Committee of the Institute of Medical Science, the University of Tokyo.

Cells. Madin-Darby canine kidney (MDCK) cells were maintained in Eagle's minimal essential medium (MEM) containing 5% newborn calf serum (NCS). Human lung carcinoma A549 cells were maintained in Ham's F-12K medium containing 10% fetal calf serum (FCS). Human embryonic kidney 293T cells were maintained in Dulbecco's modified Eagle's medium (DMEM) containing 10% FCS. SPYMEG cells (MBL), which are a fusion partner cell line for human hybridoma, were generated by the fusion of the mouse myeloma cell line SP2/0 with the human leukemia cell line MEG-01 and were maintained in DMEM containing 15% FCS (17). These cells were incubated at 37°C under 5% CO_2. Expi293F cells (Thermo Fisher Scientific) were maintained in Expi293 Expression Medium (Thermo Fisher Scientific) at 37°C under 8% CO_2.

Viruses. I used the following seven A(H1N1)pdm09 viruses: A/California/04/2009 (CA/04/09 or CA04; clade 1), A/Hiroshima/66/2011 (clade 5), A/Osaka/83/2011 (clade 7), A/Osaka/33/2013 (clade 6C), A/Osaka/6/2014 (clade 6B), A/Yokohama/50/2015 (clade 6B), and A/Yokohama/94/2015 (YO/94/15; clade 6B.1); five H1N1pre2009 viruses (A/Kumamoto/37/79, A/Kamata/8/80, A/Tokyo/913/88, A/Minato/131/92, and A/Brisbane/59/2007); two H3N2 viruses (A/Perth/16/2009 and A/Hong Kong/4801/2014); and an H5N1 virus (A/Vietnam/1203/2004). All of these viruses were propagated in MDCK cells. Mutant CA04 viruses were generated by use of reverse genetics (59) as described below.

Plasmid-based reverse genetics. The reassortant viruses, the NA mutant viruses, and the challenge virus were generated by plasmid-based reverse genetics, as described previously (59). For the HA mutant viruses, plasmids encoding mutated CA04-HA were generated by a standard PCR technique based on pPol I encoding CA04-HA. The pPol I encoding CA04-HA and the remaining 7 pPol I plasmids were cotransfected into 293T cells. For reassortant viruses, two pPol I plasmids encoding the HA and NA segments derived from the YO/94/15 or CA/04/09 viruses and six pPol I plasmids encoding the remaining segments of CA/04/09 virus were used for the plasmid transfection. For preparation of the NA mutant viruses, pPol I plasmids encoding HA and wild-type or mutated NA derived from YO/94/15 virus and six pPol I plasmids encoding the remaining segments of CA/04/09 virus were used. For preparation of the challenge virus, I used pPol I plasmids encoding the HA and

NA segments of YO/94/15 virus and six pPol I plasmids encoding the remaining segments of mouse-adapted CA/04/09 (120). These 8 pPol I plasmids along with protein expression plasmids for PB2, PB1, PA, and NP derived from A/Puerto Rico/8/34 were transfected into 293T cells by use of TransIT 293 (Mirus) according to the manufacturer's instructions. At 48 h post-transfection, the supernatants were harvested and inoculated into MDCK cells. The rescued viruses were sequenced to ensure the absence of unwanted mutations. Primer sequences are available upon request.

Hybridoma generation. Peripheral blood mononuclear cells (PBMCs) were isolated from volunteers, who were vaccinated with the 2014–2015 seasonal influenza vaccine (78) or the H5-HA vaccine (79), or were infected with influenza viruses during 2015-2016 influenza season, by using Ficoll Paque Plus (GE Healthcare). An inactivated, adjuvanted whole-virus vaccine to A/Egypt/N03072/2010 (H5N1, clade 2.2.1) was used as the H5-HA vaccine. To obtain hybridomas, the isolated PBMCs were fused with SPYMEG cells (MBL), which are fusion partner cells. The hybridomas were cultured in DMEM supplemented with 15% FCS in 96-well culture plates for 10–14 days in the presence of hypoxanthine-aminopterin-thymidine. The first screening for antibody characterization was performed by using an enzyme-linked immunosorbent assay (ELISA), as described below. Antibody-positive wells were cloned by several rounds of dilution.

ELISA. ELISA plates (96-well) were coated with 2 μg/mL of recombinant HA derived from A/California/07/2009 (H1N1pdm09), A/Perth/16/2009 (H3N2), A/Egypt/N05056/2009 (H5N1), A/Netherland/219/2003 (H7N7), B/Florida/4/2006 (Yamagata-lineage), and B/Malaysia/2506/2004 (Victoria-lineage), or 2 μg/mL of purified viruses. All recombinant HAs were purchased from Sino Biological. After being blocked with 5 times-diluted Blocking One (Nakarai), these plates were incubated with the culture medium of the hybridomas or 1 μg/mL of purified mAb. A horseradish peroxidase (HRP)-conjugated goat anti-human IgG, Fcγ Fragment-specific antibody (Jackson Immuno-Research) was used as the secondary antibody, and the signal was developed using 3, 3', 5, 5'-tetramethylbenzidine (TMB) (Thermo Fisher Scientific) as the substrate. The reaction was stopped with 2N sulfuric acid, and OD_{450} values were then measured. OD_{450} values of 0.1 or more were considered to indicate binding.

Purification of a human monoclonal IgG from hybridoma cells. Adaptation of hybridoma cells to serum-free medium, Hybridoma-SFM (GIBCO), was performed by passaging. The human antibody in the serum-free medium was purified by using a HiTrap rProtein A FF column (GE Healthcare) and the automated chromatography system ÄKTA pure 25 (GE Healthcare).

Construction and expression of monoclonal human IgG. Human mAbs were expressed and purified as described previously (79). Briefly, the VH and VL genes of the antibodies were cloned into the

expression vector Mammalian PowerExpress System (TOYOBO), together with the constant gamma heavy (IgG1), kappa light, or lambda light coding sequence. Antibodies were transiently expressed by Expi293F cells and were purified by using a HiTrap rProtein A FF column (GE Healthcare) and the automated chromatography system ÄKTA pure 25 (GE Healthcare).

Nucleotide sequence determinations. cDNA encoding the Fab region of a human antibody was PCR-amplified and directly sequenced. Determined nucleotide sequences of a heavy chain and a light chain were analyzed by using the IgBlast software (http://www.ncbi.nlm.nih.gov/igblast/).

K_D determination. K_D was determined by bio-layer interferometry (BLI) using an Octet Red 96 instrument (ForteBio). Recombinant HA derived from A/California/07/2009 (H1N1pdm09) was used for the measurements. HA (10 μg/ml) in kinetics buffer (1x PBS, pH7.4, 1% BSA, and 0.002% Tween 20) was loaded onto Ni-NTA biosensors (ForteBio) and incubated with various concentrations of 1428A33/1, 1428B5/1, F3A19, or CR9114. All binding data were collected at 30°C. The experiments comprised 4 steps: (1) HA loading onto the biosensor until the shift reached 0.35 nm; (2) baseline acquisition (300 s); (3) association of 1428A33/1, 1428B5/1, F3A19, or CR9114 for the measurement of k_{on} (300 s); and (4) dissociation of each mAb for the measurement of k_{off} (1200 s). Four concentrations (33.3, 11.1, 3.7, and 1.23 nM) of 1428A33/1, 1428B5/1, F3A19, or CR9114 were used.

Baseline and dissociation steps were carried out in buffer only. The ratio of k_{on} to k_{off} determined the K_D.

In vitro microneutralization assay. To assess the neutralization capability of the monoclonal antibodies, 100 $TCID_{50}$ (Median tissue culture infectious dose) of each indicated virus in MEM containing 0.3% bovine serum albumin (BSA-MEM) was incubated with two-fold diluted antibodies (50–0.012 μg/mL) at 37°C for 30 min. MDCK cells were washed with BSA-MEM and then incubated with the antibody-virus mixture in quadruplicate at 37°C for 1 h. After the cells were washed twice with BSA-MEM, the cells were incubated with BSA-MEM containing 1 μg/ml L-(tosylamido-2-phenyl) ethyl chloromethyl ketone (TPCK)-treated trypsin for 3 days at 37°C before the cytopathic effect (CPE) was examined. Antibody titers required to reduce virus replication by 50% (IC_{50}) were calculated by using the Reed and Muench method.

To assess the neutralization capability of human sera, serum samples were treated with Receptor-Destroying Enzyme (Denka Seiken Co., Ltd.) in accordance with the manufacturer's instructions. The sera were then serially diluted two-fold in PBS before being incubated with 100 $TCID_{50}$ of virus at 37°C for 30 min. The serum-virus mixture was added to pre-washed MDCK monolayers, which were then incubated at 37°C for 1 h. After the cells were washed once with BSA-MEM, they were incubated with BSA-MEM containing 1 μg/ml TPCK-treated trypsin at 37°C. The cells were observed for CPE at 3 days post-infection; neutralization titers were defined as the lowest

dilution at which a CPE did not appear.

Selection of escape mutants. Escape mutants were selected by passaging CA04 virus in the presence of indicated mAbs. Each two-fold diluted antibody was incubated with 10- or 100-fold diluted virus for 30 min at 37 °C. MDCK cells were washed and then incubated with the antibody-virus mixture at 37 °C for 1 h. After the inoculum was removed, the cells were incubated with BSA-MEM containing 1 μg/ml TPCK-treated trypsin for 3 days at 37 °C. Virus-containing supernatant was harvested from the CPE-positive well that contained the highest antibody concentration and was used for the next passage. I regarded a virus to be an escape mutant when it replicated well in the presence of mAbs at 50 μg/ml.

Viral growth kinetics. Triplicate wells of confluent A549 cells or MDCK cells were infected with virus at a multiplicity of infection (MOI) of 0.0001 and incubated with Ham's F-12K medium containing 0.3% BSA and 1 μg/ml TPCK-treated trypsin or BSA-MEM containing 1 μg/ml TPCK-treated trypsin, respectively, at 37°C. Supernatants were harvested at 12, 24, 48, and 72 hours post-infection (hpi). Virus titers were determined by use of plaque assays with MDCK cells.

Competitive replication assay with droplet digital PCR system. The mutant CA04 viruses possessing each indicated mutation and the wild-type virus or the K166Q mutant virus were premixed

at 1:1 ratio based on their PFU (plaque forming unit) titers. Triplicate wells of confluent A549 cells were infected with the virus mixtures at an estimated MOI of 0.0001, and incubated with Ham's F-12K medium containing 0.3% BSA and 1 μg/ml TPCK-treated trypsin at 37 °C. Supernatants were harvested at 12, 24, 48, and 72 hpi. The viral RNA was isolated from each supernatant using ISOGEN LS (Nippon gene). The relative proportions of wild-type and mutant viruses in each sample were determined by using a QX200 droplet digital PCR (ddPCR) system (Bio-Rad, Pleasanton, CA). FAM- and HEX-labeled primer/probe mixes were designed by the Bio-Rad online service. The ddPCR reaction mixture, consisting of ddPCR Supermix (Bio-Rad), the primer/probe mix, and the template cDNA, was loaded into a cartridge with droplet generation oil (Bio-Rad), and the cartridge was placed into the droplet generator (Bio-Rad). PCR amplification was carried out using the following thermal profile: 95°C for 10 min, followed by 40 cycles of 94°C for 30 s and 56°C for 1 min, 1 cycle of 98°C for 10 min, and ending at 4°C. After amplification, the droplets from each well of the plate were read by the droplet reader (Bio-Rad) to count the number of positive and negative droplets. ddPCR data were analyzed with QuantaSoft analysis software (Bio-Rad), and the threshold was set manually at the highest point of the negative droplet cluster. The concentration of each target gene is determined by applying a Poisson distribution calculation across all droplets, and is presented as the number of copies per μl of PCR mixture. The percentage of virus populations shows the ratio of the copy number of mutant viruses and wild-type viruses.

ELLA. The inhibition of NA activity was measured by using an enzyme-linked lectin assay (ELLA), as described previously (122). Briefly, two-fold diluted antibodies (4000–7.8 ng/mL) were mixed with a predetermined amount of purified YO/94/15 virus diluted in PBS containing 1% BSA and 0.05% Tween 20 (PBS-T). The mixture was transferred to 96-well plates coated with fetuin (Sigma) and then incubated for 16 h at 37°C. The plates were washed with PBS-T and then peroxidase-conjugated peanut agglutinin (PNA; Sigma) was added to detect galactose exposed by removal of the sialic acids on fetuin. The plates were incubated at room temperature for 2 h in the dark and then washed with PBS-T before the addition of o-phenylenediamine dihydrochloride (OPD) substrate (Sigma). The reaction was stopped by the addition of 1N sulfuric acid and OD_{490} values were read. The relative NA inhibition (NI) activity was calculated by dividing the OD_{490} value of the test well by the OD_{490} value of the "virus only" well and multiplying by 100. The 50% inhibitory concentration (IC_{50}) was determined by use of nonlinear regression analysis (GraphPad Prism software) assuming that the molecular weight of the antibody was 150 kDa.

Plaque size reduction assay. MDCK cells were infected with 100 plaque-forming units (pfu) of YO/94/15 virus for 1 h at 37°C. After removal of the inoculum, the cells were washed with MEM containing 0.3% bovine serum albumin (BSA-MEM) and overlaid with agar containing the indicated amount of the indicated mAb and 1 μg/ml L-(tosylamido-2-phenyl) ethyl chloromethyl ketone

(TPCK)-treated trypsin. The cells were incubated at 37°C under 5% CO_2 for 2 days and then stained with crystal violet solution to visualize the plaques. The plaque images were obtained by scanning assay plates with a photo scanner (GT-X900, EPSON). The total plaque size of each well was measured using a script written in MATLAB (Mathworks), and the average plaque size was calculated by dividing by the number of plaques. Infected cells overlaid with agar that lacked mAb served as a control. The reduction in plaque size was calculated by dividing the average plaque size in the presence of each mAb by the control plaque size.

ADCC and ADCP reporter assays. ADCC and ADCP reporter assays were performed by using ADCC and ADCP Reporter Bioassay Kits (Promega), according to the manufacturer's instructions. ADCC and ADCP signaling activations in effector cells were measured by using two kinds of target cells: A549 cells infected with YO/94/15 virus and 293T cells expressing NA derived from YO/94/15 virus. Briefly, A549 cells were plated at a density of 10,000 cells/well in a flat-bottom white 96-well plate. After 24 h, the cells were infected with YO/94/15 virus at a multiplicity of infection (MOI) of 10. At 12 h post-infection, the cells were used as target cells. For the second kind of target cell, two days before the reporter assays were performed, 293T cells in a 6-well plate were transfected with a plasmid encoding YO/94/15-NA by using Trans-IT 293. The next day, the transfected cells were harvested and seeded at 20,000 cells/well into a white 96-well plate. Twenty-four hours later, the cells were used as target cells. In the ADCC or ADCP reporter assays, the medium of the target cells was

replaced with five-fold diluted mAb (10–0.016 μg/ml) in the assay buffer (Promega). ADCC or ADCP Bioassay effector cells (a Jurkat cell line stably expressing human FcγRIIIa or FcγRIIa, human CD3γ, and an NFAT-response element driving expression of a firefly luciferase) were added to the antibody-treated target cells and incubated for 6 h at 37°C. The firefly luciferase activity was then measured using luciferase assay regents (Promega).

In vivo protection test. Four six-week-old female BALB/c mice (Japan SLC) per group were intraperitoneally injected with PBS or each indicated antibody at 30, 15, 3, 0.6, or 0.12 mg/kg in 250 μl of PBS. After 24 h, the mice were anesthetized with isoflurane and intranasally challenged with 10 MLD_{50} (50% mouse lethal dose) of the challenge virus in 50 μl of PBS. Weight was monitored daily for 14 days and mice that lost 25% or more of their initial body weight were scored as dead and euthanized according to institutional guidelines.

Competitive binding assay. For antigen preparation, 293T cells were transfected with pCAGGS plasmids encoding ebolavirus matrix protein VP40 and each indicated NA by using TransIT 293. After 2 days, the supernatant of the transfected cells was harvested and centrifuged at 28,000 rpm with a 20% sucrose cushion. The pellet containing VP40-induced VLPs presenting NA was resuspended in PBS. ELISA plates were coated overnight at 4°C with 5 μg/ml of the VLPs. After being blocked with 5 times-diluted Blocking One, these plates were incubated with a two-fold diluted cocktail of the seven

anti-NA mAbs (DA05C23, HP02C70, DA05B02, HP02B69, HP02E74, HP02E63, and HP02B24) or with individual monoclonal antibodies (HP02E63 or HP02B24), which possessed the Fc region of mouse IgG2a, or with PBS for 1 h. The plates were then washed with PBS-T, followed by the addition of diluted serum samples. The serum samples used in this assay were collected from patients infected with A(H1N1)pdm09 virus during the 2015–2016 influenza season. After 1 h, an HRP-conjugated goat anti-human IgG, Fcγ Fragment-specific antibody was added as the secondary antibody. The plates were incubated for 1 h, and then washed with PBS-T before the addition of the TMB substrate. The reaction was stopped with 2N sulfuric acid, and OD_{450} values were then measured. The wells to which PBS was added instead of monoclonal antibody served as control wells for each serum sample.

Entropy. For each amino acid position of the aligned isolate sequences, an entropy value was computed by using the formula $-\Sigma Pi \times \ln(Pi)$, as described by Chen *et al.* (123). This formula follows the definition of Shannon entropy (124) that has been used to evaluate diversity. In this study, entropy was used to measure the variability of amino acids at a given position, where $i = 1$ to 20 represents the 20 different amino acid residues, and Pi represents the probability density of the respective residue. Entropy values range from 0 (only 1 residue present at that position) to 2.996 (all 20 residues are equally represented). The calculation was based on the NA sequences of 19,034 A(H1N1)pdm09 isolates, 4,626 A(H1N1)pre2009 isolates, and 40,516 A(H3N2) isolates obtained from the GISAID database.

Cell-based ELISA. 293T cells were transfected with FLAG-tagged wild-type or mutant NA-expression plasmids or an empty plasmid as a control using TransIT 293. At 48 h after the transfection, the cells were fixed with 4% paraformaldehyde phosphate buffer solution for 30 min at room temperature. The cells were then washed with PBS-T, and blocked with 5 times-diluted Blocking One for 1 h. The cells were then incubated for 1 h with two-fold diluted serum samples, which were collected from volunteer schoolchildren and their parents who were seropositive for A(H1N1)pdm09 virus between November 2009 and March 2010 (114), followed by incubation for 1 h with an HRP-conjugated goat anti-human IgG, Fcγ Fragment-specific antibody. The signal was developed using TMB as the substrate and stopped with 2N sulfuric acid. OD_{450} values were then measured. Expression of NA was normalized with an anti-FLAG tag antibody (Wako). The mean OD_{450} at each dilution was obtained by subtracting the OD_{450} value for the control well (empty plasmid transfected cells). The end-point titers of serum samples were determined as the reciprocal of the highest dilution providing an OD_{450} value of greater than 0.1.

K_D determination. K_D values were determined from Scatchard plots using ELISA data (125). In the ELISA, VP40-induced VLPs presenting YO/94/15-NA were used as the antigen. After being blocked with 5-times-diluted Blocking One, antigen-coated plates were incubated with the two-fold diluted anti-NA mAb (10–0.005 μg/ml). The HRP-conjugated goat anti-human IgG, Fcγ Fragment-specific

antibody was used as the secondary antibody, and the signal was developed using TMB as the substrate. The reaction was stopped with 2N sulfuric acid, and OD_{450} values were then measured. Based on the OD_{450} values, the concentrations of antibody bound to antigen and of free antibody were calculated (assuming that the molecular weight of the antibody was 150 kDa). When the ratio of bound to free antibody concentration was plotted against the bound antibody concentration, the negative inverse of the resulting slope was determined as the K_D.

Structural analysis. Amino acid positions were plotted on the crystal structure of the NA protein of CA/04/09, A/Brevig Mission/1/1918 (H1N1pre2009), or A/Memphis/31/1998 (H3N2) (PDB accession code, 4B7R, 3B7E, or 4H53, respectively) by using the PyMOL molecular graphics system.

Statistical analysis. Two-way analysis of variance (ANOVA) followed by Dunnett's test, one-way ANOVA followed by Dunnett's test, the log-rank test, and Wilcoxon signed rank test were performed using GraphPad Prism software. *P* values < 0.01 were considered significantly different. No samples were excluded from the analysis.

Data availability. All data analyzed during this study are included in this article. The datasets generated and analyzed during the current study are available from the corresponding author on reasonable request.

CONCLUDING REMARKS

Influenza is an important infectious disease, because it can cause considerable morbidity and mortality worldwide. To prevent influenza virus infection, researchers have undertaken a variety of approaches, such as surveillance studies, elucidation of the virus replication cycle, functional and structural characterization of antiviral antibodies, and the development of protective vaccines and antiviral reagents. Although numerous vaccines and antiviral reagents have been developed, we cannot claim to have influenza under control. There remains an urgent need to establish novel approaches to vaccine development and treatment options for the control of influenza virus infections.

In chapter I, I selected potential antigenic drift mutants by means of in vitro selection with human monoclonal antibodies. In combination with computational analyses and other methods, in vitro selection of future antigenic variants may improve the selection of vaccine seed viruses. In chapter II, I isolated and characterized human neutralizing monoclonal antibodies that recognize functionally conserved epitopes in or around the receptor-binding site of HA, and revealed that antibodies against the receptor-binding site have the potential to be anti-influenza agents with a low propensity for the development of resistant viruses. In chapter III, I found that anti-NA lateral surface antibodies with low or no NI activity can contribute to protection from influenza virus infection, and that these mAbs may be involved in the antigenic drift of NA via Fcγ receptor-mediated antiviral activity. These findings suggest that the assessment of antigenic drift by using the NI assay alone is insufficient and that methods that allow us to consider antigenic changes that cannot be detected using NI assays need

to be developed for better selection of vaccine candidate strains.

Despite the development of antiviral drugs and vaccines against influenza virus, we still need to overcome many obstacles to control influenza virus infection. My working hypothesis for my doctoral research was that characterization of human monoclonal antibodies induced by vaccination or infection would lead to more effective therapeutic strategies. Through my studies, I made several important findings regarding protection; however, more information is still needed to achieve influenza virus control (especially for the prediction of pandemics and epidemics). I hope my findings will be useful for future research on the prevention and treatment of influenza virus infection.

ACKNOWLEDGMENTS

I would like to offer my deepest gratitude to Prof. Yoshihiro Kawaoka for his insightful suggestions, constructive comments, and warm encouragement. I especially would like to express my deepest appreciation to my supervisors, Dr. Seiya Yamayoshi and Dr. Shinya Yamada for their precise and intelligent advice, and warm encouragement. Also, I would like to acknowledge Dr. Maki Kiso, Dr. Kyoko Iwatsuki-Horimoto, Dr. Masaki Imai, Dr. Yuko Sakai-Tagawa, and Dr. Mutsumi Ito, for their helpful suggestions, guidance, and support.

I am very grateful to my collaborators, Chiharu Kawakami, Emi Takashita, and Setsuko Nakajima, for providing us with influenza viruses; Tadahiro Sasaki and Kazuyoshi Ikuta for providing the techniques for hybridoma generation; Dr. Patrick C. Wilson for providing us with anti-NA mAbs; and Drs. Jessica I-Hsuan Wang, Tomohiko Koibuchi, Michiko Koga, Eisuke Adachi, and Tadashi Kikuchi for assistance with experiments.

I also thank Dr. Susan Watson for scientific editing, and Dr. Kohei Oishi and Dr. Ryuta Uraki for helpful support and discussions. I would also like to offer my deepest appreciation to Ms. Misako Konno for her warm support, and all of the members of the Division of Virology, the Institute of Medical Science, University of Tokyo.

Finally, I would like to offer my special thanks to my family for their warm support.

REFERENCES

1. Molinari NA, Ortega-Sanchez IR, Messonnier ML, Thompson WW, Wortley PM, Weintraub E, Bridges CB. 2007. The annual impact of seasonal influenza in the US: measuring disease burden and costs. Vaccine 25:5086-96.
2. Stöhr K. 2002. Influenza—WHO cares. The Lancet infectious diseases 2:517.
3. ANDREWES CH, BANG FB, BURNET FM. 1955. A short description of the Myxovirus group (influenza and related viruses). Virology 1:176-84.
4. Hause BM, Collin EA, Liu R, Huang B, Sheng Z, Lu W, Wang D, Nelson EA, Li F. 2014. Characterization of a novel influenza virus in cattle and Swine: proposal for a new genus in the Orthomyxoviridae family. MBio 5:e00031-14.
5. Webby R, Webster R. 2001. Emergence of influenza A viruses. Philosophical Transactions of the Royal Society of London Series B 356:1817.
6. Kreijtz JH, Fouchier RA, Rimmelzwaan GF. 2011. Immune responses to influenza virus infection. Virus Res 162:19-30.
7. Tong S, Zhu X, Li Y, Shi M, Zhang J, Bourgeois M, Yang H, Chen X, Recuenco S, Gomez J, Chen LM, Johnson A, Tao Y, Dreyfus C, Yu W, McBride R, Carney PJ, Gilbert AT, Chang J, Guo Z, Davis CT, Paulson JC, Stevens J, Rupprecht CE, Holmes EC, Wilson IA, Donis RO. 2013. New world bats harbor diverse influenza A viruses. PLoS Pathog 9:e1003657.
8. Kamali A, Holodniy M. 2013. Influenza treatment and prophylaxis with neuraminidase inhibitors: a review. Infect Drug Resist 6:187-98.
9. Job ER, Bottazzi B, Gilbertson B, Edenborough KM, Brown LE, Mantovani A, Brooks AG, Reading PC. 2013. Serum amyloid P is a sialylated glycoprotein inhibitor of influenza A viruses. PLoS One 8:e59623.
10. Palese P, Tobita K, Ueda M, Compans RW. 1974. Characterization of temperature sensitive influenza virus mutants defective in neuraminidase. Virology 61:397-410.
11. Dharan NJ, Gubareva LV, Meyer JJ, Okomo-Adhiambo M, McClinton RC, Marshall SA, George KS, Epperson S, Brammer L, Klimov AI. 2009. Infections with oseltamivir-resistant influenza A (H1N1) virus in the United States. Jama 301:1034-1041.
12. Hurt AC, Ernest J, Deng Y-M, Iannello P, Besselaar TG, Birch C, Buchy P, Chittaganpitch M, Chiu S-C, Dwyer D. 2009. Emergence and spread of oseltamivir-resistant A (H1N1) influenza viruses in Oceania, South East Asia and South Africa. Antiviral research 83:90-93.
13. Baranovich T, Wong S-S, Armstrong J, Marjuki H, Webby RJ, Webster RG, Govorkova EA. 2013. T-705 (favipiravir) induces lethal mutagenesis in influenza A H1N1 viruses in vitro. Journal of virology:JVI. 02346-12.
14. Ren H, Zhou P. 2016. Epitope-focused vaccine design against influenza A and B viruses. Curr Opin Immunol 42:83-90.
15. Russell CJ. 2014. Acid-induced membrane fusion by the hemagglutinin protein and its role in

influenza virus biology. Curr Top Microbiol Immunol 385:93-116.
16. de Graaf M, Fouchier RA. 2014. Role of receptor binding specificity in influenza A virus transmission and pathogenesis. EMBO J 33:823-41.
17. Kubota-Koketsu R, Mizuta H, Oshita M, Ideno S, Yunoki M, Kuhara M, Yamamoto N, Okuno Y, Ikuta K. 2009. Broad neutralizing human monoclonal antibodies against influenza virus from vaccinated healthy donors. Biochem Biophys Res Commun 387:180-5.
18. Whittle JR, Zhang R, Khurana S, King LR, Manischewitz J, Golding H, Dormitzer PR, Haynes BF, Walter EB, Moody MA, Kepler TB, Liao HX, Harrison SC. 2011. Broadly neutralizing human antibody that recognizes the receptor-binding pocket of influenza virus hemagglutinin. Proc Natl Acad Sci U S A 108:14216-21.
19. Schmidt AG, Xu H, Khan AR, O'Donnell T, Khurana S, King LR, Manischewitz J, Golding H, Suphaphiphat P, Carfi A, Settembre EC, Dormitzer PR, Kepler TB, Zhang R, Moody MA, Haynes BF, Liao HX, Shaw DE, Harrison SC. 2013. Preconfiguration of the antigen-binding site during affinity maturation of a broadly neutralizing influenza virus antibody. Proc Natl Acad Sci U S A 110:264-9.
20. Krause JC, Tsibane T, Tumpey TM, Huffman CJ, Basler CF, Crowe JE. 2011. A broadly neutralizing human monoclonal antibody that recognizes a conserved, novel epitope on the globular head of the influenza H1N1 virus hemagglutinin. J Virol 85:10905-8.
21. Tharakaraman K, Subramanian V, Cain D, Sasisekharan V, Sasisekharan R. 2014. Broadly neutralizing influenza hemagglutinin stem-specific antibody CR8020 targets residues that are prone to escape due to host selection pressure. Cell Host Microbe 15:644-51.
22. Gupta P, Kamath AV, Park S, Chiu H, Lutman J, Maia M, Tan MW, Xu M, Swem L, Deng R. 2016. Preclinical pharmacokinetics of MHAA4549A, a human monoclonal antibody to influenza A virus, and the prediction of its efficacious clinical dose for the treatment of patients hospitalized with influenza A. MAbs 8:991-7.
23. Kallewaard NL, Corti D, Collins PJ, Neu U, McAuliffe JM, Benjamin E, Wachter-Rosati L, Palmer-Hill FJ, Yuan AQ, Walker PA, Vorlaender MK, Bianchi S, Guarino B, De Marco A, Vanzetta F, Agatic G, Foglierini M, Pinna D, Fernandez-Rodriguez B, Fruehwirth A, Silacci C, Ogrodowicz RW, Martin SR, Sallusto F, Suzich JA, Lanzavecchia A, Zhu Q, Gamblin SJ, Skehel JJ. 2016. Structure and Function Analysis of an Antibody Recognizing All Influenza A Subtypes. Cell 166:596-608.
24. Nabel GJ, Fauci AS. 2010. Induction of unnatural immunity: prospects for a broadly protective universal influenza vaccine. Nat Med 16:1389-91.
25. Lambert LC, Fauci AS. 2010. Influenza vaccines for the future. N Engl J Med 363:2036-44.
26. Hensley SE, Das SR, Bailey AL, Schmidt LM, Hickman HD, Jayaraman A, Viswanathan K, Raman R, Sasisekharan R, Bennink JR. 2009. Hemagglutinin receptor binding avidity drives influenza A virus antigenic drift. Science 326:734-736.
27. Schulman JL, Khakpour M, Kilbourne ED. 1968. Protective effects of specific immunity to

viral neuraminidase on influenza virus infection of mice. J Virol 2:778-86.
28. Webster RG, Laver WG. 1967. Preparation and properties of antibody directed specifically against the neuraminidase of influenza virus. J Immunol 99:49-55.
29. Wilson JR, Guo Z, Reber A, Kamal RP, Music N, Gansebom S, Bai Y, Levine M, Carney P, Tzeng WP, Stevens J, York IA. 2016. An influenza A virus (H7N9) anti-neuraminidase monoclonal antibody with prophylactic and therapeutic activity in vivo. Antiviral Res 135:48-55.
30. Wohlbold TJ, Podolsky KA, Chromikova V, Kirkpatrick E, Falconieri V, Meade P, Amanat F, Tan J, tenOever BR, Tan GS, Subramaniam S, Palese P, Krammer F. 2017. Broadly protective murine monoclonal antibodies against influenza B virus target highly conserved neuraminidase epitopes. Nat Microbiol 2:1415-1424.
31. Chen YQ, Wohlbold TJ, Zheng NY, Huang M, Huang Y, Neu KE, Lee J, Wan H, Rojas KT, Kirkpatrick E, Henry C, Palm AE, Stamper CT, Lan LY, Topham DJ, Treanor J, Wrammert J, Ahmed R, Eichelberger MC, Georgiou G, Krammer F, Wilson PC. 2018. Influenza Infection in Humans Induces Broadly Cross-Reactive and Protective Neuraminidase-Reactive Antibodies. Cell 173:417-429.e10.
32. Dawood FS, Jain S, Finelli L, Shaw MW, Lindstrom S, Garten RJ, Gubareva LV, Xu X, Bridges CB, Uyeki TM, Team NS-OIAHNVI. 2009. Emergence of a novel swine-origin influenza A (H1N1) virus in humans. N Engl J Med 360:2605-15.
33. Itoh Y, Shinya K, Kiso M, Watanabe T, Sakoda Y, Hatta M, Muramoto Y, Tamura D, Sakai-Tagawa Y, Noda T, Sakabe S, Imai M, Hatta Y, Watanabe S, Li C, Yamada S, Fujii K, Murakami S, Imai H, Kakugawa S, Ito M, Takano R, Iwatsuki-Horimoto K, Shimojima M, Horimoto T, Goto H, Takahashi K, Makino A, Ishigaki H, Nakayama M, Okamatsu M, Warshauer D, Shult PA, Saito R, Suzuki H, Furuta Y, Yamashita M, Mitamura K, Nakano K, Nakamura M, Brockman-Schneider R, Mitamura H, Yamazaki M, Sugaya N, Suresh M, Ozawa M, Neumann G, Gern J, Kida H, Ogasawara K, et al. 2009. In vitro and in vivo characterization of new swine-origin H1N1 influenza viruses. Nature 460:1021-5.
34. Organization WH. Recommended composition of influenza virus vaccines for use in the 2016-2017 northern hemisphere influenza season. 25th February 2016.
35. (ECDC) ECfDPaC. 2016. Influenza virus characterization, summary Europe, February 2016, Available from: http://ecdc.europa.eu/en/publications/Publications/influenza-virus-characterisation-february-2016.pdf.
36. Anonymous. 2016. Recommended composition of influenza virus vaccines for use in the 2017 southern hemisphere influenza season. Wkly Epidemiol Rec 91:469-84.
37. Team EE. 2017. WHO recommendations on the composition of the 2017/18 influenza virus vaccines in the northern hemisphere. Eurosurveillance 22.
38. Wright P, Neumann G, Kawaoka Y. 2007. Orthomyxoviruses. In" Fields Virology"(DM Knipe, and Howley, PM, Ed.). Lippincott Williams & Wilkins., Philadelphia.

39. Caton AJ, Brownlee GG, Yewdell JW, Gerhard W. 1982. The antigenic structure of the influenza virus A/PR/8/34 hemagglutinin (H1 subtype). Cell 31:417-27.
40. Matsuzaki Y, Sugawara K, Nakauchi M, Takahashi Y, Onodera T, Tsunetsugu-Yokota Y, Matsumura T, Ato M, Kobayashi K, Shimotai Y, Mizuta K, Hongo S, Tashiro M, Nobusawa E. 2014. Epitope mapping of the hemagglutinin molecule of A/(H1N1)pdm09 influenza virus by using monoclonal antibody escape mutants. J Virol 88:12364-73.
41. Gerhard W, Yewdell J, Frankel ME, Webster R. 1981. Antigenic structure of influenza virus haemagglutinin defined by hybridoma antibodies. Nature 290:713-7.
42. Xu R, Ekiert DC, Krause JC, Hai R, Crowe JE, Wilson IA. 2010. Structural basis of preexisting immunity to the 2009 H1N1 pandemic influenza virus. Science 328:357-60.
43. Linderman SL, Chambers BS, Zost SJ, Parkhouse K, Li Y, Herrmann C, Ellebedy AH, Carter DM, Andrews SF, Zheng NY, Huang M, Huang Y, Strauss D, Shaz BH, Hodinka RL, Reyes-Terán G, Ross TM, Wilson PC, Ahmed R, Bloom JD, Hensley SE. 2014. Potential antigenic explanation for atypical H1N1 infections among middle-aged adults during the 2013-2014 influenza season. Proc Natl Acad Sci U S A 111:15798-803.
44. Petrie JG, Parkhouse K, Ohmit SE, Malosh RE, Monto AS, Hensley SE. 2016. Antibodies Against the Current Influenza A (H1N1) Vaccine Strain Do Not Protect Some Individuals From Infection With Contemporary Circulating Influenza A (H1N1) Virus Strains. Journal of Infectious Diseases 214:1947-1951.
45. Chambers C, Skowronski DM, Sabaiduc S, Winter AL, Dickinson JA, De Serres G, Gubbay JB, Drews SJ, Martineau C, Eshaghi A, Krajden M, Bastien N, Li Y. 2016. Interim estimates of 2015/16 vaccine effectiveness against influenza A(H1N1)pdm09, Canada, February 2016. Euro Surveill 21:30168.
46. Krause JC, Tsibane T, Tumpey TM, Huffman CJ, Briney BS, Smith SA, Basler CF, Crowe JE. 2011. Epitope-specific human influenza antibody repertoires diversify by B cell intraclonal sequence divergence and interclonal convergence. J Immunol 187:3704-11.
47. Li GM, Chiu C, Wrammert J, McCausland M, Andrews SF, Zheng NY, Lee JH, Huang M, Qu X, Edupuganti S, Mulligan M, Das SR, Yewdell JW, Mehta AK, Wilson PC, Ahmed R. 2012. Pandemic H1N1 influenza vaccine induces a recall response in humans that favors broadly cross-reactive memory B cells. Proc Natl Acad Sci U S A 109:9047-52.
48. Huang KY, Rijal P, Schimanski L, Powell TJ, Lin TY, McCauley JW, Daniels RS, Townsend AR. 2015. Focused antibody response to influenza linked to antigenic drift. J Clin Invest 125:2631-45.
49. Dreyfus C, Laursen NS, Kwaks T, Zuijdgeest D, Khayat R, Ekiert DC, Lee JH, Metlagel Z, Bujny MV, Jongeneelen M, van der Vlugt R, Lamrani M, Korse HJ, Geelen E, Sahin Ö, Sieuwerts M, Brakenhoff JP, Vogels R, Li OT, Poon LL, Peiris M, Koudstaal W, Ward AB, Wilson IA, Goudsmit J, Friesen RH. 2012. Highly conserved protective epitopes on influenza B viruses. Science 337:1343-8.

50. Klimov AI, Garten R, Russell C, Barr IG, Besselaar TG, Daniels R, Engelhardt OG, Grohmann G, Itamura S, Kelso A, McCauley J, Odagiri T, Smith D, Tashiro M, Xu X, Webby R, Wang D, Ye Z, Yuelong S, Zhang W, Cox N, 2012 WCotWHOCoSHIVCf. 2012. WHO recommendations for the viruses to be used in the 2012 Southern Hemisphere Influenza Vaccine: epidemiology, antigenic and genetic characteristics of influenza A(H1N1)pdm09, A(H3N2) and B influenza viruses collected from February to September 2011. Vaccine 30:6461-71.
51. Rudneva I, Ignatieva A, Timofeeva T, Shilov A, Kushch A, Masalova O, Klimova R, Bovin N, Mochalova L, Kaverin N. 2012. Escape mutants of pandemic influenza A/H1N1 2009 virus: variations in antigenic specificity and receptor affinity of the hemagglutinin. Virus Res 166:61-7.
52. Korsun N, Angelova S, Gregory V, Daniels R, Georgieva I, McCauley J. 2017. Antigenic and genetic characterization of influenza viruses circulating in Bulgaria during the 2015/2016 season. Infect Genet Evol 49:241-250.
53. Ilyicheva T, Durymanov A, Susloparov I, Kolosova N, Goncharova N, Svyatchenko S, Petrova O, Bondar A, Mikheev V, Ryzhikov A. 2016. Fatal Cases of Seasonal Influenza in Russia in 2015-2016. PLoS One 11:e0165332.
54. Strengell M, Ikonen N, Ziegler T, Julkunen I. 2011. Minor changes in the hemagglutinin of influenza A(H1N1)2009 virus alter its antigenic properties. PLoS One 6:e25848.
55. Wei CJ, Boyington JC, Dai K, Houser KV, Pearce MB, Kong WP, Yang ZY, Tumpey TM, Nabel GJ. 2010. Cross-neutralization of 1918 and 2009 influenza viruses: role of glycans in viral evolution and vaccine design. Sci Transl Med 2:24ra21.
56. Krause JC, Ekiert DC, Tumpey TM, Smith PB, Wilson IA, Crowe JE. 2011. An insertion mutation that distorts antibody binding site architecture enhances function of a human antibody. MBio 2:e00345-10.
57. Krause JC, Tumpey TM, Huffman CJ, McGraw PA, Pearce MB, Tsibane T, Hai R, Basler CF, Crowe JE. 2010. Naturally occurring human monoclonal antibodies neutralize both 1918 and 2009 pandemic influenza A (H1N1) viruses. J Virol 84:3127-30.
58. Bush RM, Bender CA, Subbarao K, Cox NJ, Fitch WM. 1999. Predicting the evolution of human influenza A. Science 286:1921-5.
59. Neumann G, Watanabe T, Ito H, Watanabe S, Goto H, Gao P, Hughes M, Perez DR, Donis R, Hoffmann E, Hobom G, Kawaoka Y. 1999. Generation of influenza A viruses entirely from cloned cDNAs. Proc Natl Acad Sci U S A 96:9345-50.
60. Wilson IA, Skehel JJ, Wiley DC. 1981. Structure of the haemagglutinin membrane glycoprotein of influenza virus at 3 A resolution. Nature 289:366-73.
61. Weis W, Brown JH, Cusack S, Paulson JC, Skehel JJ, Wiley DC. 1988. Structure of the influenza virus haemagglutinin complexed with its receptor, sialic acid. Nature 333:426-31.
62. Knossow M, Skehel JJ. 2006. Variation and infectivity neutralization in influenza. Immunology

119:1-7.

63. Brownlee GG, Fodor E. 2001. The predicted antigenicity of the haemagglutinin of the 1918 Spanish influenza pandemic suggests an avian origin. Philos Trans R Soc Lond B Biol Sci 356:1871-6.
64. Chen C, Liu L, Xiao Y, Cui S, Wang J, Jin Q. 2018. Structural Insight into a Human Neutralizing Antibody against Influenza Virus H7N9. J Virol 92.
65. Ekiert DC, Kashyap AK, Steel J, Rubrum A, Bhabha G, Khayat R, Lee JH, Dillon MA, O'Neil RE, Faynboym AM, Horowitz M, Horowitz L, Ward AB, Palese P, Webby R, Lerner RA, Bhatt RR, Wilson IA. 2012. Cross-neutralization of influenza A viruses mediated by a single antibody loop. Nature 489:526-32.
66. Lee PS, Ohshima N, Stanfield RL, Yu W, Iba Y, Okuno Y, Kurosawa Y, Wilson IA. 2014. Receptor mimicry by antibody F045-092 facilitates universal binding to the H3 subtype of influenza virus. Nat Commun 5:3614.
67. Xu R, Krause JC, McBride R, Paulson JC, Crowe JE, Wilson IA. 2013. A recurring motif for antibody recognition of the receptor-binding site of influenza hemagglutinin. Nat Struct Mol Biol 20:363-70.
68. Tsibane T, Ekiert DC, Krause JC, Martinez O, Crowe JE, Wilson IA, Basler CF. 2012. Influenza human monoclonal antibody 1F1 interacts with three major antigenic sites and residues mediating human receptor specificity in H1N1 viruses. PLoS Pathog 8:e1003067.
69. Schmidt AG, Therkelsen MD, Stewart S, Kepler TB, Liao HX, Moody MA, Haynes BF, Harrison SC. 2015. Viral receptor-binding site antibodies with diverse germline origins. Cell 161:1026-1034.
70. Hong M, Lee PS, Hoffman RM, Zhu X, Krause JC, Laursen NS, Yoon SI, Song L, Tussey L, Crowe JE, Ward AB, Wilson IA. 2013. Antibody recognition of the pandemic H1N1 Influenza virus hemagglutinin receptor binding site. J Virol 87:12471-80.
71. Winarski KL, Thornburg NJ, Yu Y, Sapparapu G, Crowe JE, Spiller BW. 2015. Vaccine-elicited antibody that neutralizes H5N1 influenza and variants binds the receptor site and polymorphic sites. Proc Natl Acad Sci U S A 112:9346-51.
72. Krause JC, Tsibane T, Tumpey TM, Huffman CJ, Albrecht R, Blum DL, Ramos I, Fernandez-Sesma A, Edwards KM, García-Sastre A, Basler CF, Crowe JE. 2012. Human monoclonal antibodies to pandemic 1957 H2N2 and pandemic 1968 H3N2 influenza viruses. J Virol 86:6334-40.
73. Ohshima N, Iba Y, Kubota-Koketsu R, Asano Y, Okuno Y, Kurosawa Y. 2011. Naturally occurring antibodies in humans can neutralize a variety of influenza virus strains, including H3, H1, H2, and H5. J Virol 85:11048-57.
74. Khurana S, Suguitan AL, Rivera Y, Simmons CP, Lanzavecchia A, Sallusto F, Manischewitz J, King LR, Subbarao K, Golding H. 2009. Antigenic fingerprinting of H5N1 avian influenza using convalescent sera and monoclonal antibodies reveals potential vaccine and diagnostic

targets. PLoS Med 6:e1000049.

75. Xiong X, Corti D, Liu J, Pinna D, Foglierini M, Calder LJ, Martin SR, Lin YP, Walker PA, Collins PJ, Monne I, Suguitan AL, Santos C, Temperton NJ, Subbarao K, Lanzavecchia A, Gamblin SJ, Skehel JJ. 2015. Structures of complexes formed by H5 influenza hemagglutinin with a potent broadly neutralizing human monoclonal antibody. Proc Natl Acad Sci U S A 112:9430-5.
76. Sun L, Lu X, Li C, Wang M, Liu Q, Li Z, Hu X, Li J, Liu F, Li Q, Belser JA, Hancock K, Shu Y, Katz JM, Liang M, Li D. 2009. Generation, characterization and epitope mapping of two neutralizing and protective human recombinant antibodies against influenza A H5N1 viruses. PLoS One 4:e5476.
77. Chen Z, Wang J, Bao L, Guo L, Zhang W, Xue Y, Zhou H, Xiao Y, Wu F, Deng Y, Qin C, Jin Q. 2015. Human monoclonal antibodies targeting the haemagglutinin glycoprotein can neutralize H7N9 influenza virus. Nat Commun 6:6714.
78. Yasuhara A, Yamayoshi S, Soni P, Takenaga T, Kawakami C, Takashita E, Sakai-Tagawa Y, Uraki R, Ito M, Iwatsuki-Horimoto K, Sasaki T, Ikuta K, Yamada S, Kawaoka Y. 2017. Diversity of antigenic mutants of influenza A(H1N1)pdm09 virus escaped from human monoclonal antibodies. Sci Rep 7:17735.
79. Yamayoshi S, Uraki R, Ito M, Kiso M, Nakatsu S, Yasuhara A, Oishi K, Sasaki T, Ikuta K, Kawaoka Y. 2017. A Broadly Reactive Human Anti-hemagglutinin Stem Monoclonal Antibody That Inhibits Influenza A Virus Particle Release. EBioMedicine 17:182-191.
80. Skehel JJ, Wiley DC. 2000. Receptor binding and membrane fusion in virus entry: the influenza hemagglutinin. Annu Rev Biochem 69:531-69.
81. Ha Y, Stevens DJ, Skehel JJ, Wiley DC. 2001. X-ray structures of H5 avian and H9 swine influenza virus hemagglutinins bound to avian and human receptor analogs. Proc Natl Acad Sci U S A 98:11181-6.
82. Crotty S. 2014. T follicular helper cell differentiation, function, and roles in disease. Immunity 41:529-42.
83. Dogan I, Bertocci B, Vilmont V, Delbos F, Mégret J, Storck S, Reynaud CA, Weill JC. 2009. Multiple layers of B cell memory with different effector functions. Nat Immunol 10:1292-9.
84. de Vries RP, de Vries E, Martínez-Romero C, McBride R, van Kuppeveld FJ, Rottier PJ, García-Sastre A, Paulson JC, de Haan CA. 2013. Evolution of the hemagglutinin protein of the new pandemic H1N1 influenza virus: maintaining optimal receptor binding by compensatory substitutions. J Virol 87:13868-77.
85. Nunthaboot N, Rungrotmongkol T, Malaisree M, Kaiyawet N, Decha P, Sompornpisut P, Poovorawan Y, Hannongbua S. 2010. Evolution of human receptor binding affinity of H1N1 hemagglutinins from 1918 to 2009 pandemic influenza A virus. J Chem Inf Model 50:1410-7.
86. Schmier S, Mostafa A, Haarmann T, Bannert N, Ziebuhr J, Veljkovic V, Dietrich U, Pleschka S. 2015. In Silico Prediction and Experimental Confirmation of HA Residues Conferring

Enhanced Human Receptor Specificity of H5N1 Influenza A Viruses. Sci Rep 5:11434.
87. Daidoji T, Watanabe Y, Ibrahim MS, Yasugi M, Maruyama H, Masuda T, Arai F, Ohba T, Honda A, Ikuta K, Nakaya T. 2015. Avian Influenza Virus Infection of Immortalized Human Respiratory Epithelial Cells Depends upon a Delicate Balance between Hemagglutinin Acid Stability and Endosomal pH. J Biol Chem 290:10627-42.
88. Barbey-Martin C, Gigant B, Bizebard T, Calder LJ, Wharton SA, Skehel JJ, Knossow M. 2002. An antibody that prevents the hemagglutinin low pH fusogenic transition. Virology 294:70-4.
89. Fleury D, Wharton SA, Skehel JJ, Knossow M, Bizebard T. 1998. Antigen distortion allows influenza virus to escape neutralization. Nat Struct Biol 5:119-23.
90. Bizebard T, Gigant B, Rigolet P, Rasmussen B, Diat O, Bösecke P, Wharton SA, Skehel JJ, Knossow M. 1995. Structure of influenza virus haemagglutinin complexed with a neutralizing antibody. Nature 376:92-4.
91. Ilyushina NA, Khalenkov AM, Seiler JP, Forrest HL, Bovin NV, Marjuki H, Barman S, Webster RG, Webby RJ. 2010. Adaptation of pandemic H1N1 influenza viruses in mice. J Virol 84:8607-16.
92. Matrosovich MN, Matrosovich TY, Gray T, Roberts NA, Klenk HD. 2004. Neuraminidase is important for the initiation of influenza virus infection in human airway epithelium. J Virol 78:12665-7.
93. Potter CW, Oxford JS. 1979. Determinants of immunity to influenza infection in man. Br Med Bull 35:69-75.
94. Hobson D, Curry RL, Beare AS, Ward-Gardner A. 1972. The role of serum haemagglutination-inhibiting antibody in protection against challenge infection with influenza A2 and B viruses. J Hyg (Lond) 70:767-77.
95. Wrammert J, Koutsonanos D, Li GM, Edupuganti S, Sui J, Morrissey M, McCausland M, Skountzou I, Hornig M, Lipkin WI, Mehta A, Razavi B, Del Rio C, Zheng NY, Lee JH, Huang M, Ali Z, Kaur K, Andrews S, Amara RR, Wang Y, Das SR, O'Donnell CD, Yewdell JW, Subbarao K, Marasco WA, Mulligan MJ, Compans R, Ahmed R, Wilson PC. 2011. Broadly cross-reactive antibodies dominate the human B cell response against 2009 pandemic H1N1 influenza virus infection. J Exp Med 208:181-93.
96. Brandenburg B, Koudstaal W, Goudsmit J, Klaren V, Tang C, Bujny MV, Korse HJ, Kwaks T, Otterstrom JJ, Juraszek J, van Oijen AM, Vogels R, Friesen RH. 2013. Mechanisms of hemagglutinin targeted influenza virus neutralization. PLoS One 8:e80034.
97. Bosch BJ, Bodewes R, de Vries RP, Kreijtz JH, Bartelink W, van Amerongen G, Rimmelzwaan GF, de Haan CA, Osterhaus AD, Rottier PJ. 2010. Recombinant soluble, multimeric HA and NA exhibit distinctive types of protection against pandemic swine-origin 2009 A(H1N1) influenza virus infection in ferrets. J Virol 84:10366-74.
98. Seto JT, Chang FS. 1969. Functional significance of sialidase during influenza virus multiplication: an electron microscope study. J Virol 4:58-66.

99. Monto AS, Petrie JG, Cross RT, Johnson E, Liu M, Zhong W, Levine M, Katz JM, Ohmit SE. 2015. Antibody to Influenza Virus Neuraminidase: An Independent Correlate of Protection. J Infect Dis 212:1191-9.
100. Monto AS, Kendal AP. 1973. Effect of neuraminidase antibody on Hong Kong influenza. Lancet 1:623-5.
101. DiLillo DJ, Palese P, Wilson PC, Ravetch JV. 2016. Broadly neutralizing anti-influenza antibodies require Fc receptor engagement for in vivo protection. J Clin Invest 126:605-10.
102. Perussia B, Starr S, Abraham S, Fanning V, Trinchieri G. 1983. Human natural killer cells analyzed by B73.1, a monoclonal antibody blocking Fc receptor functions. I. Characterization of the lymphocyte subset reactive with B73.1. J Immunol 130:2133-41.
103. Stuart SG, Simister NE, Clarkson SB, Kacinski BM, Shapiro M, Mellman I. 1989. Human IgG Fc receptor (hFcRII; CD32) exists as multiple isoforms in macrophages, lymphocytes and IgG-transporting placental epithelium. EMBO J 8:3657-66.
104. Futosi K, Fodor S, Mócsai A. 2013. Neutrophil cell surface receptors and their intracellular signal transduction pathways. Int Immunopharmacol 17:638-50.
105. Bournazos S, DiLillo DJ, Ravetch JV. 2015. The role of Fc-FcγR interactions in IgG-mediated microbial neutralization. J Exp Med 212:1361-9.
106. Pincetic A, Bournazos S, DiLillo DJ, Maamary J, Wang TT, Dahan R, Fiebiger BM, Ravetch JV. 2014. Type I and type II Fc receptors regulate innate and adaptive immunity. Nat Immunol 15:707-16.
107. Laver WG, Air GM, Webster RG, Markoff LJ. 1982. Amino acid sequence changes in antigenic variants of type A influenza virus N2 neuraminidase. Virology 122:450-60.
108. Luther P, Bergmann KC, Oxford JS. 1984. An investigation of antigenic drift of neuraminidases of influenza A (H1N1) viruses. J Hyg (Lond) 92:223-9.
109. Webster RG, Laver WG, Air GM, Schild GC. 1982. Molecular mechanisms of variation in influenza viruses. Nature 296:115-21.
110. Air GM, Els MC, Brown LE, Laver WG, Webster RG. 1985. Location of antigenic sites on the three-dimensional structure of the influenza N2 virus neuraminidase. Virology 145:237-48.
111. Colman PM, Varghese JN, Laver WG. 1983. Structure of the catalytic and antigenic sites in influenza virus neuraminidase. Nature 303:41-4.
112. Fanning TG, Reid AH, Taubenberger JK. 2000. Influenza A virus neuraminidase: regions of the protein potentially involved in virus-host interactions. Virology 276:417-23.
113. Simonelli L, Pedotti M, Beltramello M, Livoti E, Calzolai L, Sallusto F, Lanzavecchia A, Varani L. 2013. Rational engineering of a human anti-dengue antibody through experimentally validated computational docking. PLoS One 8:e55561.
114. Iwatsuki-Horimoto K, Horimoto T, Tamura D, Kiso M, Kawakami E, Hatakeyama S, Ebihara Y, Koibuchi T, Fujii T, Takahashi K, Shimojima M, Sakai-Tagawa Y, Ito M, Sakabe S, Iwasa A, Ishii T, Gorai T, Tsuji K, Iwamoto A, Kawaoka Y. 2011. Seroprevalence of pandemic 2009

(H1N1) influenza A virus among schoolchildren and their parents in Tokyo, Japan. Clin Vaccine Immunol 18:860-6.

115. Murphy BR, Kasel JA, Chanock RM. 1972. Association of serum anti-neuraminidase antibody with resistance to influenza in man. N Engl J Med 286:1329-32.
116. Bragstad K, Nielsen LP, Fomsgaard A. 2008. The evolution of human influenza A viruses from 1999 to 2006: a complete genome study. Virol J 5:40.
117. Memoli MJ, Shaw PA, Han A, Czajkowski L, Reed S, Athota R, Bristol T, Fargis S, Risos K, Powers JH, Davey RT, Taubenberger JK. 2016. Evaluation of Antihemagglutinin and Antineuraminidase Antibodies as Correlates of Protection in an Influenza A/H1N1 Virus Healthy Human Challenge Model. MBio 7:e00417-16.
118. Wan H, Yang H, Shore DA, Garten RJ, Couzens L, Gao J, Jiang L, Carney PJ, Villanueva J, Stevens J, Eichelberger MC. 2015. Structural characterization of a protective epitope spanning A(H1N1)pdm09 influenza virus neuraminidase monomers. Nat Commun 6:6114.
119. Jiang L, Fantoni G, Couzens L, Gao J, Plant E, Ye Z, Eichelberger MC, Wan H. 2015. Comparative Efficacy of Monoclonal Antibodies That Bind to Different Epitopes of the 2009 Pandemic H1N1 Influenza Virus Neuraminidase. J Virol 90:117-28.
120. Sakabe S, Ozawa M, Takano R, Iwastuki-Horimoto K, Kawaoka Y. 2011. Mutations in PA, NP, and HA of a pandemic (H1N1) 2009 influenza virus contribute to its adaptation to mice. Virus Res 158:124-9.
121. Yamayoshi S, Ito M, Uraki R, Sasaki T, Ikuta K, Kawaoka Y. 2017. Human protective monoclonal antibodies against the HA stem of group 2 HAs derived from an H3N2 virus-infected human. J Infect.
122. Couzens L, Gao J, Westgeest K, Sandbulte M, Lugovtsev V, Fouchier R, Eichelberger M. 2014. An optimized enzyme-linked lectin assay to measure influenza A virus neuraminidase inhibition antibody titers in human sera. J Virol Methods 210:7-14.
123. Chen GW, Chang SC, Mok CK, Lo YL, Kung YN, Huang JH, Shih YH, Wang JY, Chiang C, Chen CJ, Shih SR. 2006. Genomic signatures of human versus avian influenza A viruses. Emerg Infect Dis 12:1353-60.
124. Shannon CE. 2001. A mathematical theory of communication. ACM SIGMOBILE mobile computing and communications review 5:3-55.
125. Ottaviano Y, Gerace L. 1985. Phosphorylation of the nuclear lamins during interphase and mitosis. J Biol Chem 260:624-32.